Addis Ababa University

College of Health Sciences

School of Pharmacy

Department of Pharmaceutics and Social Pharmacy

Physico-chemical Characterization of Native and Microcrystalline Cellulose from Sugarcane Bagasse and Evaluation of the Microcrystalline Cellulose as Directly Compressible Tablet Excipient

Natanim Degefu (B. Pharm)

July, 2019

Addis Ababa

Physico-chemical Characterization of Native and Microcrystalline Cellulose from Sugarcane Bagasse and Evaluation of the Microcrystalline Cellulose as Directly Compressible Tablet Excipient

A Thesis Submitted to Addis Ababa University, College of Health Sciences, School of Pharmacy, Department of Pharmaceutics and Social Pharmacy, in Partial Fulfillment of the Requirements for the Degree of Master of Science in Pharmaceutics

Natanim Degefu (B. Pharm)

Under the Supervision of Prof. Tsige Gebre-Mariam and Dr. Anteneh Belete, Department of Pharmaceutics and Social Pharmacy, School of Pharmacy, Addis Ababa University

July, 2019

Addis Ababa

Addis Ababa University School of Graduate Studies

This is to certify that the thesis undertaken by Natanim Degefu, entitled "Physico-chemical Characterization of Native and Microcrystalline Cellulose from Sugarcane Bagasse and Evaluation of the Microcrystalline Cellulose as Directly Compressible Tablet Excipient" and submitted in partial fulfillment of the requirements for the Degree of Master of Science in Pharmaceutics complies with the regulations of the University and meets the accepted standards with respect to originality and quality.

Approved and signed by the Examining Committee:

Name	**Signature**	**Date**
1. Prof. Tsige Gebre-Mariam (Advisor)	_____	_____
2. Dr. Anteneh Belete (Advisor)	_____	_____
3. Prof. Kaleab Asres (Examiner)	_____	_____
4. Dr. Nisha Mary Joseph (Examiner)	_____	_____

Head, Department of Pharmaceutics and Social Pharmacy, School of Pharmacy, Addis Ababa University

ACKNOWLEDGEMENTS

First and foremost, I would like to praise Almighty God for giving me strength and courage to accomplish this study.

I wish to express my sincere gratitude to my supervisors, Prof. Tsige Gebre-Mariam and Dr. Anteneh Belete, for their guidance, encouragement and insightful comments throughout the research work. They helped me to understand and enrich my research work.

I am highly thankful to Metehara Sugar Factory for providing me with sugarcane bagasse. I would also like to acknowledge Ethiopian Pharmaceuticals Manufacturing Share Company (EPHARM) for FTIR study and providing the model drug; East Africa Pharmaceuticals for allowing me access to tablet compression machine; and Ethiopian Public Health Institute for the determination of ash value.

I am thankful to Addis Ababa University, Institute of Technology, Department of Chemical Engineering, for giving me access to their laboratory (spray dryer), and Department of Pharmacognosy for allowing me to use Soxhlet apparatus and column chromatogram. My special thank also goes to Adama Science and Technology University, Department of Materials Science Engineering, for crystallinity and thermal analysis; and Leather Industry Development Institute for SEM analysis.

My special appreciation also goes to Tesfaye Gebriel for his guidance throughout the research work. I am highly indebted to all other staff members of Department of Pharmaceutics and Social Pharmacy. Furthermore, I also thank all my classmates for their helpful collaboration and friendship during the time of research.

I would like to acknowledge Addis Ababa and Haramaya Universities for sponsoring my postgraduate studies.

Finally, I wish to thank my family for their endless support during this work.

Table of Contents

ACKNOWLEDGEMENTS I

LIST OF FIGURES VI

LIST OF TABLES VII

ABBREVIATIONS and ACRONYMS VIII

ABSTRACT X

1. INTRODUCTION 1

1.1. Cellulose 1

1.2. Sources of Cellulose 2

1.3. Sugarcane Bagasse 2

1.4. Cellulose Extraction Methods 4

1.4.1. Acid pretreatment in cellulose isolation 7

1.5. Cellulose Modification 8

1.6. Microcrystalline Cellulose 8

1.7. Physico-chemical Characterization of Cellulose and Microcrystalline Cellulose 9

1.7.1. Structure of cellulose 9

1.7.2. Degree of polymerization 10

1.7.3. Morphological characterization 11

1.7.4. Crystalline structure 11

1.7.5. Thermal analysis 12

1.8. Powder Properties of Microcrystalline Cellulose 13

1.9. Applications of Cellulose and Microcrystalline Cellulose 14

1.9.1. Pharmaceutical applications 14

1.9.2. Other applications 14

1.10. Directly Compressible Tablet Diluent 15

1.11. Present Study 16
1.12. Research Questions 17
1.13. Objectives 17
1.13.1. General objective 17
1.13.2. Specific objectives 17
2. EXPERIMENTAL 18
2.1. Materials 18
2.2. Methods 18
2.2.1. Isolation of cellulose 18
2.2.2. Preparation of microcrystalline cellulose 19
2.2.3. Determination of percent yield 20
2.2.4. Characterization of cellulose and microcrystalline cellulose 20
2.2.4.1. Organoleptic characteristics 20
2.2.4.2. Chemical identification test 20
2.2.4.3. Determination of degree of polymerization 21
2.2.4.4. Moisture content 22
2.2.4.5. Fourier transform infrared spectroscopy 22
2.2.4.6. X-ray diffraction 22
2.2.4.7. Morphological characterization 23
2.2.4.8. Thermal analysis 23
2.2.5. Determination of chemical composition of microcrystalline cellulose 23
2.2.5.1. Determination of water-soluble substances 23
2.2.5.2. Determination of ether-soluble substances 24
2.2.5.3. Ash value 24
2.2.5.4. pH determination 24

2.2.6. Characterization of powder properties of microcrystalline celluloses 25
2.2.6.1. Particle size analysis 25
2.2.6.2. Densities and related properties 25
2.2.6.3. Hydration capacity 27
2.2.6.4. Moisture sorption pattern 27
2.2.7. Drug-excipient interaction study 28
2.2.8. Preparation of tablets 28
2.2.9. Evaluation of tablets 29
2.2.9.1. Lubricant sensitivity ratio 29
2.2.9.2. Weight and thickness 29
2.2.9.3. Crushing strength 29
2.2.9.4. Tensile strength 29
2.2.9.5. Friability 30
2.2.9.6. Disintegration test 30
2.2.9.7. Construction of UV calibration curve 30
2.2.9.8. In-vitro drug dissolution test 30
2.2.10. Statistical analysis 31
3. RESULTS AND DISCUSSION 32
3.1. Physico-chemical Properties of Cellulose and Microcrystalline Cellulose 32
3.1.1. Organoleptic characteristics and chemical identification test 32
3.1.2. Percent yield of cellulose and microcrystalline cellulose 32
3.1.3. Degree of polymerization 33
3.1.4. Fourier transform infrared analysis 34
3.1.5. X-ray Diffraction studies 39
3.1.6. Morphological characterization 42

3.1.7. Thermal analysis 43
3.2. Chemical Composition and Hydration Capacity of Microcrystalline Cellulose 46
3.3. Micromeritic Properties of Microcrystalline Cellulose 47
3.3.1. Particle size and particle size distribution 47
3.3.2. Density and related properties 51
3.4. Moisture Sorption Pattern 54
3.5. Mechanical Properties of Plain MCC Tablets 55
3.6. Lubricant Sensitivity Ratio 58
3.7. Drug-Excipient Compatibility Study 59
3.8. Dilution Potential 61
3.8.1. Weight variation and thickness 62
3.8.2. Crushing strength, tensile strength and friability 62
3.8.3. Disintegration time of directly compressed paracetamol tablets 65
3.8.4. UV calibration curve of paracetamol 66
3.8.5. Dissolution of directly compressed paracetamol tablets 67
4. CONCLUSIONS 69
5. SUGGESTIONS FOR FURTHER WORK 70
REFERENCES 71

LIST OF FIGURES

Figure 1-1: Production of SCB (left) and bundle of SCB (right) at Metehara Sugar Factory.....3
Figure 1-2: Molecular structure of cellulose 10
Figure 3-1: FTIR spectrum of SCBC. 35
Figure 3-2: FTIR spectrum of DSCBC.....36
Figure 3-3: FTIR spectrum of SCB-MCC.....37
Figure 3-4: FTIR spectrum of DSCB-MCC.....38
Figure 3-5: FTIR spectrum of Avicel PH-101.....39
Figure 3-6: XRD patterns of SCBC and DSCBC.....40
Figure 3-7: XRD patterns of SCB-MCCI, SCB-MCCOD, SCB-MCCSD and Avicel PH-101. 40
Figure 3-8: XRD patterns of DSCB-MCCI, DSCB-MCCOD, DSCB-MCCSD and Avicel PH-101.....41
Figure 3-9: SEM images of the DSCBC (A) and DSCB-MCCI (B).....43
Figure 3-10: TGA (A) and DTA (B) curves.....45
Figure 3-11: Hydration Capacity.....47
Figure 3-12: Volumeteric particle size distribution.....50
Figure 3-13: Moisture sorption patterns. 54
Figure 3-14: The FTIR spectrum of paracetamol.....60
Figure 3-15: FTIR spectrum physical mixture of paracetamol and SCB-MCC.....60
Figure 3-16: FTIR spectrum physical mixture of paracetamol and DSCB-MCC.....61
Figure 3-17: Effects of concentration of paracetamol on the hardness of tablets. 63
Figure 3-18: Effects of concentration of paracetamol on the tensile strength of tablets. 64
Figure 3-19: Effects of concentration of paracetamol on the friability of tablets. 65
Figure 3-20: Effects of concentration of paracetamol on the disintegration times. 66
Figure 3-21: Standard calibration curve of paracetamol in phosphate buffer 67
Figure 3-22: Dissolution profiles of tablets with different concentrations of paracetamol.....68

LIST OF TABLES

Table 3.1: Organoleptic Characteristics. 32
Table 3.2: DP and molecular weight 34
Table 3.3: Crystallinity index (CrI) and apparent crystal size 42
Table 3.4: Some Physico-chemical properties. 46
Table 3.5: Particle size and size distribution. 48
Table 3.6: Densities and related properties. 53
Table 3.7: Hardness, tensile strength, friability and disintegration time of plain tablets. 57
Table 3.8: Tensile Strengths and LSRs of the Compacts Using Pure and Lubricated Materials. 58
Table 3.9: Paracetamol tablet weight and thickness at different paracetamol concentration. ... 62

ABBREVIATIONS and ACRONYMS

AFEX:	Ammonia fiber explosion
AGU:	D-anhydroglucopyranose units
CF:	Compression Force
Cuam:	Cuprammonium hydroxide
DP:	Degree of Polymerization
DSC:	Differential Scanning Calorimetry
DSCBC:	Dewaxed Sugarcane Bagasse Cellulose
DSCB-MCC:	Dewaxed Sugarcane Bagasse Microcrystalline Cellulose
DSCB-MCCI:	Oven Dried Dewaxed Sugarcane Bagasse Microcrystalline Cellulose prepared without mechanical shearing
DSCB-MCCOD:	Oven Dried Dewaxed Sugarcane Bagasse Microcrystalline Cellulose
DSCB-MCCSD:	Spray Dried Dewaxed Sugarcane Bagasse Microcrystalline Cellulose
DTA:	Differential Thermal Analysis
FTIR:	Fourier Transform Infrared
LSR:	Lubricant Sensitivity Ratio
MCC:	Microcrystalline Cellulose
PFA/PAA:	Performic acid/ peracetic acid
RH:	Relative Humidity
rpm:	Revolution per Minute
SCB:	Sugarcane Bagasse
SCBC:	Sugarcane Bagasse Cellulose
SCB-MCC:	Sugarcane Bagasse Microcrystalline Cellulose

SCB-MCCI:	Oven Dried Sugarcane Bagasse Microcrystalline Cellulose prepared without mechanical shearing
SCB-MCCOD:	Oven Dried Sugarcane Bagasse Microcrystalline Cellulose
SCB-MCCSD:	Spray Dried Sugarcane Bagasse Microcrystalline Cellulose
SEM:	Scanning Electron Microscope
TGA:	Thermogravimetric Analysis
XRD:	X-Ray Diffraction/ Diffractometer

ABSTRACT

Sugarcane bagasse (SCB) is an abundant agricultural lignocellulose byproduct. In this study, cellulose was extracted from SCB by two methods, by acid treatment with or without dewaxing. Microcrystalline cellulose (MCC) was prepared from extracted cellulose by HCl hydrolysis with or without mechanical shearing either by oven or spray drying. Physico-chemical characteristics of cellulose and MCC were assessed. Mechanical properties of plain MCC tablets and dilution capacities of MCC, using paracetamol as a model drug, were also investigated. Cellulose yields on the dry weight basis were found to be 42.8% ± 1.10 and 43.5% ± 0.5 from non-dewaxed and dewaxed SCB, respectively. Whereas, dewaxed SCB cellulose (DSCBC) provided better yield of MCC (DSCB-MCCI) (81.0% ± 0.57) than non-dewaxed SCB cellulose (SCBC) yield of MCC (SCB-MCCI) (70.0% ± 0.90). The degree of polymerization (DP) of SCBC and DSCBC were 580.56 and 592.75, respectively, while DP of MCC preparations ranged from 230.10 - 256.14. Scanning electron microscopy of DSCBC showed characteristic morphology that was fibrous while SEM of DSCB-MCCI revealed it was rod in shape. Both dewaxed cellulose and MCC exhibited better heat stability than non-dewaxed products. The degree of crystallinity values of dewaxed cellulose (77.34%) and MCC (79.56 - 83.00%) were higher than non-dewaxed cellulose (74.50%) and MCC (78.11 - 81.93%). In contrast to non-dewaxed MCC preparation, ether-soluble substances of dewaxed MCC preparations were within the acceptable range. Except MCC prepared without mechanical shearing, all exhibited a monomodal normal particle size distribution. Mechanically sheared dewaxed MCC and Avicel PH-101 had comparable density and flow property. Both plain and paracetamol loaded tablets of spray dried MCC preparations showed significantly higher crushing and tensile strength than respective oven dried MCC preparations. All MCC preparations from SCB showed lower crushing and tensile strengths than Avicel PH-101. The disintegration times and dissolution profiles of all paracetamol loaded tablets prepared from dewaxed SCB-MCC and Avicel PH-101 were comparable and within the acceptable range. However, tablets of non-dewaxed SCB-MCC preparations had prolonged disintegration times and retarded *in-vitro* dissolution. Therefore, dewaxed SCB could be a promising locally available potential source of cellulose and MCC.

Keywords: Cellulose, Dilution capacity, Microcrystalline Cellulose, Sugarcane Bagasse

1. INTRODUCTION

1.1. Cellulose

Cellulose is the world's most abundant naturally occurring organic substance. It has been estimated that nature synthesizes from 100 to 1000 billion metric tons of cellulose per year (Coffey *et al.,* 2006; Marques-Marinho and Vianna-Soares, 2013). Cellulose has been the subject of intensive research over many decades occupying a vast body of published literature reporting its preparative and analytical methods, molecular structure, physical, chemical and biochemical properties, functionality and uses (Shanmugam *et al.,* 2015). Cellulose was first isolated from plant matter by French chemist Anselme Payen in 1839. He reported that cellulose has an identical structure as starch, but it exhibits a difference in structure and properties (Zugenmaier, 2008).

Cellulose is present in the cell wall of a great diversity of organisms, from bacteria (Cyanobacteria), prokaryotes (*Acetobacter, Rhizobium, Agrobacterium*) to eukaryotes (fungi, amoebae, green algae, freshwater and marine algae, mosses, ferns, angiosperms, gymnosperms). It is also produced by some animals, the tunicates (urochordates) (Marques-Marinho and Vianna-Soares, 2013). Among various biological species that synthesize cellulose, plants are by far the most prolific producers (Kim *et al*., 2013; Yu *et al.,* 2005). Plant fibers are mainly composed of cellulose, hemicellulose and lignin. Cellulose, which awards the mechanical properties of the complete natural fiber, is ordered in micro-fibrils enclosed by the other two main components, hemicellulose and lignin. Cellulose microfibrils can be found as intertwined microfibrils in the cell wall (Morán *et al.,* 2008).

Research in natural polymeric materials, such as cellulose, has witnessed growing interest and attention. This is attributed to a number of factors that include their relative abundance, low cost, and biodegradable and eco-friendly profiles (Marques-Marinho and Vianna-Soares, 2013). Cellulose and its derivatives have versatile uses in many industries such as food, pharmaceutical, paper, cloth and cosmetic industries (Shokri and Adibkia, 2013). The global cellulose market is expected to reach USD 36.96 Billion in 2020 at a compound annual growth rate of 9.49% over the period between 2015 and 2020 (Rohan, 2015).

1.2. Sources of Cellulose

Various biological species, mainly plants, synthesize cellulose. In plants, cellulose is synthesized by protein complexes embedded and traveling in plasma membranes of cells and excreted as a fibrillar form consisting of 24 - 36 chains into extracellular matrices where the cellulose fibrils are deposited and mixed with other polysaccharides forming cell wall (Kim *et al*., 2013).

Major commercial sources of cellulose are wood and cotton. Cotton may contain as high as ~98% of cellulose, and some types of wood may have as much as ~90% (Figueiredo *et al.*, 2010). However, high cost and a shortage of wood pulp, because of depleting forest resources, necessitate investigation of other potential sources (Suvachitanont and Ratanapan, 2011). Agricultural crop residues are an important source for isolation of cellulosic fibers in many countries, especially those that do not have a forest (Hassan, 2015). Agricultural wastes, such as banana plant waste (Ibrahim *et al.*, 2013), wheat straw (Zhong *et al.*, 2013), sugarcane bagasse (SCB) (Sun *et al.*, 2004) and sugarcane straw (Candido and Gonçalves, 2016), have been studied as a source of cellulose.

1.3. Sugarcane Bagasse

Sugarcane is largely grown in tropical and subtropical places where the wet and dry season is alternate such as Brazil, Australia, India, South Africa, Cuba, Peru and Mexico (Rípoli *et al.*, 2000). In 2011, 1.7 billion tons of sugarcane were produced worldwide (Michel *et al.*, 2013).

SCB is a fibrous residue obtained from sugarcane stalk after it is crushed to get juice used for sugar and ethanol production (Figure 1-1) (Mothé and Miranda, 2009). It is an abundant agricultural lignocellulose byproduct on earth. About 60 million tons of dry SCB are produced annually throughout the world (Huang *et al.*, 2012). It is mainly used to generate energy for the local industries and to feed animals (Michel *et al.*, 2013). SCB has also been used in many countries for papermaking and board making (Hassan, 2015).

SCB contains cellulose (40 - 50%), hemicellulose (25 - 35%) (amorphous polymers usually composed of xylose, arabinose, galactose, glucose and mannose), lignin (15 - 20%) and the remainder lesser amounts of mineral, wax (0.8 - 1.2%), ash (2.3%) and other compounds (Asl

et al., 2017; Lam *et al.*, 2017; Sun *et al.*, 2004). Since it has high concentration of cellulose, SCB becomes a potential source for cellulose preparations (Lam *et al.*, 2017; Mandal and Chakrabarty, 2011).

Figure 1-1: Production of SCB (left) and bundle of SCB (right) at Metehara Sugar Factory (Photos by Natanim Degefu, 2018).

Ethiopia has suitable soil, adequate water and conducive climate for sugarcane plantation. It is estimated that the country has a production capacity of 36,944,467 tons of sugarcane per year and 10,651,090 tons of SCB per year (Fenta, 2010). In Ethiopia, there are eight large-scale sugar establishments; namely Wonji-Shoa, Metehara, Fincha, Tendaho, Kessem, Arjo-Didessa and Omo-Kuraz Sugar Factory (II and III) (Ethiopian Sugar Corporation, Semonegna, 2018). These industries produce sugar with a large quantity of SCB as a byproduct. In 2017, Metehara sugar factory produced 2,134,677 tons of SCB. This is mainly used as a fuel to power the sugar mill and to feed animals. However, the remaining bagasse still continues to be a menace to the environment. Thus, using SCB as a source of cellulose has tremendous importance.

1.4. Cellulose Extraction Methods

In all biomass processing methods, the main technological problem is to liberate the cellulose material from the plant in a reasonable yield without large losses. This process is generally referred to as ‘‘treatment or pretreatment’’ of the biomass (Ramos, 2003). Pretreatment can be explained as a disruption of the cell-wall matrix which is the connection between carbohydrates and lignin, as well as depolymerizing and solubilizing hemicellulose polymers. During the pretreatment process, the compact lignocellulosic structure is disrupted and cellulose fiber is exposed (Amin *et al.,* 2017). Pretreatment also changes the degree of crystallinity of cellulose (Kumar *et al.,* 2015; Ramos 2003).

Pretreatment technologies are usually classified into physical, chemical, physico-chemical, and biological (Brodeur *et al.,* 2011; Ibrahim *et al.*, 2013). Combination of two or more techniques from the same or different categories are most commonly used (Ibrahim *et al.,* 2013; McMillan, 1994). Selection of particular pretreatment is dependent on the cellulose source material and to a lesser degree on the desired morphology of the starting cellulose particles (Moon *et al*., 2011; Radotić and Mićić, 2016).

Physical pretreatment methods, including mechanical operations, microwave radiation and ultrasonic pretreatment, have been utilized to enhance the accessibility to hydrolyzable polymers within lignocellulosic material. Among the physical pretreatments, mechanical pretreatment is widely used for waste materials, such as agricultural residues or any other crops and forestry residues. All pretreatment processes involve an initial mechanical step in which the biomass is comminuted by a combination of chipping, grinding and milling (McMillan, 1994). It is an important step for improving the bioconversion affectivity and chemical accessibility (Amin *et al.,* 2017). Ultrasound-assisted extraction can be explained by the mechanical action of the ultrasound on the cell wall resulting in increased accessibility and extractability of the hemicellulosic and lignin components (Liu *et al.,* 2006; Sun *et al.,* 2004). Microwave radiation also accelerates biological, chemical and physical processes because of heat and extensive collisions brought about by the vibration of polar molecules and ion movement. However, its performance is influenced by the dielectric properties of the lignocellulosic material (Amin *et al.,* 2017).

Chemical, alkali or acid, pretreatment methods are most commonly used pretreatment method with the primary goal of removing lignin and/or hemicellulose (Ibrahim *et al.*, 2013; McMillan, 1994). Alkaline pretreatment involves the use of bases, such as sodium, potassium, calcium and ammonium hydroxide, for the pretreatment of lignocellulosic biomass. The use of an alkali causes the degradation of ester and glycosidic side chains resulting in structural alteration of lignin, cellulose swelling, partial decrystallization of cellulose and partial solvation of hemicellulose (Brodeur *et al.*, 2011; Mashego, 2016). The efficacy of alkali pretreatment is dependent upon lignin content (McMillan, 1994), whereas acid pretreatment involves the use of concentrated or diluted acids to break the rigid structure of the lignocellulosic material. The most commonly used acids are sulphuric, hydrochloric, phosphoric, acetic, formic and nitric acid (Brodeur *et al.*, 2011; McMillan, 1994).

Physico-chemical pretreatment methods, including liquid hot water pretreatment, steam explosion, ammonia explosion or ammonia fiber explosion (AFEX) and supercritical fluid pretreatment, can also be used in cellulose extraction. Liquid hot water pretreatment uses water at elevated temperatures and high pressures to maintain its liquid form in order to promote disintegration and separation of the lignocellulosic matrix. Temperatures of liquid hot water pretreatment can range from 160 ^{o}C to 240 ^{o}C and over lengths of time ranging from a few minutes up to an hour. It solubilizes hemicellulose and separates it from the rest of the solid material while reducing the formation of inhibitors (Brodeur *et al.*, 2011). Steam explosion is another process used to treat lignocellulosic material under high pressure and with a rapid pressure drop, at the end. It is the most commonly used pretreatment method for depolymerization of the lignocellulosic material that helps in loosening the bonds between cellulose, hemicellulose and lignin (Amin *et al.*, 2017; Kumar *et al.*, 2015; McMillan, 1994). AFEX pretreatment has been demonstrated to markedly improve the saccharification rates of numerous herbaceous crops and grasses. There are two mechanisms by which AFEX pretreatment acts. First, the reactivity of cellulose is increased by exposure to liquid NH_3. Penetration of liquid NH_3 into the lignocellulose matrix is relatively rapid. Second, accessible surface area increases following AFEX treatment, probably as a combined effect of hemicellulose hydrolysis and explosive decompression (McMillan, 1994).

Biological pretreatment by using bacteria (*Actinomycetes)* has been observed to be effective on grasses. Fungi can also be used as sources of commercial plant cell wall-degrading enzymes. Some of the disadvantages of biological pretreatment that make it less suitable for industry include a long residence time of 10 - 14 days, extremely precise growth conditions and the need for a large space to perform the biological pretreatment. Another potential disadvantage is that some fraction of the carbohydrate is consumed by the microorganisms. Biological pretreatment can be exploited as a first step, default pretreatment in combination with another pretreatment method or on its own if the biomass has a low lignin content (Amin *et al.,* 2017).

Bleaching is another consecutive step in cellulose extraction. It has the purpose of increasing their brightness by chemical means. Chemical such as sodium hypochlorite/glacial acetic acid or hydrogen peroxide/sodium hydroxide mixture can be used as a bleaching agent. Currently, with the development of totally chlorine-free bleaching technologies, there is a growing interest in the use of hydrogen peroxide as one of the oxidants replacing chlorine-based reagents. It is generally accepted that perhydroxyl anion HOO^- is the most important active species involved in the suppression of chromophores in lignin macromolecules. On the other hand, radicals such as $HO^{\cdot}$ and $O^{\cdot}{}_2$ produced at high pH levels can participate in lignin degradation and hemicellulose dissolution (Sun *et al.,* 2004; Yiannoulakis, 2015).

Natural fibers contain wax in addition to cellulose, hemicelluloses, lignin, pectin and water-soluble substances (Rosli *et al.,* 2013). Epicuticular wax, the outermost lipophilic layer covered on the plants surface, provides protection for the plant against environmental stress. Sugarcane can produce epicuticular wax on the stems and leaves. During the milling process of sugarcane, a large portion of the wax detaches from the bagasse and mixes with the expressed juice, and then removed to the press mud (filter cake) during the subsequent clarification step. The rest of the wax still attaches on the surface of the SCB (Qi *et al.,* 2016). Residual wax and any other hydrophobic components are thought to compromise the disintegration properties of microcrystalline cellulose (MCC) (Padmadisastra and Gonda, 1989). Therefore, dewaxing procedure is required in addition to the pretreatment procedure in cellulose extraction.

Several research reports indicate that extractions with toluene-ethanol or chloroform-methanol gave larger amounts of hydrophobic extractives (Sun and Tompkinson, 2003). Usually, these

two solvent mixtures are used for dewaxing of natural fibers. Other solvents that are sometimes used include benzene, methyl isobutyl ketone, propane, petroleum naphtha, ethylene dichloride and methylene chloride. In addition to the solvent type, the duration of extraction period can have a significant change in the dewaxing effectiveness. As reported by Sin (2012), extracting for 4 hrs gave a percentage of about 15% and when extraction period prolonged, six hours, extraction effectiveness was reduced (< 12%).

Different investigators follow different procedures for dewaxing lignocellulosic biomass. Lu and Hsieh (2012) dewaxed rice straw powder with toluene/ethanol (2:1 v/v) mixture for 20 hrs by maceration with 1:15 solid to liquor ratio. In another study, the solid residue was subjected to toluene-methanol, (2:1 v/v) with stirring at a constant temperature of 60 ^{o}C (Kumar *et al.*, 2015). Zhong *et al.* (2013) dewaxed wheat straw in Soxhlet apparatus with toluene-ethanol (2:1 v/v) for 5 hrs. Kapok fiber was dewaxed by refluxing in $CHCl_3$ for 4 hrs at 65 ^{o}C. Then, the mixture was filtered, washed with methanol and dried (Draman *et al.,* 2016). Attard *et al.* (2015) dewaxed milled biomass (sugarcane rind or leaves) in Soxhlet apparatus for 4 hrs. After this procedure, the fiber was allowed to dry in an oven at 60 ^{o}C for 16 hrs (Attard *et al.*, 2015; Sun *et al.*, 2004).

1.4.1. Acid pretreatment in cellulose isolation

Acid pretreatment is one of chemical pretreatment techniques. The most commonly used acids are sulphuric, hydrochloric, phosphoric, acetic, formic and nitric acids. Since their ability to remove hemicellulose and lignin, acid pretreatments have been used as parts of the overall process in fractionating the components of lignocellulosic biomass (Brodeur *et al*., 2011).

The acetic or formic acid process is an effective method to fractionate lignocellulosic materials to produce cellulosic pulp/other products. The process can be carried out at atmospheric pressure. The acid used in the process can be easily recovered by distillation and reused in the process. The method has been used to separate cellulose, hemicellulose and lignin from lignocellulosic materials. The lignin thus obtained is an optimal feedstock. The sugars from hemicellulose are readily convertible to chemicals and fuels (Jahan *et al.*, 2011).

Acetic acid cooking needs sulfuric acid as a catalyst for delignification. Therefore, the presence of sulfuric acid in the black liquor complicates the recycling of the cooking chemicals and also creates corrosion problems. Formic acid effectively fractionates lignin, hemicelluloses and pulp. In the spent liquor, a considerable amount of acetic acid is generated from the bound acetyl group in hemicelluloses during formic acid/performic acid delignification process. The separation of acetic acid from the spent liquor makes the recovery system complicated. In addition, increasing formic acid concentration in the acid mixture improves the delignification rate but reduces levels of cellulose, hemicellulose, lignin and pulp yield (Hidayati *et al.*, 2017, Jahan *et al.*, 2011; Jahan *et al.*, 2014). Thus, combination of formic and acetic acid can be used as an alternative method because its investment cost is relatively low; does not pollute the environment, and obtaining cellulose from lignocellulosic with product properties of high yield, low residual lignin content, high brightness and good strength (Hidayati *et al.*, 2017, Jahan *et al.*, 2011).

1.5. Cellulose Modification

Cellulose can be physically modified, like microfibrillated cellulose and MCC, or chemically modified, such as ethyl cellulose, hydroxyethyl cellulose, hydroxypropyl cellulose and carboxymethyl cellulose. They majorly differ from cellulose by the extent of crystallization with crystal-forming hydrogen bonds (Coffey *et al.*, 2006; Shokri and Adibkia, 2013).

1.6. Microcrystalline Cellulose

MCC is a cellulose derivative obtained by treating the alpha cellulose contained in fibrous plants using acid solutions, hydrochloric or sulfuric acid. MCC was discovered in 1955 by Battista and Smith. It was first commercialized under the brand name Avicel® and first registered in the supplement to the National Formulary, twelfth edition, in 1966 MCC (Coffey *et al.*, 2006; Huang *et al.*, 2012).

During MCC preparation, the hinges of amorphous cellulose which link the naturally occurring microcrystals are preferentially removed by severe acid hydrolysis, yielding cellulose with a degree of polymerization (DP) of about 200 to 300. After acid hydrolysis, microcrystals rebind together randomly as aggregates. These microcrystals are freed from their fibrous, packed

structure by mechanical shearing of a water slurry and obtained as a powder by drying. By varying the hydrolytic, shearing and drying conditions, the particle size and the moisture content of MCC change, and such changes give rise to different commercial MCC grades currently available. Note that the degree of crystallinity of the MCC products varies a lot and is not necessarily higher than that of the original cellulose because intensive agitation may destroy the crystal structure and short macromolecular chains are unfavorable to the formation of crystalline regions (Doelker *et al.*, 1987; Doelker, 1993).

MCC occurs as white, odourless and tasteless crystalline powder composed of porous particles (Suvachitanont and Ratanapan, 2011). It is generally considered as a diluent having the best binding properties and as one of the preferred direct compressible binders. In addition to its dry binding properties, MCC is self-disintegrating with low lubricant requirement because of its extremely low coefficient of friction and its very low residual die wall pressure. MCC offers other advantages including broad compatibility with active pharmaceutical ingredients, physiological inertness and ease of handling (Thoorens *et al.*, 2014).

1.7. Physico-chemical Characterization of Cellulose and Microcrystalline Cellulose

1.7.1. Structure of cellulose

Cellulose is a linear syndiotactic homopolymer composed of D-anhydroglucopyranose units (AGU), which are linked together by β-(l—>4)-glycosidic bonds. Taking the dimer cellobiose as the basic unit, cellulose can be considered as an isotactic polymer of cellobiose (Figure 1-2) (Klemm *et al..,* 1998). Each of the AGU has three hydroxyl (OH) groups at C-2, C-3 and C-6 positions. This multiple OH groups on cellulose molecule and its linear structure enable the formation of crystalline fiber bonded by extensive hydrogen bonds (Kusumattaqiin and Chonkaew, 2015). These hydroxy groups at C-2, C-3 and C-6 positions are capable of undergoing the typical reactions known for primary and secondary alcohols. The hydroxy groups at both ends of the cellulose chain show different behavior. The C-1 end has reducing properties while the glucose end group with a free C-4 hydroxy group is non-reducing. The bridging and the ring oxygen atom are predominantly involved in intramolecular and intermolecular interactions, mainly hydrogen bonds and in degradation reactions (Klemm *et al*., 1998).

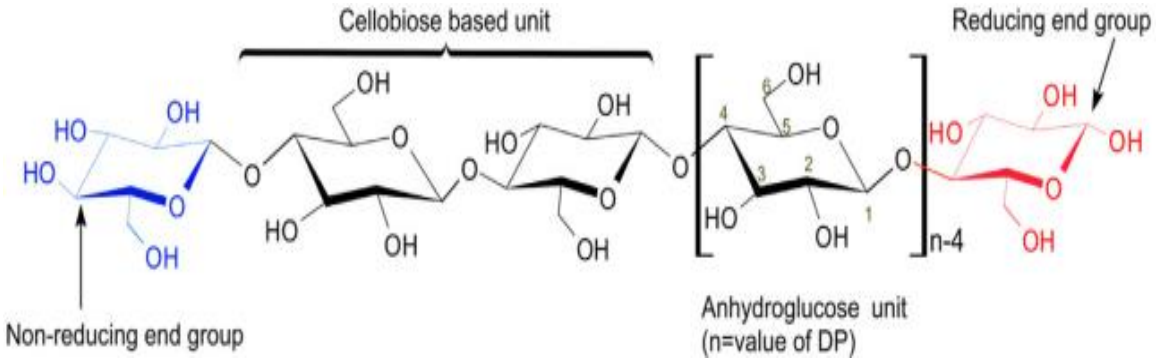

Figure 1-2: Molecular structure of cellulose showing the numbering of carbon atoms, the reducing end with a hemiacetal, and the non-reducing end with a free hydroxyl at C4 (Trache *et al*., 2016).

1.7.2. Degree of polymerization

The molecular size of polymer molecules can be conveniently described in terms of DP, which is an average value of the number of monomer units. The DP of cellulose can be estimated by various physical techniques (intrinsic viscosity measurement, light scattering, etc.) (Coffey *et al.*, 2006). The determination of the DP is usually performed viscosimetrically after dissolving the sample in complexing aqueous solvents, like cuprammonium hydroxide (Cuam) or copper ethylene diamine (Cuen) (Klemm *et al*., 1998).

DP is merely an identity test to distinguish MCC (DP < 350) from powdered cellulose (DP > 440). Level-off degree of polymerization (LODP) is unique to particular raw material, commonly in the range of 200 – 300, after which it is difficult to further hydrolyze the MCC. DP values higher than the plateau LODP are more difficult to control because of their greater sensitivity to hydrolysis conditions. Above the LODP, MCC retains more of the fibrous cellulose characteristics, which would result in a lower bulk density, may improve tabletability but would hinder powder flow. Below the LODP, MCC is less fibrous, denser and less tabletable. Within a single MCC grade, in order to meet DP and bulk density specifications, MCC manufacturers need to tightly control the hydrolysis conditions to avoid producing out of specification material (Thoorens *et al.*, 2014).

1.7.3. Morphological characterization

Morphology of cellulose and MCC can be studied by electron microscopy techniques such as scanning (SEM) or transmission (TEM) electron microscopy (Granström, 2009). SEM analysis reveals the finer details of the processed sample (Kumar *et al*., 2015). The morphological structure of cellulose comprises a well-organized architecture of fibrillar elements. In native cellulose, the hierarchy of the fibrillar entities is organized in layers with differing fibrillar textures (Granström, 2009). MCC is also fibrous (rod-shaped) particles and had a short length when compared to cellulose (Obae *et al.*, 1999). There is not much difference in the MCC surface morphology as compared with several types of sources such as MCC from alfa fiber, rice hulls, bean hulls, bagasse, cotton silver, jute, rice straw, cotton straw and oil palm empty fruit brunch, as well as commercial MCC. It seems that when the cellulose sample undergoes hydrolysis treatment, the surface morphology of MCC changes in terms of size and level of smoothness (Trache *et al*., 2016), whereas different grades of MCC have different scanning electron micrograph. For example, Avicel PH-101 has a matchstick-like or rod-like structure, and Avicel PH-102 is a mixture of primary particles and agglomerates. The primary particles are composed of fibrils with a radius of 10 to 15 nm with a hollow axis of about 2 nm. These intraparticle pores account for 90% of the total surface area (Bolhuis and de Waard, 2011).

1.7.4. Crystalline structure

Cellulose is considered as a two-phase system consisting of amorphous and crystalline domains. The physico-chemical behavior of cellulose is strongly related to its degree of crystallinity. It influences directly the accessibility for chemical derivatization, swelling and water-binding. Therefore, the degree of crystallinity is a very important property which needs to be taken into account when considering the manufacturing and applications of cellulose (Cybulska *et al.*, 2011). The naturally produced crystalline cellulose can have two polymorphic structures: Iα and Iβ. Algae and lower plants produce mostly Iα allomorph, whereas higher plants produce mostly Iβ allomorph. Cellulose II produced by treating cellulose Iα and Iβ with high concentration alkaline and neutralizing with ammonia or obtained through coagulation with water of a fully dissolved cellulose solution in strong ionic solvents. When cellulose I or II are treated with liquid ammonia, then they convert to III_I and III_{II}, respectively. Another polymorphic form is cellulose

IV. It is reported to be formed through high temperature treatments of cellulose III in glycerol. Certain young primary cell walls of cotton were claimed to produce cellulose IV (Kim *et al.*, 2013).

The degree of crystallinity of cellulose and MCC can be determined either by X-Ray Diffractometer (XRD) or infrared spectroscopy. The values of the degree of crystallinity for cellulose and MCC can be varied depending on the method used to determine this parameter. Modifying the hydrolysis conditions, including temperature, time and acid concentration, also have very little impact on the degree of crystallinity. This indicates that crystallinity cannot be controlled at the hydrolysis stage. Crystallinity appears to be more dependent on pulp source rather than on processing conditions (Sun *et al.,* 2008; Thoorens *et al*., 2014).

Various studies demonstrated that crystallinity index of MCC showed the highest value compared to cellulose when tested under XRD. This higher crystallinity in MCC is caused by the removal of amorphous regions of cellulose by hydrolysis process which prompts hydrolytic cleavage of glycosidic bonds and leads to rearrangement of cellulose molecules (Trache *et al*., 2016).

The degree of crystallinity of MCC can affect its tabletability. Furthermore, the total amount of sorbed water in MCC is proportional to the fraction of amorphous. Therefore, MCC powders with a lower degree of crystallinity may contain more water than their counterparts with a higher degree. Despite the controversial impact of crystallinity, it may influence the adsorption of water on cellulose microfibrils, which may in turn influence flowability, tabletability and stability of the drug product (Suzuki and Nakagami, 1999)

1.7.5. Thermal analysis

Both thermogravimetric analysis (TGA) and differential scanning calorimetry (DSC) are commonly used to investigate the thermal and degradation properties of cellulose sample (Trache *et al*., 2016). The thermal stability of the cellulose increased with its purity (Draman *et al.,* 2016; Sun *et al.,* 2004). Compared to cellulose, MCC requires high energy to be degraded because of the high degree of molecular ordering (Trache *et al*., 2016).

1.8. Powder Properties of Microcrystalline Cellulose

Density is an important factor for the application of MCC. A decrease in bulk and tap density is accompanied by an increase in DP. Tensile strength of MCC tablets increased with decreased bulk and tapped density. It could be due to MCC with lower density has a higher surface roughness, which contributes to mechanical interlocking during formation (Liao *et al.*, 2012).

MCC is one of the most commonly used tabletting excipients and many of its properties depend on its moisture content (Mihranyan *et al.,* 2004). Moisture affects the flow, mixing rheology, compaction, true density and mechanical properties of granules as well as tablets. The amount of water associated with a solid at a particular relative humidity (RH) and temperature depends on its chemical affinity, surface area and available sites of interaction (Patel *et al.,* 2006). Moisture within the pores of MCC may act as an internal lubricant, reduce frictional forces, and facilitate slippage and plastic flow within the individual microcrystals. The lubricating properties of water may also reduce tablet density variation by providing a better transmission of the compression force through the compact and by decreasing the adhesion of the tablet to the die wall (Nokhodchi, 2005). Tablets containing MCC became harder as the moisture content increased, whereas a lack of moisture was responsible for tablet lamination because of increased yield force and elastic recovery. It has been explained by adsorbed water functioning as a surface-restructuring medium, thus increasing the amount of solid bridges. Another possible explanation for increasing tensile strength is that immobile water layers sorbed at particle surfaces can enhance particle-particle interaction (Patel *et al.*, 2006). According to specifications to the USP monograph loss on drying is not more than 7.0% (USP 30/NF 25, 2007).

The crystallite portion of MCC does not adsorb water and the extent of water adsorption by cellulose should thus be proportional to the amount of amorphous present in cellulose. Therefore, water is sorbed almost exclusively by the amorphous regions of MCC (Kachrimanis *et al.,* 2006). In general, water sorption can occur either on the surfaces or in the bulk of a material. Moisture uptake by cellulose powder is recognized as predominantly occurring in the bulk of disordered regions. Moisture sorption in cellulose is a complex process directly associated with and controlled by, the structural properties of cellulose, such as surface area, pore volume, and crystallinity. The extent of moisture sorption was shown to decrease with increasing crystallinity of the samples at relative humidities below 75%. At higher relative

humidities, filling of the large pore volume of the cellulose accounted for an increase in moisture content (Mihranyan *et al*., 2004; Williams *et al.*, 1997).

1.9. Applications of Cellulose and Microcrystalline Cellulose

1.9.1. Pharmaceutical applications

Cellulose and its derivatives are extensively used in food, pharmaceutical, paper and cosmetic industries. They show several interesting characteristics such as low cost, reproducibility, biocompatibility and recyclability (Marques-Marinho and Vianna-Soares, 2013; Suvachitanont and Ratanapan, 2011).

The applications of the powdered cellulose and MCC in compounding pharmacies include the oral solid dosage form as a bulking agent to increase the mass in formulations containing small amounts of the active ingredient. The powdered cellulose is a base material for powder dosage forms, a suspending agent for aqueous peroral delivery and an adsorbent and thickening agent for topical preparations (Marques-Marinho and Vianna-Soares, 2013).

MCC is a commonly used filler/binder in the pharmaceutical industry. In the colloidal form, MCC is utilized as a suspension stabilizer, a water retainer, a viscosity regulator and emulsifier in different pastes and creams. Features like lightness, stiffness, strength, fibrous nature, non-toxicity, water insolubility, crystallinity, biodegradability and renewability make MCC more attractive to be used in pharmaceutical industry (Moon *et al.,* 2011).

1.9.2. Other applications

Cellulose and its derivatives have long been used in fabricating formulated foods. The physically modified celluloses are useful in many products where bulk properties are desirable. This would include low-calorie foods, flavor oil imbibers or flowable products such as artificial sweeteners and flavor packets. The use of these cellulosics is generally due to their rheology, controlled water interaction and textural attributes and insolubility. Five important roles for the chemically modified cellulose derivatives in foods are the regulation of rheological properties, emulsification, stabilization of foams, modification of ice crystal formation and growth and water-binding capacity (Coffey *et al.*, 2006; Mashego, 2016).

1.10. Directly Compressible Tablet Diluent

Direct compression describes tablet production without prior treatment of the particulate solids. Since the introduction in the early sixties of the last century of spray dried lactose as the first excipient specially designed for direct compaction, other directly compressible excipients, commonly referred to as filler-binders, appeared on the pharmaceutical market. The introduction of the very effective filler-binder MCC (Avicel PH) in 1964 resulted in an increased interest in the production of tablets by direct compaction. The term diluent is often used in relation to direct compaction, but it only covers the bulking function. The diluent in a direct compaction formulation has a dual role, increases the bulk of the dosage unit and promotes the binding of the constituent particles of the formulation. Thus, the term filler-binder is preferred (Bolhuis and de Waard, 2011). Apart from its use in direct compression, MCC is used as a diluent in tablets prepared by wet granulation, as filler in capsules and for the production of spheres (Gohel and Jogani, 2005).

Dilution potential (or uptake capacity) defined as the amount of an active ingredient that can be satisfactorily compressed into tablets with a given filler-binder. It is not possible to give specific values on this parameter because it depends on the properties of the drug being incorporated, the compaction force utilized to produce the compacts and the rate of applying this load when dealing with viscoelastically deforming materials (Bolhuis and de Waard, 2011; Habib *et al.,* 1996).

Tablets containing a high dose of an active ingredient that has poor compactibility, poor flow properties and/or low bulk density cannot be prepared by direct compaction, because filler-binders have a limited dilution potential (uptake capacity). However, if an active ingredient is more compressible and flowable, a greater proportion can be carried successfully by a filler-binder (Bolhuis and de Waard, 2011). Most commonly, dilution potential is assessed by comparing the hardness (or tensile strength) versus compaction force (or pressure) curves for various binary mixtures of the filler and some poorly compactible substance, such as paracetamol or ascorbic acid (Kuentz *et al.,* 2000).

Dilution capacity of MCC has been investigated by different researchers. Habib *et al.* (1996) reported that Avicel PH-101, Avicel PH-102 and Avicel PH-200 had dilution capacity of 65.5,

68.0 and 47.2%, respectively, when paracetamol is used as a model drug. Similarly, Pesonen and Paronen (1986) also prepared strong tablets by using Emcocel and Avicel PH-101 at very low compressional forces. Emcocel and Avicel PH-101 had similar ability to bind paracetamol into tablets. Both of these materials were able to bind paracetamol up to 70%. In another study, with a similar model drug, dilution capacity of Avicel PH-101 was found to be 79.9% (Kuentz *et al.*, 2000). This discrepancy can be because of the different pressure ranges and extrapolation techniques that were used.

1.11. Present Study

In Ethiopia, pharmaceutical and other industries import excipients by expending a large amount of foreign currency. Cellulose and its derivatives are among the excipients frequently used in pharmaceutical industry for various purposes. The main source of cellulose is wood. Thus, the production of cellulose from forest trees is one of the main causes of deforestation. Moreover, trees have a long-life cycle (Ciacco *et al.*, 2008). These necessitate the investigation of another potential source of cellulose from locally available agricultural byproducts.

SCB is an abundant agricultural byproduct on earth. Since sugarcane is a rapidly growing plant, the use of SCB has several advantages over other sources of cellulose. For instance, producing one metric ton of paper from non-virgin materials such as SCB, kenaf and bamboo can save 17 trees, 3.3 cubic meters of landfill space, 360 L of water, 100 L of gasoline, 60 pounds of air pollutants and 10,401 kilowatts of electricity (Poopak and Reza, 2012). In addition, SCB is a residue produced in large quantities by the sugar and alcohol industries and mainly used as a fuel to power the sugar mill and feed to animals. However, the remaining SCB still continues to be a menace to the environment (Laopaiboon *et al.*, 2010; Mothé and de Miranda, 2009; Sun *et al.*, 2004).

SCB cellulose will undoubtedly help to fulfill the local demand of cellulose as it typically offers the advantages of being cheap and plentiful. Furthermore, using agricultural waste as a source of cellulose will prevent deforestation; and utilizing agricultural waste in producing cellulose will avoid environmental pollution that is caused by unexploited SCB. Thus, extraction of cellulose from locally available sources, especially from agricultural wastes, will save foreign currency and play significant role in the sustainable supply of these excipients.

The absence of a research report on cellulose and MCC from SCB in Ethiopia necessitates the need for preparation and characterization of SCB cellulose and MCC. The present study reports the composition, physico-chemical properties of SCB cellulose and MCC. And MCC potential application as a direct compressible pharmaceutical excipient. These data are compared with that of Avicel PH-101. Further, the basis for the explanation of the differences and similarities are presented. Paracetamol, which is a poorly compressible drug, was selected as a model drug for dilution capacity study.

1.12. Research Questions

1. What is the cellulose and MCC yield potential of SCB?
2. What are the physico-chemical characteristics of SCB cellulose and MCC?
3. How does SCB MCC perform when compressed with or without active pharmaceutical ingredient?

1.13. Objectives

1.13.1. General objective

- ✓ To prepare and characterize native and microcrystalline cellulose from SCB and evaluate MCC as a direct compressible pharmaceutical excipient.

1.13.2. Specific objectives

- ✓ To extract and characterize cellulose from SCB;
- ✓ To prepare and characterize MCC from SCB cellulose; and
- ✓ To evaluate the potential of SCB MCC as a directly compressible pharmaceutical excipient.

2. EXPERIMENTAL

2.1. Materials

Fresh SCB (30 kg) was collected from Metehara sugar factory, Metehara, Ethiopia. Paracetamol powder (China Associate Co Ltd, China) was kindly donated by Ethiopian Pharmaceuticals Manufacturing Share Company (EPHARM). Acetic acid (99.9%) (Sigma Aldrich, Germany), Ammonia solution (28%) (Farmitalia Carlo erba reagents S.P.A, Italy), Cupric sulphate pentahydrate (98.5%), Formic acid (85%), Potassium iodide, Silica gel, Xylene (98%, extra pure) and Zinc chloride (97%) (Loba Chemie Pvt. Ltd., India), Diethyl ether (Central drug house Ltd., India), Ethanol (96%) and Sodium chloride (99.8%) (UNI-CHEM, India), Hydrochloric acid (37%) (BDH Chemicals Ltd, England), Hydrogen peroxide (30%) (Carlo erba reagents S.A.S, France), Iodine (Hayashi pure chemical industries Ltd, Japan), Magnesium stearate (Bulvinos Chemicals Ltd, England), MCC (Avicel PH-101), Sodium hydroxide (99.8%) (Alphax Chemical industry, India), and Toluene (99.5%) (Fisher Chemicals, UK) were all used as received.

2.2. Methods

2.2.1. Isolation of cellulose

Extraction of cellulose from SCB was carried out by acid treatment with or without dewaxing following mechanical pretreatment. SCB was cleaned, dried in sunlight, reduced to 1 - 2 cm in a grinder and partially depithed by shaking on a 2 mm orifice screen (Padmadisastra and Gonda, 1989; Sun *et al.,* 2004). One half of dried SCB was treated with toluene/ethanol (2:1, v/v) for 4 hrs at 60 ^{o}C with agitation with solid to liquor ratio of 1:20 w/v. After filtration, it was washed with ethanol repeatedly and dried in an oven (Kottermann® 2711, Germany) at 60 ^{o}C for 16 hrs (Attard *et al.,* 2015; Draman *et al.,* 2016; Kumar *et al*., 2015; Qi *et al.,* 2016).

SCB and dewaxed SCB were treated with a mixture of formic and acetic acid (85% formic acid/ 99.5% acetic acid ratio of 70:30 v/v) at a fiber to liquor ratio of 1:8 w/v in a water bath (GFL, D 3006, Germany) at 100 ^{o}C for 90 min. After filtration by using nylon cloth, fibers were washed with hot distilled water and further delignified by a mixture of performic acid/ peracetic acid (PFA/PAA) solution in a water bath at 100 ^{o}C for 90 min with fiber to liquor ratio of 1:8 w/v.

PFA/PAA solution mixture was prepared in 1:1:2 v/v ratio of 85% formic acid: 99.5% acetic acid: 10% H_2O_2. Delignified fibers were then filtered by using nylon cloth and washed with hot distilled water. Finally, delignified fibers were bleached by treating with solution mixtures of 10% H_2O_2 and 4% NaOH at 100 ^oC for 60 min in a water bath with 1:10 w/v SCB ratio. After filtration by using nylon cloth, bleached fibers were washed with distilled water repeatedly and dried in an oven at 70 ^oC until constant weight was obtained. Thus, sugarcane bagasse cellulose (SCBC) and dewaxed sugarcane bagasse cellulose (DSCBC) were prepared from SCB and dewaxed SCB, respectively. DSCBC and SCBC were ground by a mechanical grinder for subsequent modification (Jahan *et al.,* 2011; Jahan *et al.,* 2014).

2.2.2. Preparation of microcrystalline cellulose

Hydrolysis of cellulose was carried out according to the method described by Battista (1950). 2.5 M HCl was heated to boiling point on a hot plate (Cimarec, Malaysia). DSCBC and SCBC (with cellulose: acid ratio of 1:20 w/v) were added into heated acid and boiled for 30 min at the same temperature with constant stirring using magnetic stirrer. The resulting sugarcane bagasse MCC (SCB-MCC) and dewaxed sugarcane bagasse MCC (DSCB-MCC) were collected by filtration and washed with distilled water. SCB-MCC and DSCB-MCC were then washed with dilute ammonium hydroxide (5%). It was then washed repeatedly with distilled water until acid-free (becomes odorless). Finally, each slurry was further treated by three different techniques:

1. SCB-MCC and DSCB-MCC slurries were filtered and dried in an oven at 70 ^oC to constant weight and pulverized by mortar and pestle and passed through 224 μm mesh size sieve. The resulting MCC preparations were then named as SCB-MCCI and DSCB-MCCI for an oven dried sugarcane bagasse MCC and an oven dried dewaxed sugarcane bagasse MCC, respectively (Battista, 1950, Yuliasmi and Husnita, 2017).
2. SCB-MCC and DSCB-MCC slurries were mechanically sheared in a juice blender, filtered and dried in an oven at 70 ^oC to a constant weight and pulverized by pulverisette (FRITSCH, Germany) to pass through 224 μm mesh size sieve (Battista and Smith, 1962). The resulting MCC preparations were then marked as SCB-MCCOD and DSCB-MCCOD for mechanically sheared oven dried sugarcane bagasse MCC and mechanically sheared oven dried dewaxed sugarcane bagasse MCC, respectively.

3. The slurry of DSCB-MCC and SCB-MCC were prepared (16% w/v of MCC) and mechanically sheared in a juice blender. The slurries were then transferred through a peristaltic pump and fed to the spraying nozzle at pumping rates of 7.5 ml/min into the drying chamber of the apparatus (Tall Form Spray Dryer, FT80, England). The in-let temperature of 175 ^{o}C and out-let temperature of 120 ^{o}C were used. A flow of heated air set at 1 bar aspirated by a pump induces the quick evaporation of the solvent from the drops, leading to the formation of solid particles. The spray dried particles were collected in a reservoir, cooled down to room temperature and stored in a bottle (Peng *et al.*, 2012). The resulting MCC preparations were then labeled as SCB-MCCSD and DSCB-MCCSD, which stand for mechanically sheared spray dried sugarcane bagasse MCC and mechanically sheared spray dried dewaxed sugarcane bagasse MCC, respectively.

2.2.3. Determination of percent yield

The yield of cellulose was calculated based on the dry weight basis by using Eq. 2.1.

$$\text{Yield of cellulose (\%)} = \frac{\text{Weight of cellulose obtained (g)}}{\text{Weight of SCB or dewaxed SCB used (g)}} \text{ X } 100 \cdots\cdots\cdots 2.1$$

Likewise, percent yield of MCC was determined based on the dry weight basis and calculated by using Eq. 2.2.

$$\text{Yield of MCC (\%)} = \frac{\text{Weight of MCC obtained (g)}}{\text{Weight of cellulose used (g)}} \text{ X } 100 \cdots\cdots\cdots\cdots\cdots 2.2$$

The results were expressed as a mean of three individual determinations.

2.2.4. Characterization of cellulose and microcrystalline cellulose

2.2.4.1. Organoleptic characteristics

The color, odor, taste and physical appearance of cellulose and MCC samples were observed.

2.2.4.2. Chemical identification test

Identification test was performed by using iodinated zinc chloride solution. Iodinated zinc chloride solution was prepared by dissolving 20 g of zinc chloride and 6.5 g of potassium iodide

in 10.5 ml of distilled water. 0.5 g of iodine was then added and shaken for 15 min. About 10 mg of sample was placed on a watch glass and dispersed in 2 ml of iodinated zinc chloride solution (USP 30/NF 25, 2007).

2.2.4.3. Determination of degree of polymerization

The DP of cellulose and MCC samples was determined according to the method described by Klemm *et al.* (1998) and Karande *et al.* (2011). The Cuam solution was prepared by dissolving freshly precipitated $Cu(OH)_2$ in aqueous ammonia. First, Cupric Sulphate Pentahydrate (28 g) was dissolved in about 600 ml of distilled water and filtered into a beaker. By adding 14 ml of 25% aqueous ammonia, $Cu(OH)_2$ was precipitated. After settling of the precipitate, a clear solution was decanted and the procedure of settling and decanting was repeated with distilled water until the decanted liquid is free of sulfate ions. The precipitate was then dissolved to 500 ml with NH_4OH (25%) to form Cuam solution. 100 mg of sample was added in the 100 ml of Cuam solution. The mixture was vigorously shaken and then placed in a water bath at 25 ^oC for 5 min. After the sample was completely dissolved in the solvent, viscosity measurement was carried out in an Ostwald Capillary viscometer (BDH, England). The viscosity was calculated from the efflux time of this cellulose solution and of the blank Cuam solution. DP was calculated according to Eq. 2.3.

$$DP = \frac{2000 \text{ x } \eta_{spec}}{c \text{ x } (1 + 0.29 \text{ x } \eta_{spec})} \quad \ldots\ldots 2.3$$

$$\eta_{spec} = \frac{\eta}{\eta_0} - 1 \quad \ldots\ldots 2.4$$

Where η_{spec} is specific viscosity; $\frac{\eta}{\eta_0}$ is relative viscosity; c is concentration in g/l; η_0 is the time required for the solvent to travel from upper graduated mark to the lower graduated mark and η is the time required for the sample to travel from upper graduated mark to the lower graduated mark. The molecular weight of cellulose and MCC samples were determined from DP by using Eq. 2.5. The determination was performed in triplicate.

$$\text{Molecular wieght} = DP \text{ X } 162 \quad \ldots\ldots 2.5$$

2.2.4.4. Moisture content

The moisture content was determined as per the American Society of Testing and Materials International (ASTM, 2003). Three grams of a sample were weighed into weighed, dried Petridish and heated in an oven at a temperature of 105 ^{o}C for about 2 hrs. The sample was then taken out of an oven and weighed. The sample was then replaced in an oven for 30 min and reweighed. This procedure was continued until a mass loss of not more than 5 mg for 30 min drying time. The result was expressed as a mean of three parallel determinations and the percentage of moisture was calculated by Eq. 2.6.

$$\text{Moisture (\%)} = \frac{\text{Mass loss on heating (g)}}{\text{Weight Sample used (g)}} \text{ X } 100 \cdots\cdots\cdots\cdots\cdots\cdots\cdots\cdots\cdots\cdots\cdots\cdots 2.6$$

2.2.4.5. Fourier transform infrared spectroscopy

Fourier transform infrared (FTIR) spectra of cellulose and MCC samples were acquired at room temperature using FTIR spectrophotometer (FTIR-8400S, SHIMADZU, Japan) in transmittance mode. The samples were first ground to reduce the average particle size. Finely ground samples were mixed with liquid paraffin in a mortar and pestle. The sample mixture was then placed onto the face of a potassium bromide plate and the second window was placed on top of the first salt plate. The sandwiched samples were placed in the infrared spectrometer and the spectra were obtained. Each IR spectrum was collected with 20 scans. Scanning was performed between wave numbers 4000 and 500 cm^{-1}. The background spectrum was collected before running each sample.

2.2.4.6. X-ray diffraction

The cellulose and MCC samples were oven dried at 105 ^{o}C for 1 hr and sieved with 224 μm mesh size sieve. The samples were then placed in the cavity of a disc sample holder of the diffractometer. The measurements were done using a diffractometer (XRD 7000S, SHIMADZU, Japan) operating in the 2θ mode using computer software. A Cu target tube operated at a power setting of 40 kV (30 mA) in the range of 10 - 40^{o} of 2θ at a speed of 3^{o}/min. Percentage crystallinity index (CrI %) was calculated by using Segal equation (Eq. 2.7).

$$\text{CrI}\ (\%) = \frac{(I_{002} - I_{am})}{I_{002}}\ \text{X}\ 100 \ldots\ldots\ldots\ldots\ldots\ldots\ldots 2.7$$

Where I_{002} represents crystalline material and I_{am} represents the amorphous material (Ahvenainen *et al.,* 2016; Gurgel *et al.,* 2012; Leão *et al.,* 2017; Segal *et al.,* 1959).

The apparent crystallite size (L) was estimated through the use of the Scherrer equation (Eq. 2.8).

$$L = \frac{K\lambda}{\beta \text{Cos}\theta} \ldots\ldots\ldots\ldots\ldots\ldots\ldots\ldots\ldots\ldots\ 2.8$$

Where K is a constant with the value of 0.94, λ is the X-ray wavelength (0.1542 nm for Cu Ka radiation), β is the half-height width of diffraction band and Θ is the Bragg angle corresponding to the (002) plane (Poletto *et al.,* 2014; Popescu *et al.,* 2011).

2.2.4.7. Morphological characterization

The morphologies of cellulose and MCC were studied using a scanning electron microscope (JSM-IT300, JEOL, Japan). The scanning electron micrographs were taken at an accelerating voltage of 20 KV. The samples were then viewed and photographed.

2.2.4.8. Thermal analysis

The thermal properties of cellulose and MCC were determined using a thermogravimetric analyzer (DTG-60H, SHIMADZU, Japan) for TGA and differential thermal analysis (DTA). The samples were heated from room temperature to 700 ^{o}C with a scanning rate of 10 ^{o}C/min under a nitrogen atmosphere. The weight of a sample was in range 10 - 16 mg.

2.2.5. Determination of chemical composition of microcrystalline cellulose

2.2.5.1. Determination of water-soluble substances

Five grams of MCC were added to 80 ml of distilled water and shaken for 10 min by shaker (Heidolph Unimax 1010, Germany). After filtration with filter paper, the filtrate was transferred to a beaker and evaporated to dryness without charring at 105 ^{o}C for 90 min on a hot plate. Finally, the beaker was weighed, and the weight of the residue was recorded as the difference

between the weights of an empty beaker and the beaker with the residue. All results are the mean of three parallel determinations (USP 30/NF 25, 2007).

2.2.5.2. Determination of ether-soluble substances

Five grams of MCC were placed in a chromatographic column to which sufficient amount of peroxide-free ether was passed through the column (Sinta Glass 1, England). The eluate was evaporated to dryness in a previously dried and tared beaker. The residue was dried at 105 ^{o}C for 30 min, cooled and weighed. The difference between the blank and sample eluate residues was taken as the amount of ether-soluble matter in the sample. Triplicate studies were conducted and mean value of ether-soluble matter was then calculated (USP 30/NF 25, 2007).

2.2.5.3. Ash value

Three grams of MCC powder were poured into a crucible, previously washed, dried at 100 ^{o}C for 30 min, and then cooled in a desiccator filled with silica gel, for 30 min and weighed. The crucible with its content was then gently heated until it was completely charred. Subsequently, the samples were put in a furnace at 550 ^{o}C for 2 hrs. The crucible with its content was allowed to cool in a desiccator and weighed. The weight of the ash was then determined and the percentage ash value calculated by using Eq. 2.9.

$$\text{Ash value } (\%) = \frac{W_A}{W_S} \text{ X } 100 \text{ . .. . .2.9}$$

Where W_A and W_S are weight of ash formed and initial weight of MCC powder, respectively.

2.2.5.4. pH determination

Five grams of MCC were shaken with 40 ml of water for 20 min, and allowed to stand. Then the pH of supernatant was determined by using pH meter (JENWAY, 3505, UK). All results are the mean of three parallel determinations (USP 30/NF 25, 2007).

2.2.6. Characterization of powder properties of microcrystalline celluloses

2.2.6.1. Particle size analysis

Particle size distribution analysis was performed using a Malvern Mastersizer 2000 laser diffraction particle size analyzer (Malvern Instruments Ltd, Worcestershire, WR14 1XZ, UK). The analysis was done under these conditions: Range (0.05–900 µm, 300RF); active beam length (2.4 mm); sample unit (MS1: Small Volume Sample Dispersion Unit); Polydisperse; standard-wet, Presentation (3OHD). A small amount of MCC was dispersed in distilled water (was already soaking into the sample port of the instrument) until an obscuration of 15 - 20% was recorded. The mean volume particle size distribution, mean particle size, specific surface area and percentile distribution of samples were obtained with Mastersizer S, PSS0003-01 software (2002). Determinations were done in triplicates.

2.2.6.2. Densities and related properties

Bulk density

Thirty grams of MCC powder were introduced into a 250 ml measuring cylinder. The cylinder was then lightly tapped twice to collect all the powder sticking on the wall of the cylinder. The volume was then read directly from the cylinder and used to calculate the bulk density. Bulk density (ρb) was determined as a mean of three measurements by using Eq. 2.10.

$$\rho b = \frac{m}{V_b} \quad \ldots\ldots\ldots\ldots\ldots\ldots 2.10$$

Where m is the weight of the powder and V_b is bulk volume.

Tapped density

Thirty grams of MCC powder were tapped in graduated measuring cylinder 10, 500, and 1250 times and the corresponding volumes V_{10}, V_{500}, and V_{1250} were read to the nearest graduated unit using tapped densitometer (ERWEKA, Germany). If the difference between V_{500} and V_{1250} was less than or equal to 2 ml, V_{1250} is the tapped volume. If the difference between V_{500} and V_{1250} exceeds 2 ml, repeat in increments such as 1250 taps, until the difference between

succeeding measurements was less than or equal to 2 ml. Tapped density (ρt) was determined as a mean of three measurements by using Eq. 2.11 (USP <616>, 2015).

$$\rho t = \frac{m}{V_t} \ldots\ldots\ldots\ldots\ldots\ldots 2.11$$

Where m is the weight of the powder and V_t is the tapped volume.

Carr's index and Hausner ratio

Carr's index (% compressibility) and Hausner ratio were calculated by using Eq. 2.12 and 2.13, respectively.

$$\text{Carr's index (\%)} = \frac{(\rho_t - \rho_b)}{\rho_t} X\ 100 \ldots\ldots\ldots\ldots\ldots 2.12$$

$$\text{Hausner ratio} = \frac{\rho_t}{\rho_b} \ldots\ldots\ldots\ldots\ldots\ldots 2.13$$

True density

True density was determined by liquid displacement method using xylene as immersion fluid. MCC sample was placed in a pycnometer, closed and weighed (the weight of the empty pycnometer and of the pycnometer filled with xylene is known). Sufficient xylene was added to wash down and overlay the sample. After 10 min, the sediment MCC was stirred with a small glass-stirring rod to release entrapped air. When the evolution of minute air bubbles through the supernatant xylene layer had stopped, the stirrer was removed and rinsed into the pycnometer with several milliliters of xylene. The sample was allowed to settle, the pycnometer filled with xylene and the meniscus was adjusted. True density (g/ml) was calculated by using Eq. 2.14. True density was measured as a mean of three measurements.

$$\rho = \frac{(W_1 \times SG)}{[(W_1 + W_2) - W_3]} \ldots\ldots\ldots\ldots\ldots 2.14$$

Where ρ = true density of MCC; W_1= weight (g) of MCC, W_2= weight (g) of the pycnometer filled with xylene, W_3= weight (g) of pycnometer with sample plus xylene, and SG = specific gravity of xylene (g/ml) (~0.862).

Powder porosity

Powder porosity was determined by using Eq. 2.15.

$$\varepsilon\,(\%) = (1 - \frac{\rho b}{\rho})\ \text{X100}. \ldots\ldots\ldots\ldots\ldots\ldots\ldots 2.15$$

Where ρb is the bulk density, ρ is the true density and ε is the porosity (Kothari *et al.*, 2002). The results were the mean of three determinations.

2.2.6.3. Hydration capacity

A 1 g of MCC was placed in each of four 15 ml plastic centrifuge tubes and 10 ml of distilled water was added and then stoppered. The tube was shaken vigorously and allowed to stand for 20 min, with shaking every 5 min. It was then centrifuged for 15 min at 2000 revolution per minute (rpm) in Beckman Coulter centrifuge (Allegra 64R, USA). The supernatant was decanted and the tube was drained for 10 min at a 45^{o} angle. The tube was weighed, and the gain in weight was expressed as a ratio. The hydration capacity was determined by using Eq. 2.16.

$$\text{Hydration Capacity} = \frac{W_2}{W_1} \ldots\ldots\ldots\ldots\ldots\ldots 2.16$$

Where W_2 is the weight of hydrated MCC and W_1 is the initial weight of MCC (Gbenga and Fatimah, 2014; Umeh *et al.*, 2014).

2.2.6.4. Moisture sorption pattern

Pyrex desiccators containing distilled water, a saturated solution of NaCl or appropriate concentrations (24.66, 31.58 and 40.00 %) of NaOH were prepared to provide different (100, 75.6, 60, 40 and 20%, respectively) RH chambers and stored at room temperature. Samples of MCC were pre-dried in an oven for 4 hrs at 105 ^{o}C. 2 g of each MCC sample was placed in a plastic plate (dried and weighed) and transferred to the RH chamber. Samples were equilibrated for 4 weeks at room temperature. The weights after 4 weeks were recorded and the moisture uptake of each sample was calculated as the weight difference of the MCC samples before and after equilibration in a given RH chamber. Water sorption capacities of the MCC samples were expressed as percent moisture uptake. Results were expressed as a mean of three parallel determinations (Sun, 2008).

2.2.7. Drug-excipient interaction study

Possible drug-excipient interaction was investigated by FTIR spectroscopy as described in Section 2.2.4.5. The FTIR spectra of paracetamol powder alone and its physical mixture with MCC sample (1:1) at 4000 - 500 cm^{-1} were recorded using FTIR-8400S, Shimadzu, Japan.

2.2.8. Preparation of tablets

Tablets containing plain SCB-MCCOD, SCB-MCCSD, DSCB-MCCOD, DSCB-MCCSD and Avicel PH-101 were compressed in a rotary tablet compression machine (ECO PRESS 200, India) fitted with 11 mm punches to study mechanical properties. Each MCC compact were produced with 400 mg size by compressing the powders at different compression force adjusted to give tablets (formulated using the standard unlubricated Avicel PH-101) crushing strength of 50 (CF1), 75 (CF2), 100 (CF3), 125 (CF4) and 150 (CF5) N.

Lubricant sensitivity of SCB-MCCOD, SCB-MCCSD, DSCB-MCCOD, DSCB-MCCSD and Avicel PH-101 were assessed as a method described by Rojas *et al.* (2013). Binary blends of excipient : lubricant (99.5:0.5) were made in a Turbula® mixer (Willy A. Bachofen AG, Turbula® 2TF, Basel, Switzerland) for 5 min. Lubricated and unlubricated compacts (400 mg) of 11 mm in diameter were compressed with a rotary tablet compression machine at constant pressure adjusted to give plain Avicel PH-101 tablets with a hardness of 120 N.

Dilution capacity of SCB-MCCOD, SCB-MCCSD, DSCB-MCCOD, DSCB-MCCSD and Avicel PH-101 was evaluated as per the method described by Kuentz and Leuenberger (2000) and Rojas *et al.* (2013). Mixture of 25, 40, 55 and 70% w/w of paracetamol and the corresponding amount of MCC powders were blended in a Turbula® mixer (Willy A. Bachofen AG, Turbula® 2TF, Basel, Switzerland) for 10 min at 45 rpm. The blend was then compressed into tablets with 400 mg size at a fixed compression force on a rotary tablet compression machine which was fitted with 11 mm diameter punches.

2.2.9. Evaluation of tablets

2.2.9.1. Lubricant sensitivity ratio

The lubricant sensitivity ratio (LSR) was measured as the breaking strength ratio of compacts and calculated according to Eq. 2.17.

$$LSR = \frac{(T_0 - T_l)}{T_0} \quad \ldots\ldots\ldots\ldots\ldots\ldots\ldots\ldots \quad 2.17$$

Where T_0 and T_l are the breaking strengths of unlubricated and lubricated compacts, respectively (Mužíková and Nováková, 2007; Rojas *et al.,* 2013).

2.2.9.2. Weight and thickness

From each batch, twenty tablets were randomly selected and weighed individually on the analytical balance and then the average weight and standard deviation was calculated. Tablet thickness and diameter (fixed 11 mm) were measured using a sliding caliper scale (Nippon Sokutei, Japan).

2.2.9.3. Crushing strength

After 24 hrs of production, ten tablets were taken from each batch and the crushing strengths of the tablets were determined using hardness tester (Caleva, THT2, England).

2.2.9.4. Tensile strength

The radial tensile strength was calculated using the data obtained from crushing strength, diameter and thickness of tablets according to Eq. 2.18.

$$\sigma x = \frac{2F}{\pi DT} \quad \ldots\ldots\ldots\ldots\ldots\ldots\ldots\ldots\ldots\ldots \quad 2.18$$

Where σx is the tensile strength, F is the crushing strength, D is the diameter of the tablet, and T is the tablet thickness.

2.2.9.5. Friability

Ten tablets of known weights from each batch were placed in a friability tester (ERWEKA, TAR 20, Germany) and subjected to combined effects of abrasion and shock by placing them in the plastic chamber that revolves at 25 rpm for 4 min. The tablets were then dedusted and weighed, and the percent loss in weight was calculated as friability.

2.2.9.6. Disintegration test

Disintegration test was carried out according to USP 30/NF 25 specification (2007). Six tablets of known weight from each batch were placed in a disintegration tester (ERWEKA, DT504, Germany) filled with distilled water at 37 ± 2 ^{o}C. The tablets were considered completely disintegrated when all the particles passed through the wire mesh.

2.2.9.7. Construction of UV calibration curve

A stock solution containing 200 µg/ml of paracetamol in phosphate buffer of pH 5.8 was prepared. From this stock solution, nine different concentrations (3.5, 5, 6.5, 8, 9.5, 11, 12.5, 14, and 15.5 µg/ml) were prepared. The UV absorbance readings of these solutions were measured at 243 nm using UV/VIS SPECTROMETER (T92+, UK). Phosphate buffer (pH = 5.8) was used as a blank. The absorbance versus concentration of the solutions was plotted, and a linear regression equation and correlation coefficient were obtained.

2.2.9.8. *In-vitro* drug dissolution test

The dissolution test was done according to the USP 30/NF 25 (2007) specification using dissolution apparatus Type II (ERWEKA, DT600, Germany) stirred at 50 rpm with 900 ml phosphate buffer (pH 5.8) as the dissolution medium at 37 ± 0.5 ^{o}C. Five ml aliquots of the dissolution medium were removed at 5, 10, 15, 20, 30, 45 and 60 min and filtered using filter paper. An equal amount of fresh medium kept at the same temperature was transferred into the dissolution vessel to maintain a sink condition. One ml of the filtered samples was diluted to 25 ml and absorbance readings were taken with UV/VIS SPECTROMETER at 243 nm. Phosphate buffer (pH = 5.8) was used as a blank. All the necessary corrections for dilution were made when calculating the drug content.

2.2.10. Statistical analysis

Statistical analysis was carried out using Analysis of Variance (ANOVA) with statistical software Origin 9.6 (OriginLabTM Corporation, USA). Tukey multiple comparison test was used to compare the individual difference in the physico-chemical and tablet properties of the MCCs. At 95% confidence interval, p values less than 0.05 were considered statistically significant. The results are reported as mean and standard deviation.

3. RESULTS AND DISCUSSION

3.1. Physico-chemical Properties of Cellulose and Microcrystalline Cellulose

3.1.1. Organoleptic characteristics and chemical identification test

The organoleptic properties of the prepared cellulose and MCC samples fulfilled USP/NF specification (USP 30/NF 25, 2007) (Table 3.1). Both non-dewaxed and dewaxed preparations had white color though dewaxed preparations had higher degree of whiteness. Identification tests were performed for all cellulose and MCC samples and all samples turned to violet-blue color confirming the presence of cellulose and MCC.

Table 3.1: Organoleptic Characteristics of SCBC, DSCBC, SCB-MCC and DSCB-MCC.

Organoleptic Characteristic	**SCBC**	**DSCBC**	**SCB-MCC**	**DSCB-MCC**
Color	White	White	White	White
Odor	Odorless	Odorless	Odorless	Odorless
Taste	Tasteless	Tasteless	Tasteless	Tasteless
Physical appearance	Fibrous	Fibrous	Fine Powder	Fine powder

3.1.2. Percent yield of cellulose and microcrystalline cellulose

The cellulose yield primarily depends on the method of cellulose extraction. Cellulose yields on the dry weight basis were found to be 42.8% ± 1.1 and 43.5% ± 0.5 from non-dewaxed and dewaxed SCB, respectively. The yield of DSCBC is slightly higher ($P > 0.05$) than yield of SCBC. In addition, DSCBC yield is comparable to the values reported by Sun *et al.* (2004), two types of cellulose were isolated from dewaxed SCB by treating with mixture of acetic acid (80%) and nitric acids (70%) at 110 °C and 120 °C for 20 min found cellulose yields of 43.6% and 43%, respectively.

The recovery yields of acid-hydrolyzed SCBC and DSCBC were 70% ± 0.9 (SCB-MCCI) and 81% ± 0.57 (DSCB-MCCI), respectively. This significantly higher ($P < 0.05$) DSCB-MCCI yield can be explained by the dewaxing step in extraction procedure, which increases purity by partially removing amorphous region (lignin and waxy materials) and preserving crystal region of cellulose. The yields of SCB-MCCI from SCB and DSCB-MCCI from dewaxed SCB were found to be 29.97% ± 1.56 and 35.24% ± 0.81, respectively.

Mechanical shearing of MCC slurry was found to increase the MCC yields, and improve the appearance and powder properties of MCC. The SCB-MCCOD and DSCB-MCCOD yields were found to be 78% ± 1.07 and 83% ± 0.74, respectively. This might be due to mechanical shearing of slurry which causes disaggregation of MCC particles (Battista and Smith, 1962). A Study by Adedokun *et al.* (2014) also revealed that yields from sugarcane were 40% and 70% of α-cellulose and MCC, respectively. Thus, sourcing cellulose and MCC from SCB appeared very cost-effective.

3.1.3. Degree of polymerization

DP is defined as the number of repeating units present in a polymer. DP of cellulose primarily depends on the method of isolation. The viscosity average DP values of the cellulose and MCC samples were determined from their viscosity in Cuam solution. The viscosity is a measure of the hydrodynamic volume occupied by a molecule and capacity of a polymer molecule to enhance the viscosity. The decrease in viscosity indicates a decrease in the hydrodynamic volume in the macromolecular chain (Bezerra *et al.*, 2016; Sun *et al.* 2004; Trache *et al*., 2016).

DP and molecular weight values of SCBC and DSCBC are presented in Table 3.2. DSCBC had a higher value of average DP and molecular weight than SCBC. The reason for these higher values is presumably because of the removal of some more amounts of low molecular weight hemicelluloses during extraction procedures, thereby increasing the viscosity and molecular weight (Liu *et al.*, 2006). Various studies indicated that SCB cellulose prepared by different isolation methods have average DP values in the range of 560 - 2238.2 (Huang *et al.*, 2012; Liu *et al.*, 2006; Sun *et al.*, 2004). The low DP values of cellulose preparations in this study possibly resulted from the use of formic acid, which cause hydrolysis of polysaccharides during pulp cooking process, and the longest duration of treatment. Chemical hydrolysis in the production of pulp with an acidic environment causes degradation reaction, and it is distinctive to glycoside-glycoside bond, glycosidic di-oligo, and polysaccharides. Accordingly, a high concentration of formic acid did not only dissolve the lignin but also reduce the DP of cellulose (Hidayati *et al.*, 2017). Correspondingly, Sun *et al.* (2004) prepared cellulose from dewaxed SCB which had DP

value of 822.5 by treating in an acidic environment (with 80% acetic acid and 70% nitric acid mixture) at 120 ^{o}C for short duration (20 min).

MCC was prepared by hydrolyzing cellulose with 2.5 M HCl. Table 3.2 also shows the DP values of MCC prepared from SCBC and DSCBC, and Avicel PH-101. The DP value obtained for MCC preparations was moderately higher than that of Avicel PH-101. El-Sakhawy and Hassan (2007) prepared MCC from SCB with DP of 299 and 317 by using H_2SO_4 and HCl, respectively while Huang *et al.* (2012) prepared MCC with DP of 189 by degradation under subcritical Water/CO_2. By mechanical shearing, DP values of the prepared MCC was slightly decreased. Furthermore, oven dried MCC preparations had slightly lower DP value than respective spray dried MCC preparations. This could have resulted from pulverization after oven drying. However, DP values of all MCC preparations were within acceptable range (< 350) (Thoorens *et al.*, 2014).

Table 3.2: DP and molecular weight of SCBC, DSCBC, SCB-MCCI, SCB-MCCOD, SCB-MCCSD, DSCB-MCCI, DSCB-MCCOD, DSCB-MCCSD and Avicel PH-101.

Samples		**DP**	**Molecular weight (g/mol)**
Cellulose	SCBC	580.56	94050.72
	DSCBC	592.75	96025.50
MCC	SCB-MCCI	238.09	38569.93
	SCB-MCCCOD	230.10	37276.20
	SCB-MCCSD	232.50	37665.00
	DSCB-MCCI	256.14	41495.33
	DSCB-MCCOD	249.08	40350.96
	DSCB-MCCSD	251.40	40726.80
	Avicel PH-101	220.94	35792.28

3.1.4. Fourier transform infrared analysis

FTIR spectroscopy is a quick and simple technique for identifying compounds. The FTIR spectrum of a given compound is unique. The FTIR spectral results are displayed in Figures 3-1, 3-2, 3-3, 3-4 and 3-5. The band absorbances in cellulose and MCC have been assigned and matched with the vibrational modes of the chemical bonds and the structures of cellulose and MCC molecules by many researchers. Cellulose and MCC have similar major peaks because both have same functional groups.

The FTIR spectra of cellulose and MCC samples are described by ten main bands, with maximum absorbance peaks around 3300, 2915, 2852, 1455, 1374, 1320, 1172, 1113, 1055 and 896 cm^{-1} (Adel *et al.*, 2010; Kumar *et al.*, 2015; Liu *et al.*, 2006; Sun *et al.*, 2005) and all these peaks were observed in SCBC, DSCBC, SCB-MCC, DSCB-MCC and Avicel PH-101.

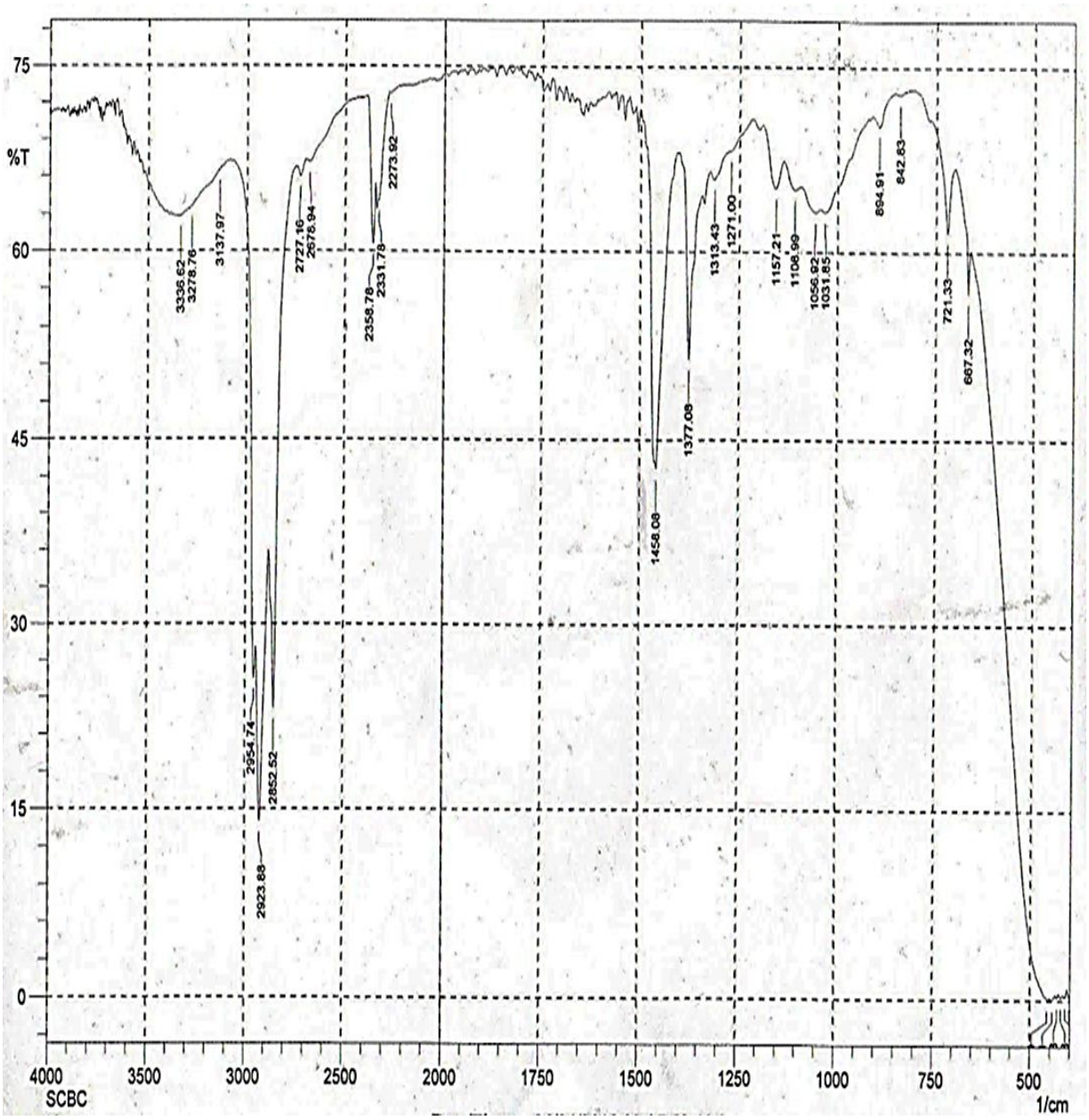

Figure 3-1: FTIR spectrum of SCBC.

FTIR spectra of all samples exhibited a broad band in the region of 3500-3200 cm^{-1}, corresponding to the O–H stretching vibration of the OH groups in cellulose molecules. Peaks

at 2923 and 2854 cm^{-1}, found in all samples, are characteristics of asymmetric and symmetric C–H stretching vibration (Mandal and Chakrabarty, 2011). The absorption band at 1623 cm^{-1} in DSCBC FTIR spectrum is presumably due to the bending mode of the absorbed water (Rosli *et al.*, 2013). The peak at 1458 and 1377 cm^{-1}, reflected in all samples, are attributed to symmetric deformation and asymmetric deformations of C–H_2 group of cellulose molecules, respectively. The peak at 1313 cm^{-1} in SCBC, SCB-MCC and Avicel PH-101 originates from CH_2 wagging vibration at C-6 position, C–C and C–O skeletal vibrations, whereas in DSCBC and DSCB-MCC it is found at 1315 cm^{-1} (Sun *et al.*, 2005).

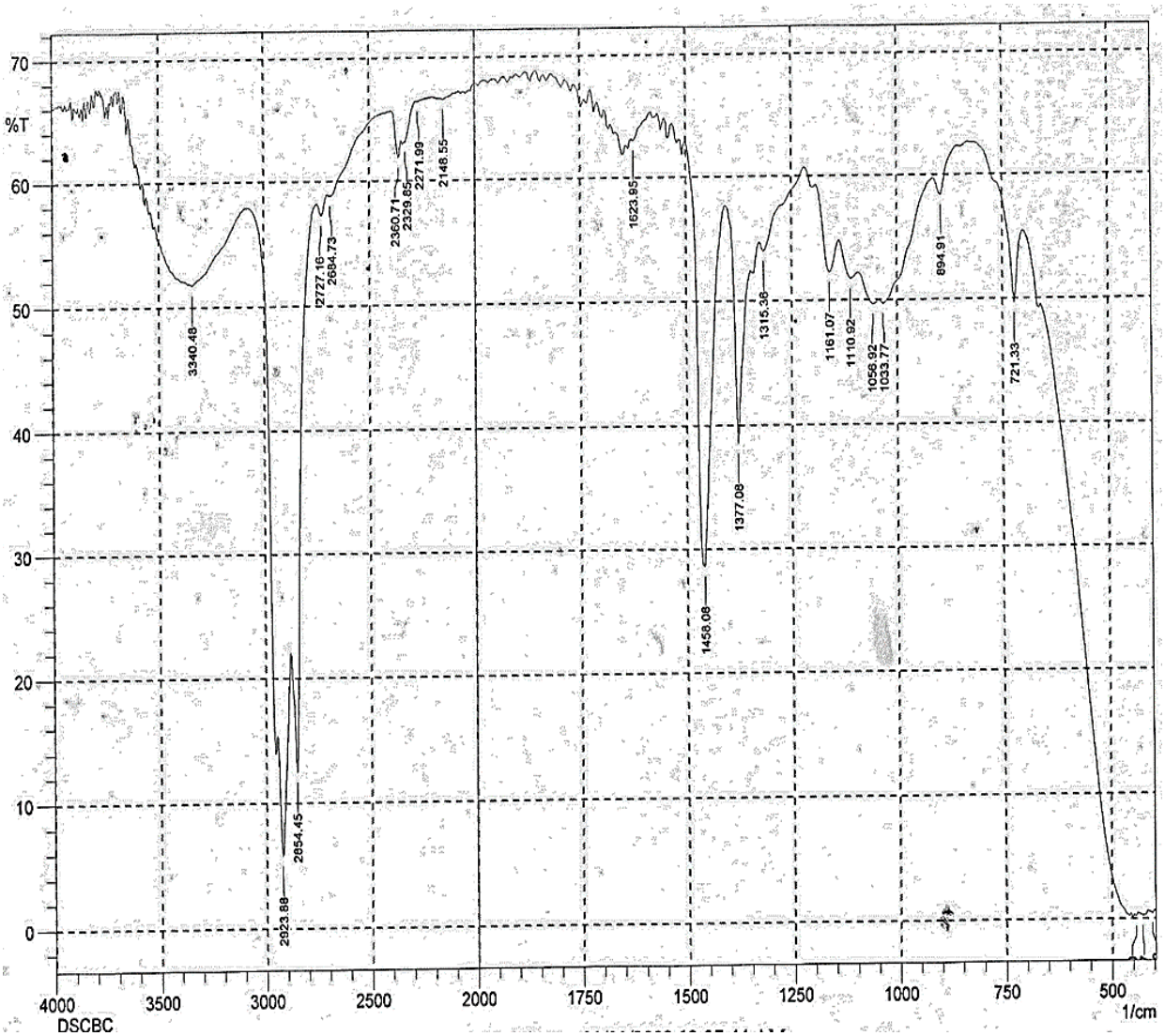

Figure 3-2: FTIR spectrum of DSCBC.

The peak at 1161 cm^{-1} in DSCBC, DSCB-MCC and Avicel PH-101 molecules is attributed to C-O-C asymmetrical stretching of β-1,4-glycosidic linkage, whereas it is found around 1157 cm^{-1} and 1159 cm^{-1} in SCBC and SCB-MCC, respectively (Mothé and Miranda, 2009). A peak at 1110,1108 and 1112 cm^{-1} in dewaxed, non-dewaxed and Avicel PH-101, respectively, represents C–OH skeletal vibration (Liu *et al.*, 2006). The peak observed in the spectra of all samples around 1055 cm^{-1} originates from C–O–C pyranose ring (antisymmetric in phase ring) stretching vibration (Sun *et al.*, 2004).

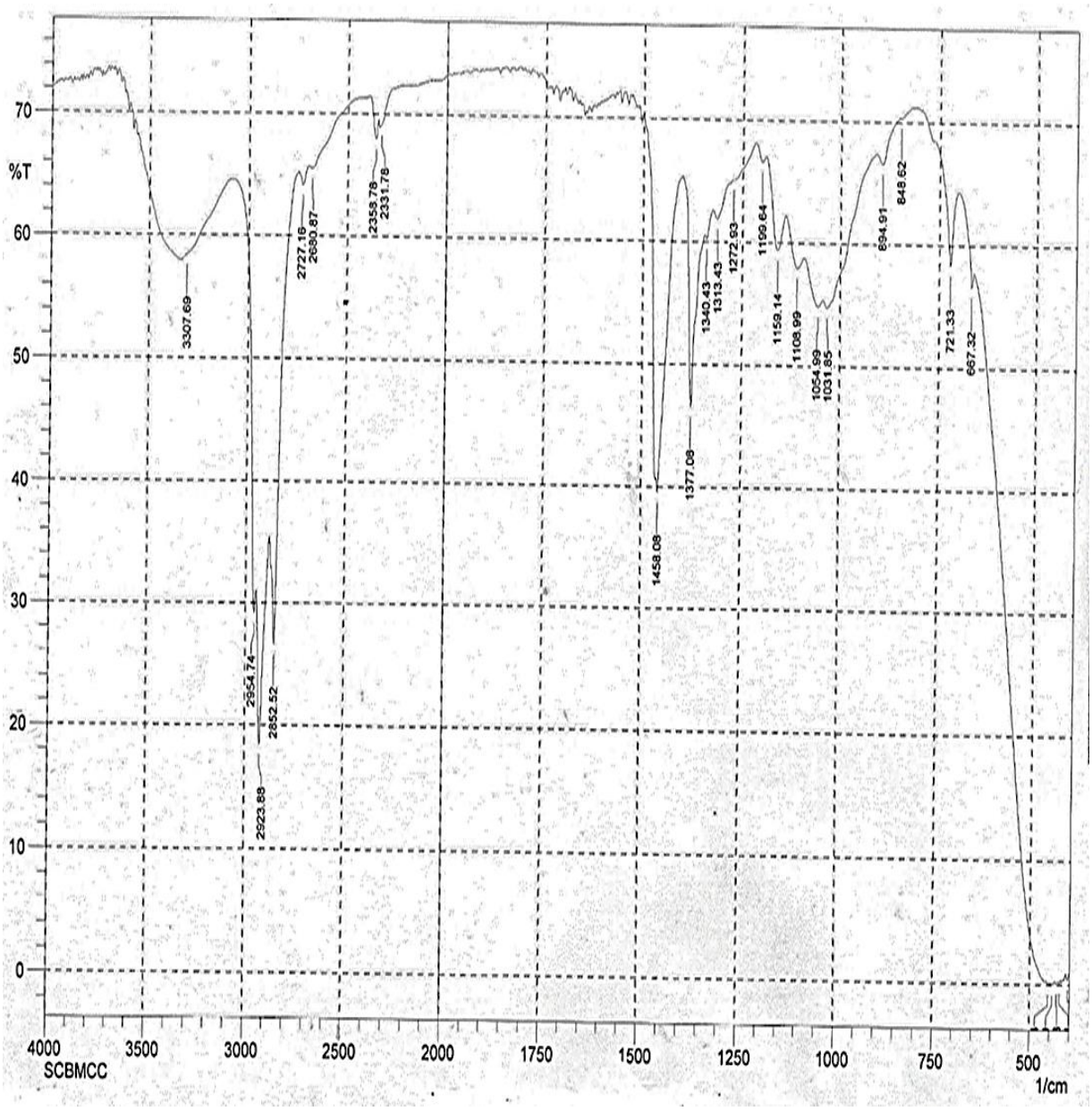

Figure 3-3: FTIR spectrum of SCB-MCC.

A small sharp peak observed at 895 cm^{-1} is associated with the glycosidic C_1–H deformation with ring vibration contribution and O–H bending, which is characteristic of β-glycosidic linkages between glucose in cellulose (Alemdar and Sain 2008; Kumar *et al.,* 2015).

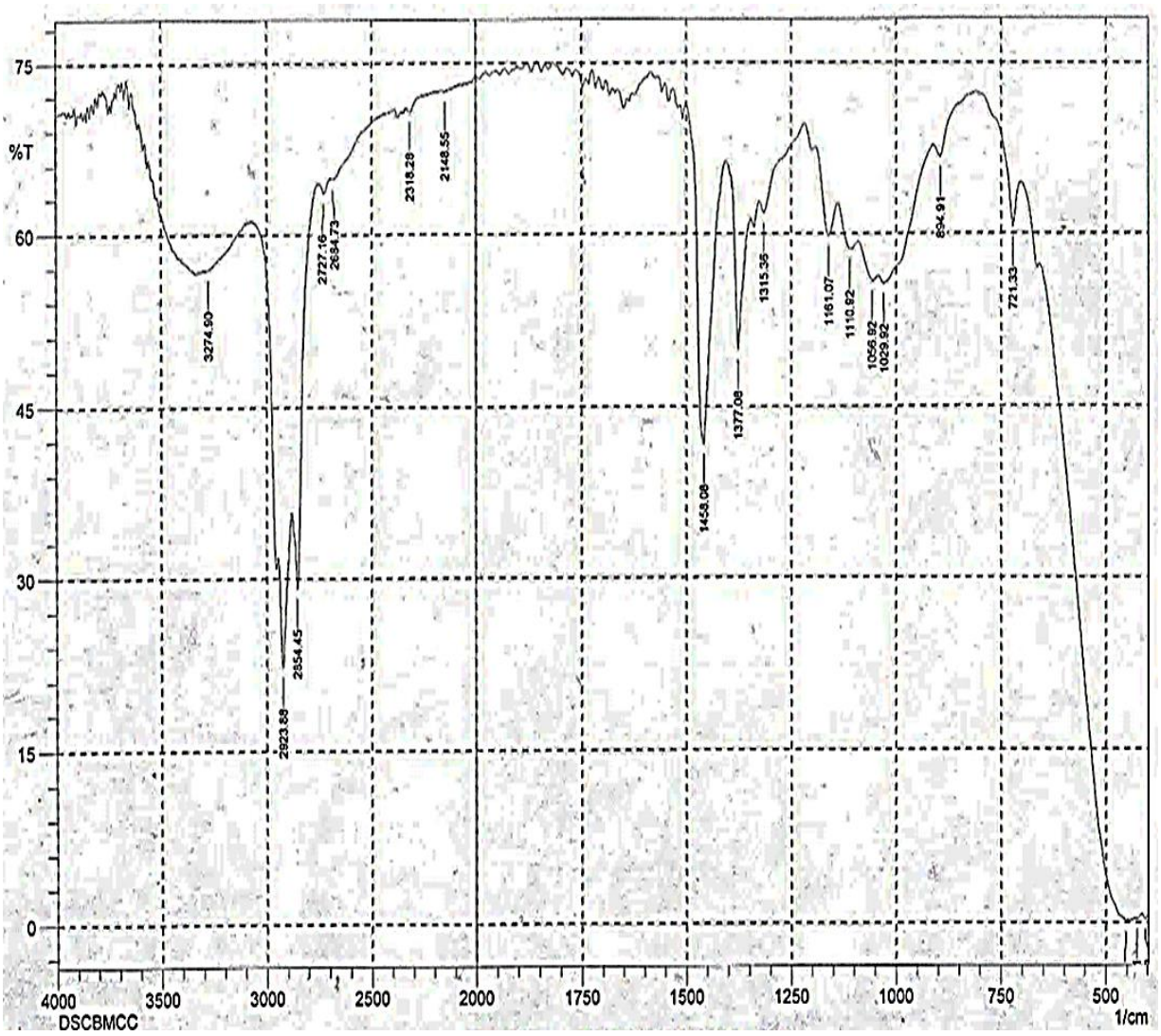

Figure 3-4: FTIR spectrum of DSCB-MCC.

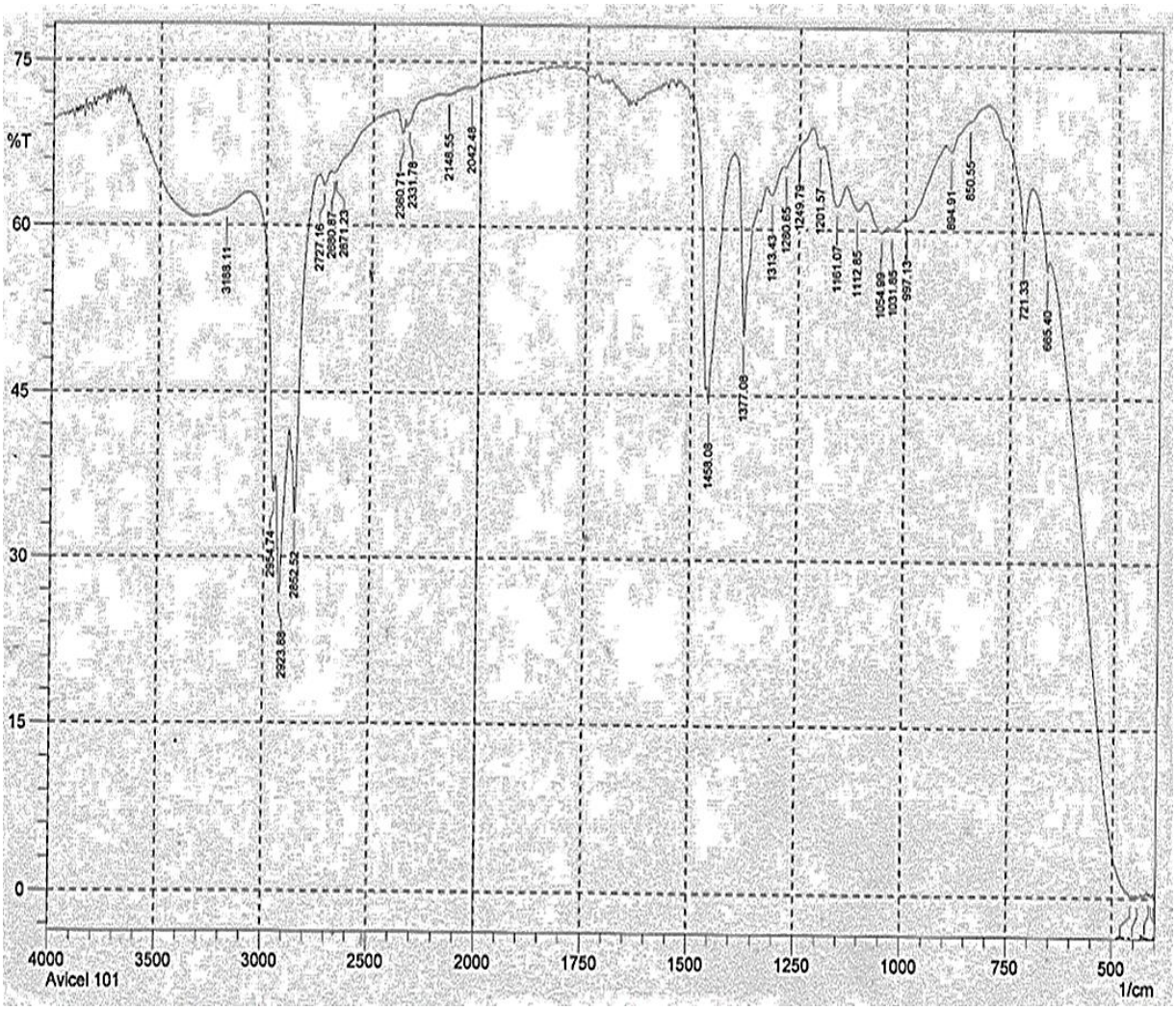

Figure 3-5: FTIR spectrum of Avicel PH-101.

3.1.5. X-ray Diffraction studies

XRD analysis was carried out in order to determine the changes of the crystalline and amorphous regions of cellulose and MCC samples. The XRD patterns of different cellulose and MCC samples are shown in Figure 3-6, 3-7 and 3-8.

XRD patterns of cellulose and MCC samples always show three typical diffraction peaks around 15.6, 22.3, and 34.5. These peaks correlate with 110, 002, and 004 lattice planes, respectively, which are believed to represent the typical cellulose Iβ structure (Chen *et al.,* 2011; Ho *et al.*, 2011). Except cellulose preparations, all MCC preparations exhibited similar peak position and are composed of cellulose Iβ. However, cellulose preparations were also present in the form of

cellulose Iβ, and not cellulose II, which arises from the fact that there is no doublet in the intensity of the main peak (002) (Morán *et al.*, 2008).

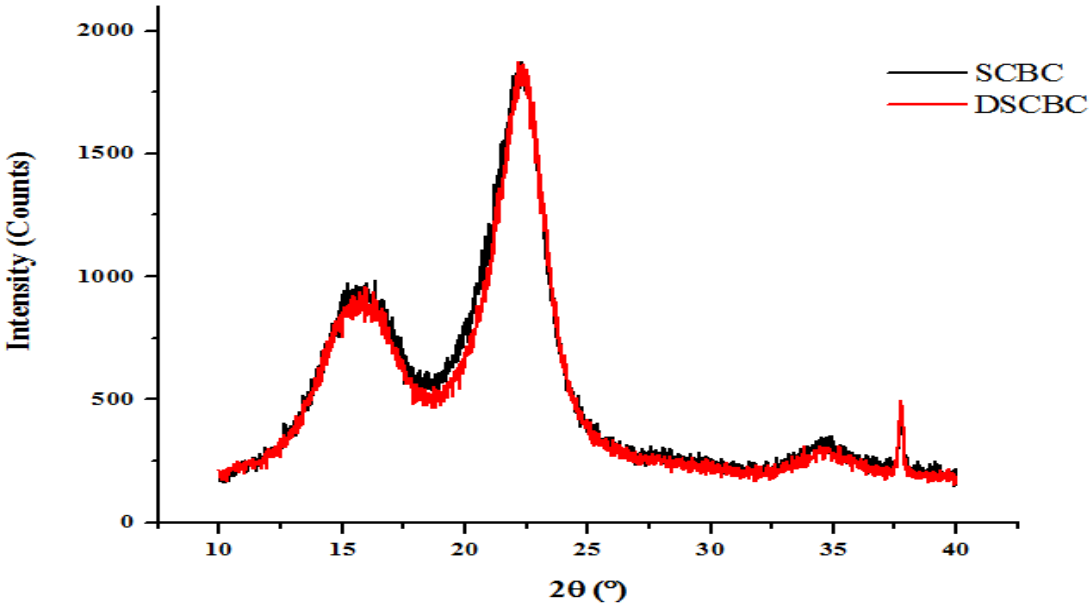

Figure 3-6: XRD patterns of SCBC and DSCBC.

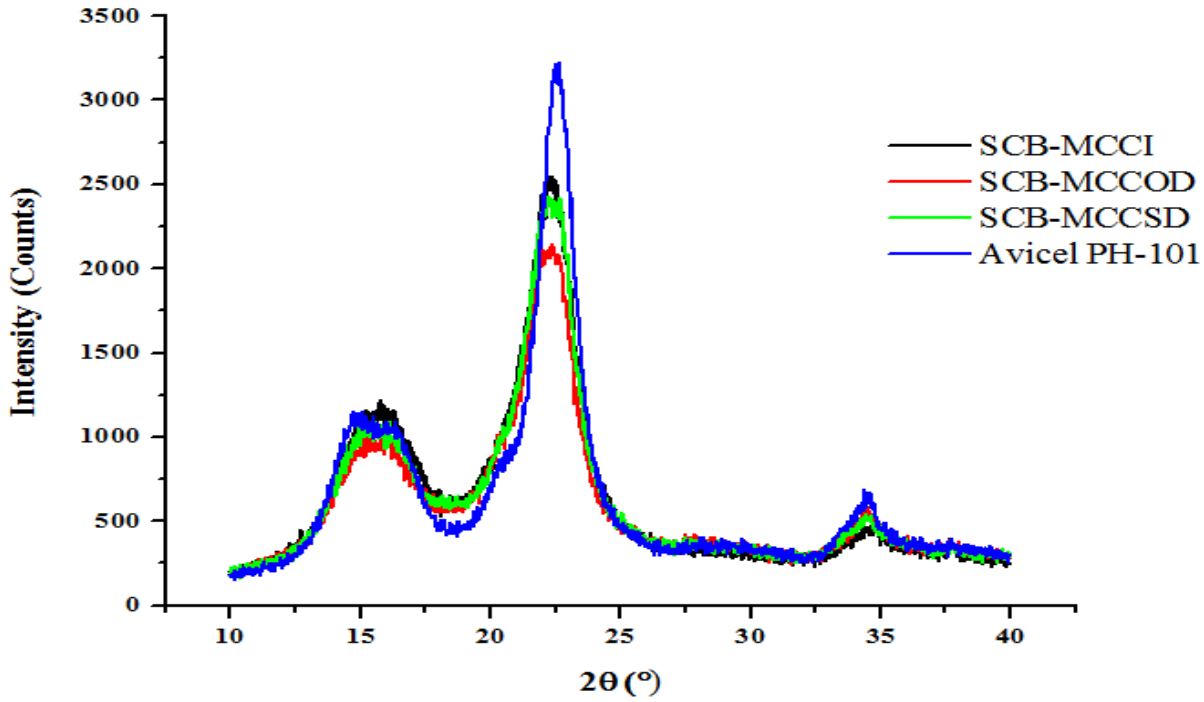

Figure 3-7: XRD patterns of SCB-MCCI, SCB-MCCOD, SCB-MCCSD and Avicel PH-101.

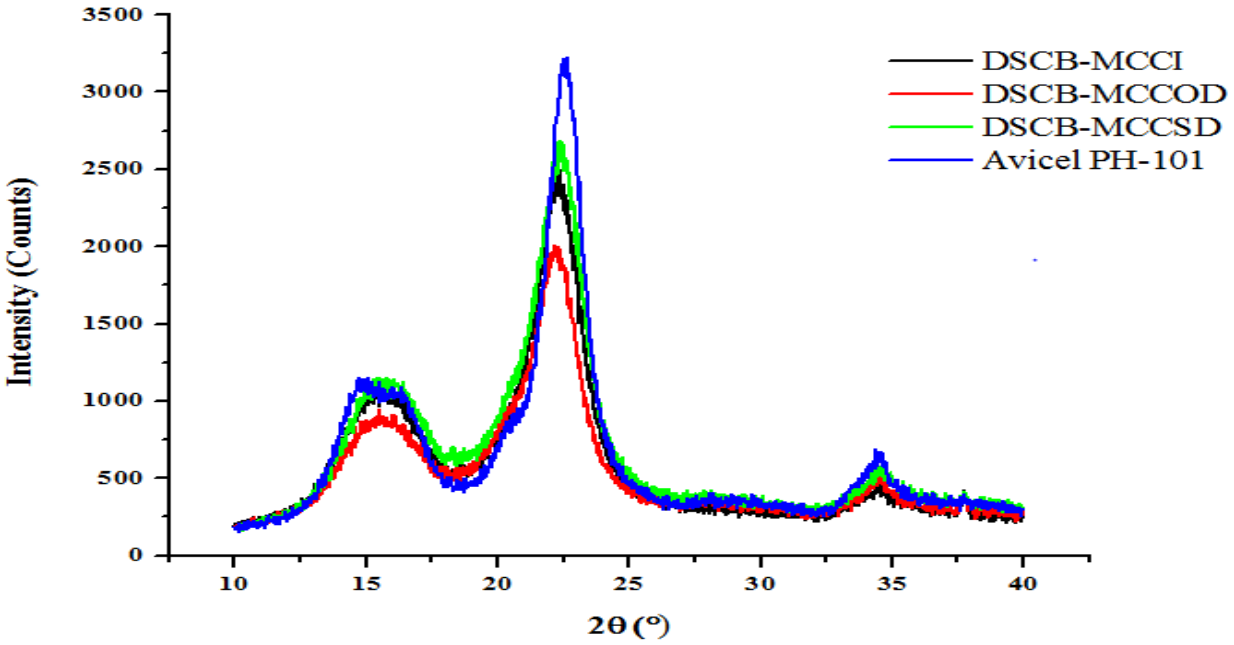

Figure 3-8: XRD patterns of DSCB-MCCI, DSCB-MCCOD, DSCB-MCCSD and Avicel PH-101.

The values of crystallinity index were calculated by using the empirical Segal equation and are summarized in Table 3.3. All values of crystallinity index were determined after subtraction of a baseline. Depending on the origin of the cellulose source and the processing variables used in their manufacture, the degree of crystallinity of cellulose and MCC products varies (Doelker *et al.*, 1987).

According to various research reports, percentage crystallinity index of MCC can be varied from 37 to 93% depending on the source material, and X-ray methods and experimental mode used (Sun *et al.*, 2008; Terinte *et al.*, 2011). The degree of crystallinity of MCC typically depends on particle size. Thus, grinding of MCC for prolonged periods of time resulted in reduced crystallinity by reducing particle size, and this is true for MCC prepared in this study (Kumar and Kothari, 1999; Padmadisastra *et al.*, 1987; Suzuki and Nakagami, 1999). SCB-MCCI had higher crystallinity index than SCB-MCCOD and SCB-MCCSD. Similarly, DSCB-MCCI had higher crystallinity index than DSCB-MCCOD and DSCB-MCCSD. This might be due to reduction of particle size by mechanical shearing in latter products (Segal *et al.*, 1959). As shown in Table 3.3, when mechanical shearing combined with pulverization crystallinity index of MCC was further decreased. Whole type dewaxed samples had slightly higher crystallinity

index than corresponding non-dewaxed samples, which is consistent with the result reported by Padmadisastra *et al.* (1989).

The apparent crystallite size (L) of cellulose and MCC preparations were estimated by using the Scherrer equation. Crystallite sizes of cellulose and MCC are presented in Table 3.3. Dewaxed cellulose and MCC had higher crystal size than respective non-dewaxed preparations. Overall, Avicel PH-101 had the highest % crystallinity index and crystal size. This might have resulted from differences in source plant, extraction method and particle size (Sun *et al.*, 2008; Thoorens *et al.*, 2014).

Table 3.3: Crystallinity index (CrI) and apparent crystal size of SCBC, DSCBC, SCB-MCCI, SCB-MCCOD, SCB-MCCSD, DSCB-MCCI, DSCB-MCCOD, DSCB-MCCSD and Avicel PH-101.

Samples		**Peak position (2θ)**		**CrI %**	**L (nm)**
		I_{am}	I_{002}		
Cellulose	SCBC	18.26	22.30	74.50	2.75
	DSCBC	18.64	22.16	77.34	3.08
MCC	SCB-MCCI	18.08	22.38	81.93	3.24
	SCB-MCCOD	18.08	22.36	78.11	2.93
	SCB-MCCSD	18.48	22.26	79.62	3.23
	DSCB-MCCI	18.02	22.40	83.00	3.54
	DSCB-MCCOD	18.02	22.14	79.56	3.24
	DSCB-MCCSD	18.44	22.38	81.87	3.35
	Avicel PH-101	18.74	22.66	89.89	4.80

3.1.6. Morphological characterization

Particle morphology is an essential property in the characterization and identification of pharmaceutical excipients. It can also be utilized to predict certain functional properties that are particularly related to flowability and compactibility of the powder. Figure 3-9 (A) shows SEM photomicrographs of DSCBC sample. The morphological structure of cellulose comprises fibrillar elements. Figure 3-9 (B) shows SEM photomicrographs of DSCB-MCCI sample. The MCC is a mixture of different size of fiber fragments. As can be noted from the figure, after acid hydrolysis shortening of fibers occurred and rod-shaped MCC formed, which is similar to the findings of various study (Adel *et al.*, 2011; El-Sakhawy and Hassan, 2007; Gurgel *et al.*, 2012).

A.

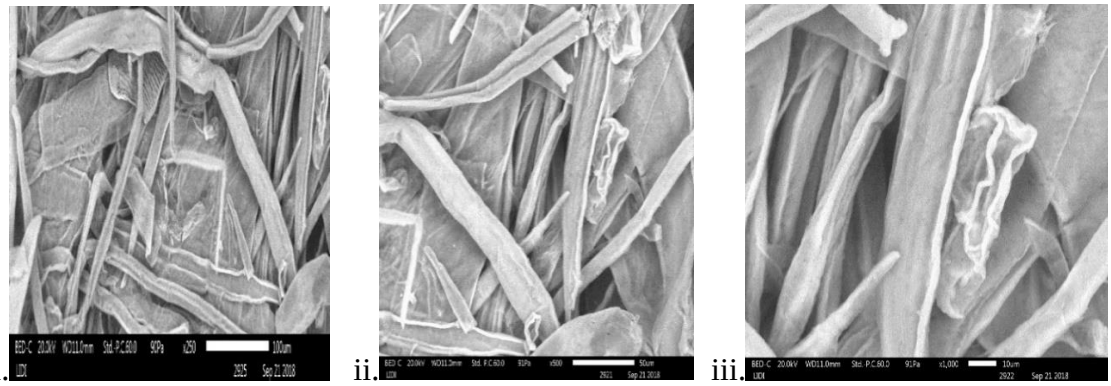

B.

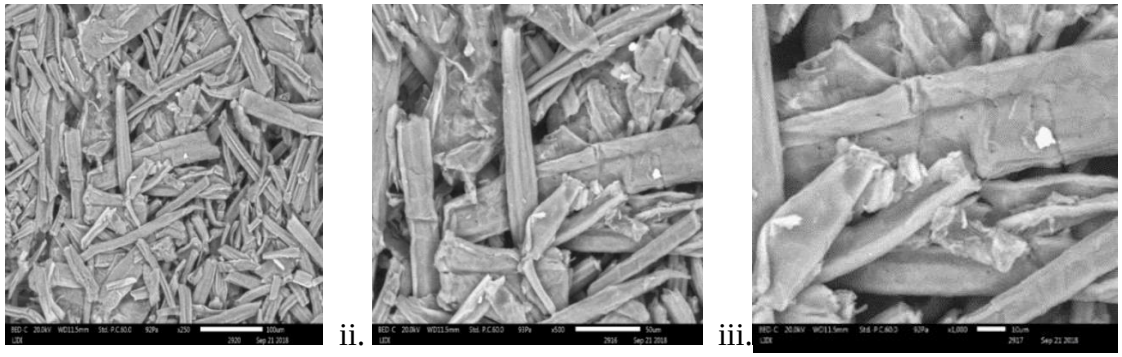

Figure 3-9: SEM images of the DSCBC (A) and DSCB-MCCI (B); *x250 (i), x500 (ii) and x1000 (iii).*

3.1.7. Thermal analysis

Thermogravimetry is one of the most widely used technique to monitor the thermal degradation of cellulose fiber and MCC. This is because different polymers and supermolecular structures of cellulose and MCC behave differently when undergoing thermal degradation (Liu *et al.*, 2006). It is a convenient, reproducible and useful method for characterizing heterogeneous organic materials (Sun *et al.*, 2005).

The decomposition temperature of cellulose and MCC mainly depends on their molecular weight and purity. In addition, the decomposition temperature is affected by polymer morphology and degree of crystallinity, high crystallinity of a polymer means high decomposition temperature (Princi *et al.*, 2005). Cellulose and MCC undergo three typical decomposition stages. The initial weight loss in the region 40 - 150 ^{o}C is mainly because of moisture evaporation (Adel *et al.*, 2011; Deepa *et al.*, 2015). The major and second decomposition peak at about 250 - 380 °C with maximum weight loss rate attained at 355 ^{o}C is attributed to thermal decarboxylation, depolymerization and decomposition of glycosyl units in

cellulose. The third stage of weight loss ranging from 380 to 700 °C is attributed to char residue formation (Jahan *et al.*, 2011; Liu *et al.*, 2006; Trache *et al.*, 2016; Yang *et al.*, 2007). The decomposition curves for SCB, SCBC, DSCBC, SCB-MCC, DSCB-MCC and Avicel PH-101 are shown in Figure 3-10. Except SCB, all samples had three decomposition stages. SCB underwent unique decomposition at a low temperature associated with the degradation of hemicellulose, wax and pectin material ranging from 170 to 230 ^{o}C (Nazir *et al.*, 2013).

An initial weight loss was detected around 42 to 114 ^{o}C for all samples because of evaporation of water in cellulose and MCC samples (Fahma *et al*., 2010). The second degradation stage of SCBC and DSCBC occurred from 224.55 - 366.22 ^{o}C and 248.65 - 374.69 ^{o}C, respectively. Whereas, SCB-MCC, DSCB-MCC and Avicel PH-101 degraded in the range of 289.5 - 361.87, 295.1 - 372.29 and 293.7 - 371.69 ^{o}C, respectively. This is attributed to cellulose degradation (Rosli *et al.*, 2013). A 50% weight loss decomposition temperature ($T_{50\%}$) of cellulose and MCC preparations occurred at 339.88, 346.83, 337.52 and 339.74 ^{o}C for SCBC, DSCBC, SCB-MCC and DSCB-MCC, respectively. This indicates that the thermal stability of the cellulose increased with its purity. The reason for this relatively higher thermal stability of the pure cellulose is likely attributed to the substantial removal of less stable hemicellulosic polymers from dewaxed SCB as noted elsewhere (Sun *et al.*, 2004). $T_{50\%}$ of Avicel PH-101 was 336.13 ^{o}C, which likely resulted from its moderately lower DP value.

DTA thermogram of the cellulose and MCC preparations contained endothermic and exothermic peaks. The area of second endothermic peak correlates with the proportion of crystallinity, higher value implying higher crystallinity. As shown in Figure 3-10 (B), DSCB-MCC possessed a higher value than SCB-MCC. This could be attributed to high crystallinity index of the former product. Avicel PH-101 had a higher area than both MCC preparations from SCB, which resulted from its higher crystallinity index. The exothermic peak of cellulose and MCC samples is attributable to the disintegration of intramolecular interaction and the decomposition of the polymer. The amount of heat emission depends on the amount of heat required for decomposition (Sun *et al.*, 2004).

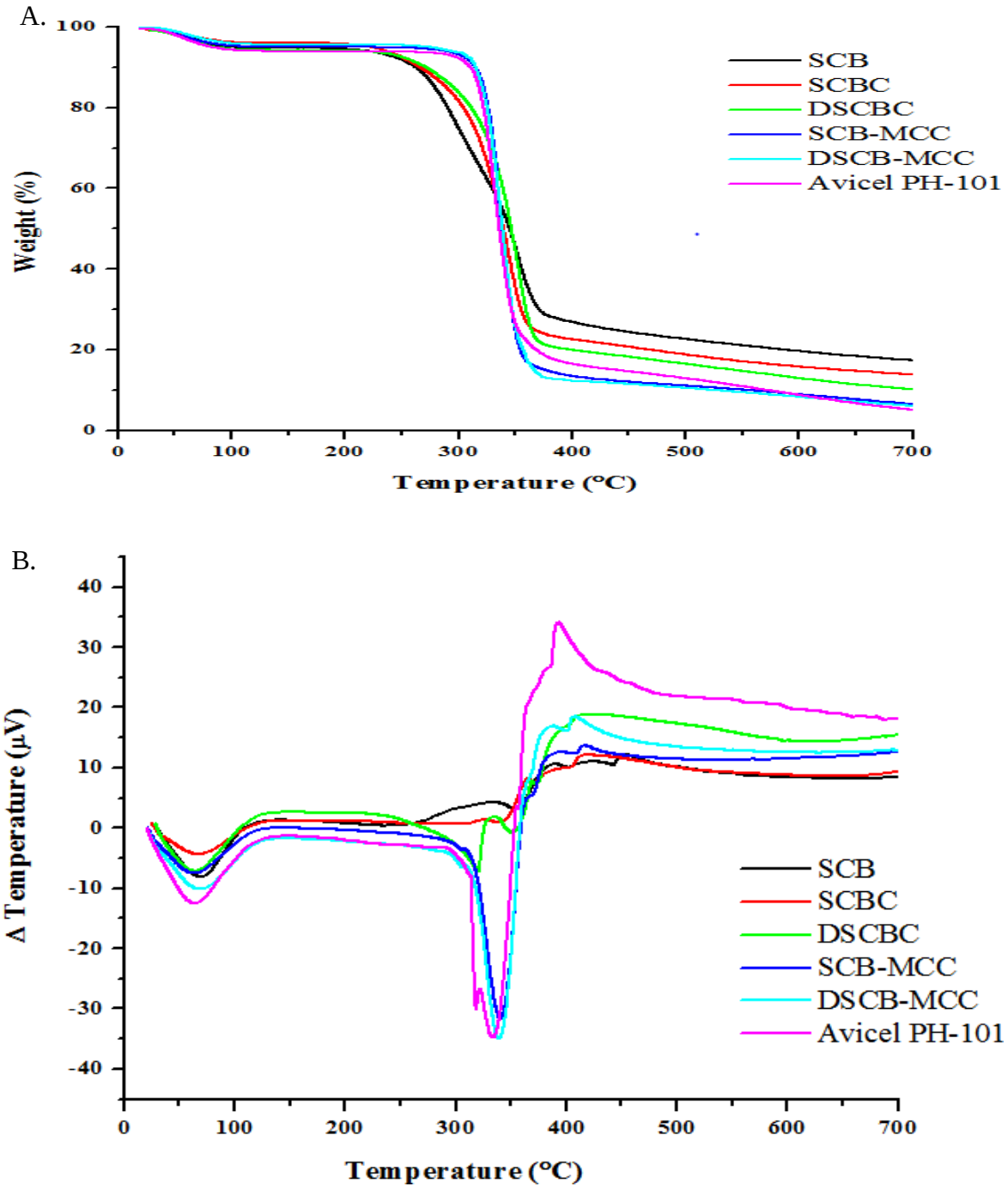

Figure 3-10: TGA (A) and DTA (B) curves of SCB, SCBC, DSCBC, SCB-MCC, DSCB-MCC and Avicel PH-101.

Thermal stability of the studied samples was increased by chemical treatment, which resulted from the removal of hemicellulose and lignin, as well as by degree of crystallinity of the treated samples. The solid residue at 700 °C was 17.32, 13.84, 10.26, 6.44, 6.01 and 5.06% for SCB, SCBC, DSCBC, SCB-MCC, DSCB-MCC and Avicel PH-101, respectively. The higher amount

of residues in the raw SCB has resulted from the presence of lignin as well as ash, which both have a slow degradation rate. On the other hand, the small amount of residue in the dewaxed samples might be the result of additional dewaxing procedure which increases removal of lignin during the extraction procedure as reported elsewhere (Rosli *et al.*, 2013).

3.2. Chemical Composition and Hydration Capacity of Microcrystalline Cellulose

Ash, pH, water-soluble and ether-soluble substance values of SCB-MCC, DSCB-MCC and Avicel PH-101 were performed and are presented in Table 3.4. Except ether-soluble substance value of SCB-MCC, all those values were within USP/NF specification (USP 30/NF 25, 2007). The ash value is indicative of the inorganic content of the sample. The value obtained for the total ash was very low. This indicates that MCC samples are almost free of inorganic compounds (Ohwoavworhua and Adelakun, 2010).

Table 3.4: Some Physico-chemical properties of SCB-MCC, DSCB-MCC and Avicel PH-101.

Tests	**SCB-MCC**	**DSCB-MCC**	**Avicel PH-101**	**Standard as per USP**
pH	6.81 ± 0.003	6.83 ± 0.001	6.25 ± 0.002	5.0 – 7.5
Ash (%)	0.02	0.02	0.06	Not more than 0.1
Water-soluble substance (%)	0.180 ± 0.020	0.160 ± 0.060	0.170 ± 0.050	Not more than 0.25
Ether-soluble substance (%)	0.710 ± 0.030	0.041 ± 0.003	0.022 ± 0.002	Not more than 0.05

The hydration capacity values of MCC samples are displayed in Figure 3-11. SCB-MCCI and DSCB-MCCI had the highest hydration capacity. Their highest porosity value might have resulted in overestimated hydration capacity. Since DSCB-MCCOD and DSCB-MCCSD contained significantly lower ($P < 0.05$) hydrophobic content, they had significantly higher ($P < 0.05$) hydration capacity than SCB-MCCOD and SCB-MCCSD. Avicel PH-101 had a higher hydration capacity than all mechanically sheared MCC preparations. This could be due to the significantly lower ($P < 0.05$) hydrophobic impurity of the former product than the prepared MCC (Padmadisastra and Gonda, 1989).

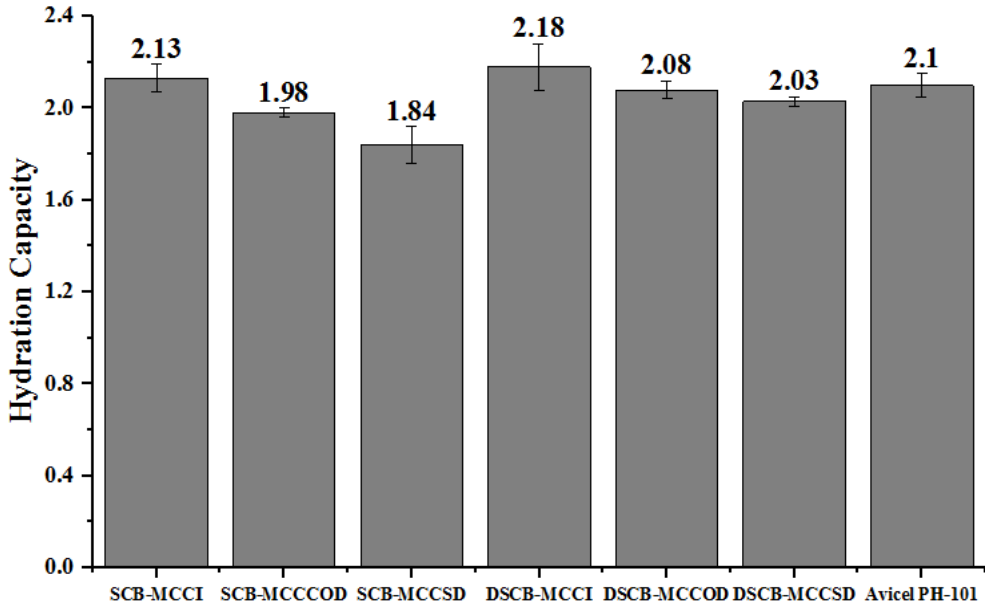

Figure 3-11: Hydration Capacity of SCB-MCCI, SCB-MCCOD, SCB-MCCSD, DSCB-MCCI, DSCB-MCCOD, DSCB-MCCSD and Avicel PH-101.

3.3. Micromeritic Properties of Microcrystalline Cellulose

3.3.1. Particle size and particle size distribution

Knowledge and control of size and size range of particles have profound importance in pharmacy (Singh, 2006). The particle size distributions of MCC samples are shown in Figure 3.12 and Table 3.5. The particle size distribution was measured by using laser diffraction particle size analyzer. In this technique the laser beam is reflected according to the volume occupied by the particles in the dispersion phase, therefore the shape of the particle influences the measured particle size (Rumman, 2009). For nonspherical particles, an equivalent sphere size distribution is obtained because the technique uses the assumption of spherical particles in its optical model. The resulting particle size distribution may be different from those obtained by methods based on other physical techniques such as sieving (USP 30/NF 25, 2007). Therefore, it does not provide accurate information about the fibrous particles size.

All MCC samples, except SCB-MCCI and DSCB-MCCI, showed a monomodal normal particle size distribution. MCC prepared without mechanical shearing had the highest mean particle size. A mean particle size of MCC was decreased after mechanical shearing of MCC slurry, as observed in the mean particle size of SCB-MCCOD, DSCB-MCCOD, SCB-MCCSD and

DSCB-MCCSD. Whereas, oven dried MCC preparations had a lower mean particle size than respective spray dried MCC preparations. This could have resulted from additional pulverization of MCC after oven drying.

FMC Specification indicates that the D_{10}, D_{50} and D_{90} of Avicel PH-101 should be within 14-30, 40-75 and 77-156 µm, respectively (FMC, 2003). Rowe *et al.* (2009) reported that the mean particle size of Avicel PH-101 is 50 µm. In this study, the mean particle size of Avicel PH-101 is significantly higher ($P < 0.05$) than the reported value and both SCB-MCCSD and DSCB-MCCSD. However, all percentiles of Avicel PH-101 were within the acceptable range.

According to various research reports, a specific surface area of Avicel PH-101 ranges from 1.06 to1.26 m^2/g (Pesonen *et al.,* 1989; Rowe *et al.*, 2009). The measured surface area can vary depending on the method of measurement. The most commonly used method for the determination of surface area is physical gas adsorption. It considers the contribution of pore surface area, which is accessible to the gas molecules. Nitrogen, krypton, and argon are some of the typically used adsorptives. Moreover, TEM and SEM can also be used to measure the surface area. Significantly lower values of the specific surface area of MCC samples in this study could be due to the type of measuring instrument, which does not consider the porosity of particle (Fan and Zhu, 1998).

Table 3.5: Particle size and size distribution of SCB-MCCI, SCB-MCCOD, SCB-MCCSD, DSCB-MCCI, DSCB-MCCOD, DSCB-MCCSD and Avicel PH-101.

Parameters	**SCB-MCCI**	**SCB-MCCOD**	**SCB-MCCSD**	**DSCB-MCCI**	**DSCB-MCCOD**	**DSCB-MCCSD**	**Avicel PH-101**
Mean particle size (µm)	104.40 ± 2.8	58.10 ± 1.5	65.20 ± 1.3	90.20 ± 1.9	44.90 ± 0.8	52.89 ± 0.6	73.14 ± 0.7
D_{10} (µm)	19.63 ± 0.6	11.20 ± 0.5	15.93 ± 0.4	17.06 ± 0.5	7.78 ± 0.2	12.39 ± 0.3	19.54 ± 0.4
D_{50} (µm)	81.58 ± 1.8	44.08 ± 0.8	51.87 ± 1.1	63.53 ± 1.5	32.43 ± 0.8	43.41 ± 0.9	61.79 ± 1.3
D_{90} (µm)	228.06 ± 5.3	126.50 ± 3.9	131.43 ± 5.5	209.48 ± 4.6	92.83 ± 2.7	108.09 ± 4.1	145.07 ± 3.7
SSA (m^2/g)	0.12 ± 0.001	0.22 ± 0.003	0.17 ± 0.002	0.14 ± 0.001	0.62±0.008	0.49 ± 0.006	0.44 ± 0.01
Span	2.56E+00	2.62E+00	2.23E+00	3.03E+00	2.62E+00	2.2E+00	2.03E+00

D_{10}: 10% of particles below, D_{50}: 50% of the particles below, D_{90}: 90% of particles below, SSA: Specific surface area, Span= $(D_{90} - D_{10})/D_{50}$

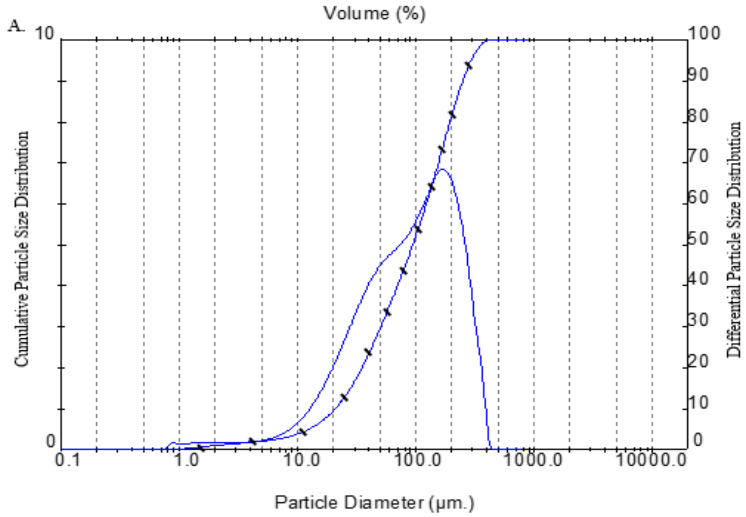
A.
Volume (%)
Cumulative Particle Size Distribution
Differential Particle Size Distribution
Particle Diameter (µm.)
10
0
100
90
80
70
60
50
40
30
20
10
0
0.1
1.0
10.0
100.0
1000.0
10000.0

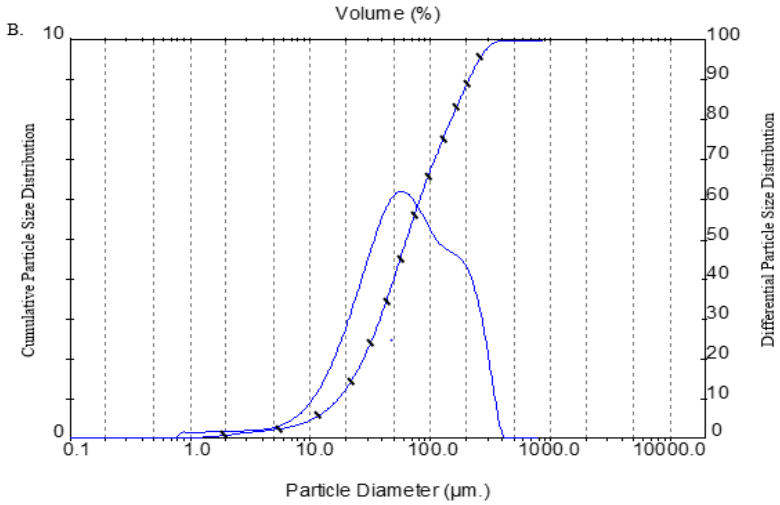
B.
Volume (%)
Cumulative Particle Size Distribution
Differential Particle Size Distribution
Particle Diameter (µm.)
10
0
100
90
80
70
60
50
40
30
20
10
0
0.1
1.0
10.0
100.0
1000.0
10000.0

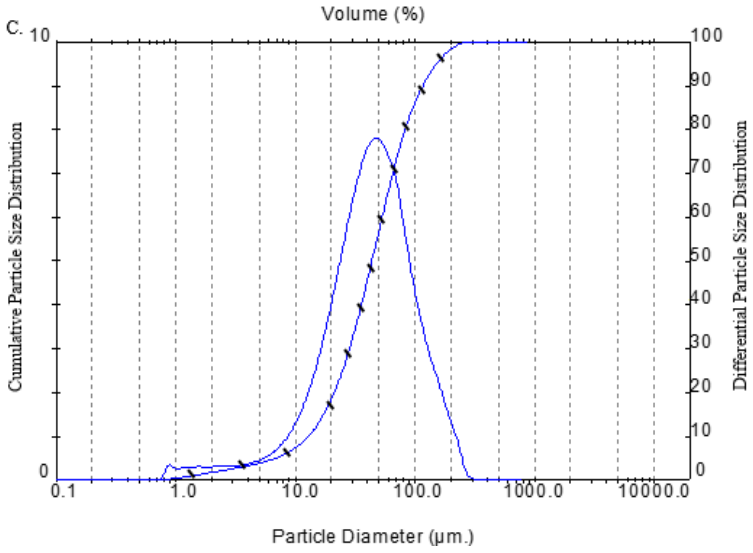
C.
Volume (%)
Cumulative Particle Size Distribution
Differential Particle Size Distribution
Particle Diameter (µm.)
10
0
100
90
80
70
60
50
40
30
20
10
0
0.1
1.0
10.0
100.0
1000.0
10000.0

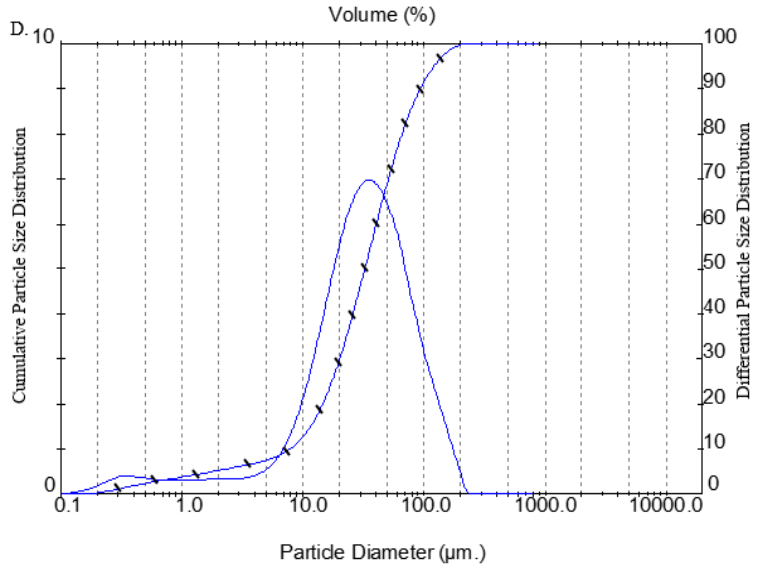
D.
Volume (%)
Cumulative Particle Size Distribution
Differential Particle Size Distribution
Particle Diameter (µm.)
10
0
100
90
80
70
60
50
40
30
20
10
0
0.1
1.0
10.0
100.0
1000.0
10000.0

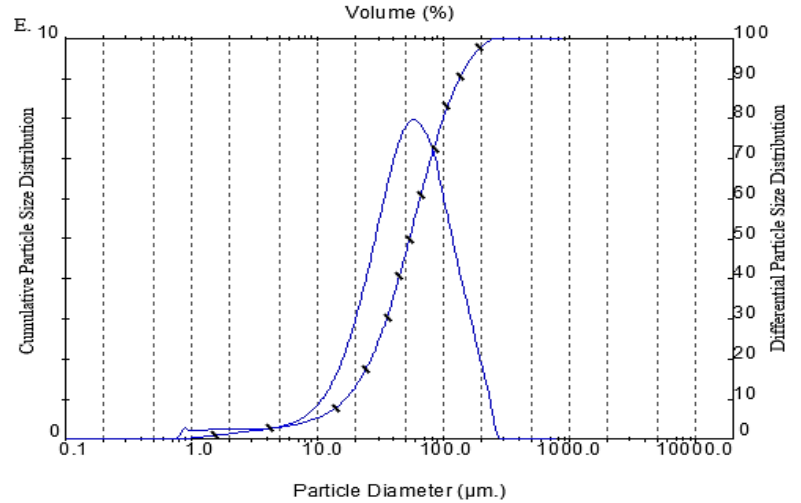

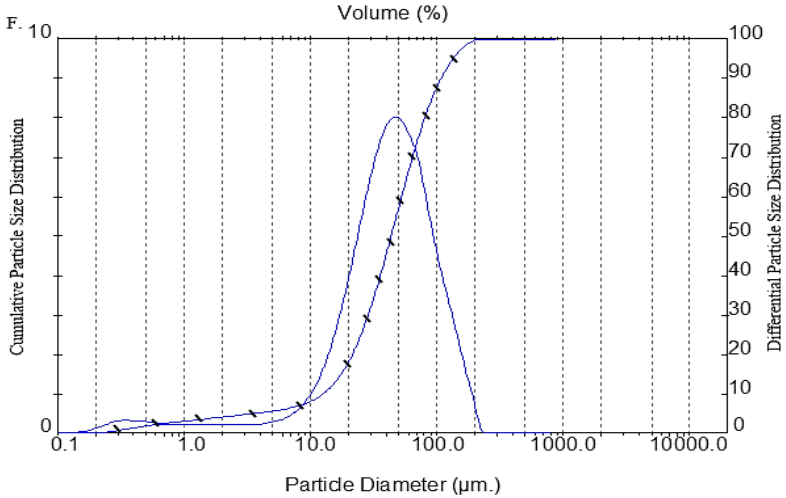

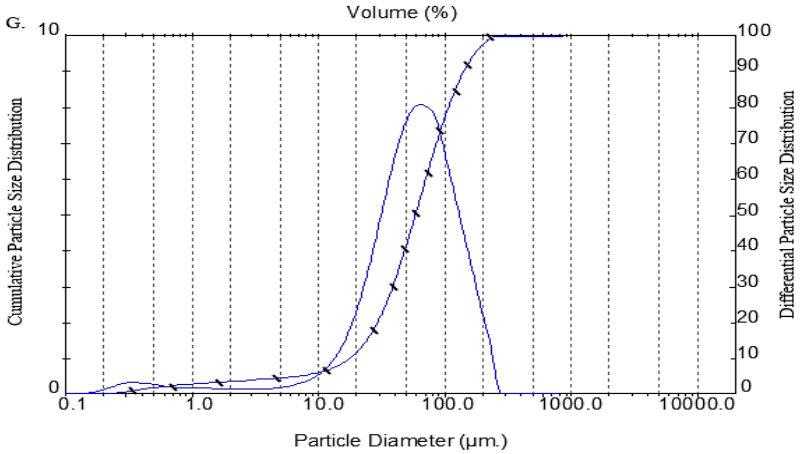

Figure 3-12: Volumeteric particle size distribution of SCB-MCCI (A), DSCB-MCCI (B), SCB-MCCOD (C), DSCB-MCCOD (D), SCB-MCCSD (E), DSCB-MCCSD (F) and Avicel PH-101 (G).

3.3.2. Density and related properties

Moisture is known to affect physicomechanical properties of pharmaceutical formulations including powder flow, compressibility/compactibility, hardness of tablets, die-wall friction and stability (physical, chemical and microbiological). Cellulose composes of a high amorphous part and it provides hygroscopic nature. Thus, it may have a higher loss on drying than MCC (Kachrimanis *et al.*, 2006). This study showed that the moisture content of SCBC and DSCBC were 5.23 (± 0.03) and 5.34 (± 0.01) %, respectively. The moisture content of SCB-MCCI, SCB-MCCOD, SCB-MCCSD, DSCB-MCCI, DSCB-MCCOD, DSCB-MCCSD and Avicel PH-101 are presented in Table 3.6. The rank order of the moisture content is DSCB-MCCOD > SCB-MCCOD > Avicel PH-101 > DSCB-MCCI > SCB-MCCI > DSCB-MCCSD > SCB-MCCSD. DSCB-MCCSD and SCB-MCCSD had a minimum moisture content. This might be because spray drying has interparticle heat contact than oven drying. In this study, all of the MCC samples had a moisture content within the limits recommended by USP (< 7%) (USP 30/NF 25, 2007). Moreover, the variability reflected in the moisture content values among the various MCC preparations suggests that not only the degree of crystallinity and drying technique but also the accessibility of the adsorption sites to water molecules determines the final moisture content value of the cellulose excipients (Kothari *et al*. 2002).

The true density value of perfect cellulose crystal is 1.56 and 1.61 g/cm3 for Iα and Iβ polymorphs, respectively, while the true density value of MCC ranges from 1.512 g/cm^3 to 1.668 g/cm^3 (Rowe *et al.*, 2009; Sun, 2008). True density values of the prepared MCC and Avicel PH-101 were within reported values.

The bulk density gives an estimate of the ability of a material to flow from a hopper into the die cavity, while the tap density is a measure of how well a powder can be packed in a confined space on repeated tapping. In general, powders with high bulk and tap densities had better flow property (Kothari *et al*. 2002). The bulk density of a powder depends primarily on particle size, particle size distribution, particle shape and the tendency of the particles to adhere to one another (Singh, 2006). Densities and related properties of MCC samples are presented in Table 3.6. DSCB-MCCOD had the greatest bulk density, whereas SCB-MCCI had the lowest bulk density. This could have resulted from the largest particle size of SCB-MCCI, which may pack in such

a way as to leave large gaps between their surfaces, resulting in powder of low bulk density (Singh, 2006). Dewaxing of SCB significantly increased ($P < 0.05$) the bulk and tapped densities of the powder. In addition, mechanical shearing of a slurry of MCC further significantly increased ($P < 0.05$) bulk and tapped densities of both dewaxed and non-dewaxed MCC preparations by decreasing particle size. A difference in crystallinity index between the prepared MCC could also result in variation of bulk and tapped densities (Pesonen *et al.,* 1989). DSCB-MCCOD, DSCB-MCCSD and Avicel PH-101 had comparable bulk and tapped densities.

The HR and CI calculated from bulk and tapped densities indicate the flow properties of powders. HR values 1.00-1.11, 1.12-1.18, 1.19-1.25, 1.26-1.34, 1.35-1.45, 1.46-1.59, and > 1.6 represent excellent, good, fair, passable, poor, very poor and very, very poor flow properties, respectively. Likewise, CI values ≤ 10, 11-15, 16-20, 21-25, 26-31, 32-37, > 38 represent excellent, good, fair, passable, poor, very poor and very, very poor flow properties, respectively (USP <1174>, 2016). Dewaxing of SCB before extraction of cellulose significantly improved ($P < 0.05$) CI and HR of MCC preparations (Table 3.6). Moreover, mechanical shearing of a slurry of both MCC preparations also improved CI and HR significantly ($P < 0.05$). CI and HR value of DSCB-MCCOD and Avicel PH-101 were not significantly different ($P < 0.05$) and had passable flow property.

The porosity values of MCC preparations were significantly affected ($P < 0.05$) by mechanical shearing, pulverization and dewaxing procedure. DSCB-MCCSD and Avicel PH-101 had comparable porosity value. Overall, spray dried MCC preparations had significantly higher ($P < 0.05$) porosity value than respective oven dried MCC preparations. This is presumably because spray dried powders have a porous structure and a relatively low bulk density (Thoorens *et al.*, 2014).

Table 3.6: Densities and related properties of SCB-MCCI, SCB-MCCOD, SCB-MCCSD, DSCB-MCCI, DSCB-MCCOD, DSCB-MCCSD and Avicel PH-101.

Parameters	**SCB-MCCI**	**SCB-MCCOD**	**SCB-MCCSD**	**DSCB-MCCI**	**DSCB-MCCOD**	**DSCB-MCCSD**	**Avicel PH-101**
Moisture Content (%)	4.72 ± 0.07	5.10 ± 0.03	4.33 ± 0.33	4.90 ± 0.05	5.14 ± 0.01	4.66 ± 0.33	5.02 ± 0.08
True density (g/ml)	1.560 ± 0.02	1.540 ± 0.01	1.548 ± 0.01	1.580 ± 0.00	1.565 ± 0.03	1.570 ± 0.01	1.577 ± 0.03
Bulk Density (g/ml)	0.151 ± 0.01	0.300 ± 0.02	0.270 ± 0.02	0.285 ± 0.01	0.385 ± 0.02	0.357 ± 0.01	0.353 ± 0.03
Tapped Density (g/ml)	0.220 ± 0.01	0.420 ± 0.02	0.390 ± 0.01	0.396 ± 0.03	0.500 ± 0.01	0.480 ± 0.01	0.462 ± 0.06
Carr's Index (%)	31.82 ± 0.69	28.57 ± 0.13	30.77 ± 0.18	28.03 ± 0.10	23.00 ± 0.02	25.78 ± 0.28	23.59 ± 0.69
Hausner Ratio	1.46 ± 0.02	1.40 ± 0.01	1.44 ± 0.02	1.39 ± 0.01	1.30 ± 0.01	1.34 ± 0.01	1.31 ± 0.01
Porosity (%)	90.32 ± 0.08	80.52 ± 0.12	82.26 ± 0.09	81.96 ± 0.10	75.4 ± 0.13	77.26 ± 0.14	77.62 ± 0.51

3.4. Moisture Sorption Pattern

Moisture modifies the flow and mechanical properties of many powders. Therefore, the moisture sorption profiles of MCC preparations were determined to extrapolate the extent of influence of a humid environment on the powder properties. The moisture sorption profiles SCB-MCCI, SCB-MCCOD, SCB-MCCSD, DSCB-MCCI, DSCB-MCCOD, DSCB-MCCSD and Avicel PH-101 are depicted in Figure 3-13. The crystallite portion of MCC does not adsorb water and that the extent of water adsorption by MCC should thus be proportional to the amount of amorphous present in MCC. Therefore, water is sorbed almost exclusively by the amorphous regions of MCC (Kachrimanis *et al.*, 2006; Thoorens *et al.*, 2014).

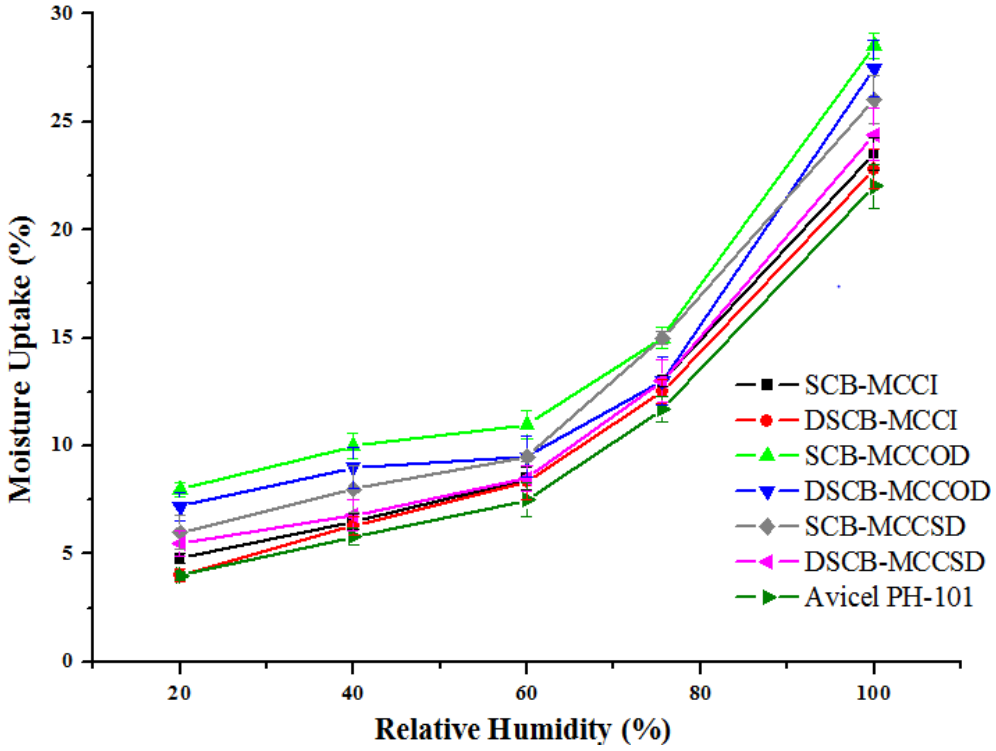

Figure 3-13: Moisture sorption patterns of SCB-MCCI, SCB-MCCOD, SCB-MCCSD, DSCB-MCCI, DSCB-MCCOD, DSCB-MCCSD and Avicel PH-101 at room temperature.

As can be noted in the above figure, the water uptake of all MCC powders slightly increased with RH at lower values but increased significantly at about 100% RH. SCB-MCCOD and DSCB-MCCOD had the highest moisture uptake. This might have resulted from their significant amorphous content. Avicel PH-101 had slightly lower moisture uptake than the MCC prepared from SCB at all relative humidities. This could be attributed to its high crystallinity index. Yet

the prepared MCC had a difference in hydrophobic content, all had comparable moisture uptake property. The possible reasons could be the high crystallinity of dewaxed MCC preparation and high porosity of non-dewaxed MCC preparations (Mihranyan *et al*., 2004; Williams *et al.*, 1997). Higher moisture sorption of the prepared MCC indicates a possible higher susceptibility to moisture-induced changes in quality. Therefore, MCC preparations from SCB require good control of moisture as compared to Avicel PH-101.

3.5. Mechanical Properties of Plain MCC Tablets

MCC is a widely used tableting excipient. It is described as a filler/binder and usually added to formulations to enhance compactibility (El-Sakhawy and Hassan, 2007). MCC is by far the most compactible material and best dry binder to date to be used in direct compression formulation. Its outstanding compactibility results from a good balance between high plasticity, viscoelasticity, low brittleness and particle interlocking (Doelker, 1993). Different MCC samples were pressed into tablets at different compression forces and their hardness, tensile strength, friability and disintegration time were evaluated (Table 3.7).

Crushing strength is often studied to describe the integrity of the compact. The strength of a compressed MCC tablet depends on various factors, the most important of which are compression force, particle size and distribution, porosity and crystallinity (Edge *et al.*, 2000; Singh, 2006). Crushing strength of SCB-MCCSD is moderately higher than that of DSCB-MCCSD, but not significantly different ($P > 0.05$), across the formulations. This might have resulted from the high waxy residue, known binder, of former product. The crushing strength of spray dried MCC preparations were significantly higher ($P < 0.05$) than oven dried MCC preparations. Spray dried excipients are characterized by a porous structure and a relatively low bulk density. This facilitates compressibility (Thoorens *et al.*, 2014; Westermarck *et al*., 1999). In addition, denser powders, oven dried MCC preparations, produce weaker tablets. Bulk and tap densities increased is accompanied by a decrease of DP, and lead to a decrease of tensile strength (Liao *et al.*, 2012). This indicates that the higher density contributes to the weaker mechanical property. For instance, SCB-MCCSD and DSCB-MCCSD had higher DP, lower bulk density and higher crushing strength than their respective oven dried MCC preparations. The crushing strength of Avicel PH-101 is significantly higher ($P < 0.05$) than MCC prepared from SCB in all compression forces. This is attributed to its higher crystallinity index.

Correspondingly, several studies reported that high crystallinity MCC powders produce harder tablets than low crystallinity powders (Doelker *et al.*, 1987; Kumar and Kothari, 1999; Nakai *et al.*, 1977).

Tensile strength is often used to describe the strength of a compact. It indicates the bonding strength, and it may provide information about the laminating and capping tendencies of the material (El-Sakhawy and Hassan, 2007). Avicel PH-101 possessed significantly higher ($P < 0.05$) tensile strength, it could be because of its high degree of crystallinity. A study by Jahan *et al.* (2011) also showed that MCC which had higher crystallinity exhibited a higher tensile strength. The results from this study indicate the need for different compression force to produce tablets from different types of MCC. Similarly, it was also reported by different authors (Bhimte and Tayade, 2007; Padmadisastra *et al.*, 1987; Padmadisastra and Gond, 1989).

Friability test is performed in order to monitor the resistance of tablets to stresses like mechanical shocks and abrasion during the manufacturing, packing and transportation processes. Such stresses can lead to capping, chipping, abrasion or even breakage of the tablets. It is therefore important that the tablet is formulated to withstand such stress without damage. A maximum weight loss of not more than 1.0% is generally considered acceptable (Akgeyik *et al.*, 2016). The compact of DSCB-MCCOD formulated at CF1 was broken during the test. Whereas, the friability results of SCB-MCCOD, SCB-MCCSD and DSCB-MCCSD were less than 1.0% except formulation prepared at CF1. The relatively low value of friability of these MCC compacts could be attributed to the strength of their compacts. Avicel PH-101 compacts had a relatively low value of friability. This could be due to their higher compacts' strength. Overall at comparable crushing strength, all MCC samples had comparable percentage friability.

Table 3.7: Hardness, tensile strength, friability and disintegration time of plain tablets of SCB-MCCOD, SCB-MCCSD, DSCB-MCCOD, DSCB-MCCSD and Avicel PH-101.

Excipients	Parameters	CF1	CF2	CF3	CF4	CF5
SCB-MCCOD	Crushing strength (N)	19.30 ± 3.60	38.90 ± 3.10	61.10 ± 4.10	80.70 ± 6.80	103.50 ± 7.70
	Tensile strength (Kg/cm^2)	1.76 ± 0.33	3.56 ± 0.28	6.46 ± 0.43	8.88 ± 0.75	12.22 ± 0.91
	Friability (%)	2.70 ± 0.05	0.95 ± 0.20	0.36 ± 0.05	0.21 ± 0.01	0.14 ± 0.06
	Disintegration time (min)	3.50 ± 1.2	10.10 ± 0.97	18.70 ± 1.78	30.80 ± 3.96	71.13 ± 7.44
SCB-MCCSD	Crushing strength (N)	30.00 ± 5.24	53.20 ± 3.09	76.70 ± 7.50	101.00 ± 4.40	124.30 ± 6.20
	Tensile strength (Kg/cm^2)	2.78 ± 0.49	5.27 ± 0.31	8.14 ± 0.80	11.14 ± 0.49	14.76 ± 0.74
	Friability (%)	1.17 ± 0.10	0.43 ± 0.04	0.18 ± 0.09	0.17 ± 0.05	0.10 ± 0.02
	Disintegration time (min)	6.80 ± 2.10	15.76 ± 1.10	29.10 ± 1.52	77.90 ± 8.37	120*
DSCB-MCCOD	Crushing strength (N)	15.00 ± 3.63	32.30 ± 4.10	54.90 ± 4.70	73.40 ± 9.10	94.70 ± 5.60
	Tensile strength (Kg/cm^2)	1.34 ± 0.33	3.19 ± 0.40	5.71 ± 0.49	7.89 ± 0.98	11.10 ± 0.66
	Friability (%)	**	1.10 ± 0.02	0.47 ± 0.07	0.23 ± 0.09	0.15 ± 0.01
	Disintegration time (min)	0.10 ± 0.01	0.23 ± 0.13	0.61 ± 0.08	0.91 ± 0.10	1.87 ± 0.27
DSCB-MCCSD	Crushing strength (N)	27.50 ± 5.90	48.80 ± 5.97	70.70 ± 4.32	92.30 ± 6.00	114.90 ± 7.10
	Tensile strength (Kg/cm^2)	2.53 ± 0.54	4.82 ± 0.59	7.44 ± 0.45	10.15 ± 0.66	13.58 ± 0.84
	Friability (%)	1.21 ± 0.09	0.55 ± 0.20	0.25 ± 0.08	0.18 ± 0.03	0.12 ± 0.01
	Disintegration time (min)	0.28 ± 0.01	0.67 ± 0.07	0.95 ± 0.03	1.93 ± 0.17	4.08 ± 0.32
Avicel PH-101	Crushing strength (N)	49.10 ± 5.20	75.90 ± 6.30	101.60 ± 7.10	125.10 ± 4.90	151.00 ± 6.40
	Tensile strength (Kg/cm^2)	4.58 ± 0.48	7.64 ± 0.63	10.87 ± 0.76	14.05 ± 0.55	18.00 ± 0.80
	Friability (%)	0.40 ± 0.07	0.19 ± 0.08	0.16 ± 0.08	0.09 ± 0.02	0.04 ± 0.01
	Disintegration time (min)	0.57 ± 0.07	0.80 ± 0.04	1.43 ± 0.21	3.95 ± 0.34	6.57 ± 0.30

*Tablets did not disintegrate during the measurement time of 2 h, ** Tablet break, CF compression force

The disintegration time increased with an increase in compaction force for all MCC preparations (Table 3.7). The penetration of water into a tablet was necessary for the disintegration as the first step and the work of dispersion of particles caused through the penetration of water had to overcome the binding work of particles caused through cohesion and adhesion (Nogami *et al.*, 1969). Non-dewaxed MCC preparations showed prolonged disintegration time than both dewaxed MCC samples and Avicel PH-101, which might have resulted from it substantial waxy residue that impedes the penetration of water into the tablets (Kothari *et al.,* 2002). Oven dried MCC preparations had fast disintegration than respective spray dried MCC preparations. It might be because of the smaller degree of crystallinity, which increases access for water molecules to enter and interact with free hydroxyl groups, and higher hydration capacity of the former materials (Kothari *et al.,* 2002). At comparable crushing strength, DSCB-MCCOD and DSCB-MCCSD had slightly higher disintegration time than Avicel PH-101. This could have resulted from a higher hydration capacity and lower hydrophobic content of the latter product.

3.6. Lubricant Sensitivity Ratio

Lubricants are frequently included in tablet formulations to reduce die wall friction during both compaction and ejection of the tablet. Their presence, however, may cause undesirable changes in tablet properties. Magnesium stearate is one of the most commonly used lubricant in tablet production (Bolhuis and Holzer, 2011; Bos *et al.,* 1987; Rojas *et al.,* 2013). During the mixing of tablet ingredients with magnesium stearate, it distributes over the powder material, either as a surface film or as a free fraction (Bolhuis and Holzer, 2011; Bos *et al.,* 1987). Magnesium stearate negatively affects the binding property of MCC prepared from SCB and Avicel PH-101, as reflected by their LSRs and tensile strengths values (Table 3.8).

Table 3.8: Tensile Strengths and LSRs of the Compacts Using Pure and Lubricated Materials.

Samples	**Tensile Strength (Kg/cm^2)**		**LSR**
	Without magnesium stearate	With 0.5% magnesium stearate	
SCB-MCCOD	7.80	6.66	0.132
SCB-MCCSD	10.14	8.64	0.104
DSCB-MCCOD	6.96	5.30	0.211
DSCB-MCCSD	9.45	7.28	0.18
Avicel PH-101	13.31	10.33	0.192

When mixed with 0.5% magnesium stearate, all samples give softer compacts than those made with the pure materials. A study by Doelker (1987) also revealed that the tensile strength of MCC tablets decreased when compacts prepared from mixtures of 0.5% magnesium stearate and MCC. The highest magnesium stearate sensitivity of DSCB-MCCOD could be attributed to its least porous structure, highest bulk density and best flow property, easing the formation of a continuous lubricant film (Bos *et al.*, 1987; Rojas *et al.*, 2013). For instance, SCB-MCCOD and SCB-MCCSD exhibited the highest porosity (80.52 and 82.26%, respectively), had more void space to accommodate lubricant, and, at the same time, a very low lubricant sensitivity (Rojas *et al.*, 2013). Sensitivity to magnesium stearate followed the rank (most to least sensitive): DSCB-MCCOD > Avicel PH-101> DSCB-MCCSD > SCB-MCCOD > SCB-MCCSD.

3.7. Drug-Excipient Compatibility Study

The FTIR spectra of paracetamol, physical mixture (1:1) of paracetamol and SCB-MCC, and paracetamol and DSCB-MCC are displayed in Figure 3-14, 3-15 and 3-16, respectively. The structure of paracetamol contains different functional groups including -NH, O-H, C=O and aromatic ring containing C=C (Mallah *et al.*, 2015). Characteristic peaks of paracetamol are at 3570 - 3200 cm^{-1} (O−H stretching), 3360 - 3310 cm^{-1} (N−H stretching), 1680 - 1630 cm^{-1} (C=O stretching), 1650 - 1504 cm^{-1} (amide II), 1615 - 1450 cm^{-1} (the aromatic ring C=C-C stretching bands), 1377 - 1040 cm^{-1} (C−N−H group), and 810 cm^{-1} (=C-H bending) (Burgina *et al.*, 2004; Coates, 2000). All characteristic peaks of paracetamol were observed in the FTIR spectra of the physical mixture of paracetamol and SCB-MCC, and paracetamol and DSCB-MCC.

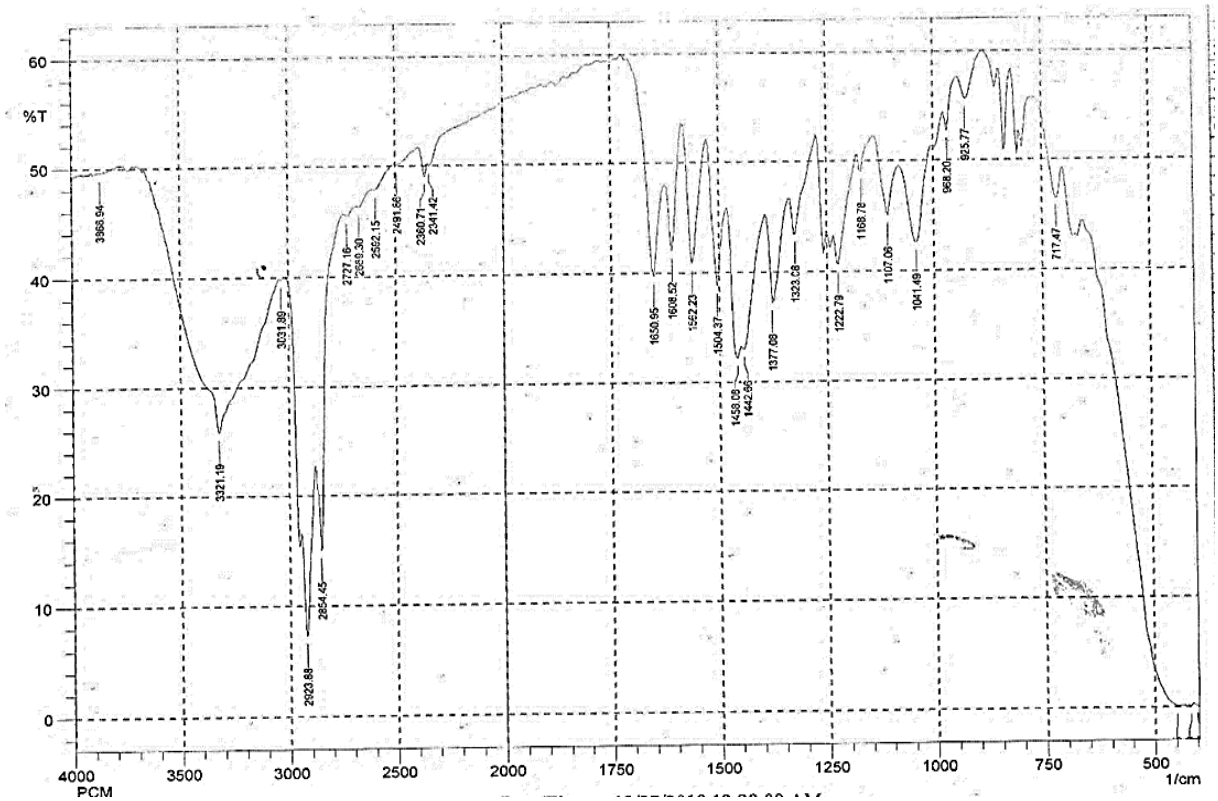

Figure 3-14: The FTIR spectrum of paracetamol.

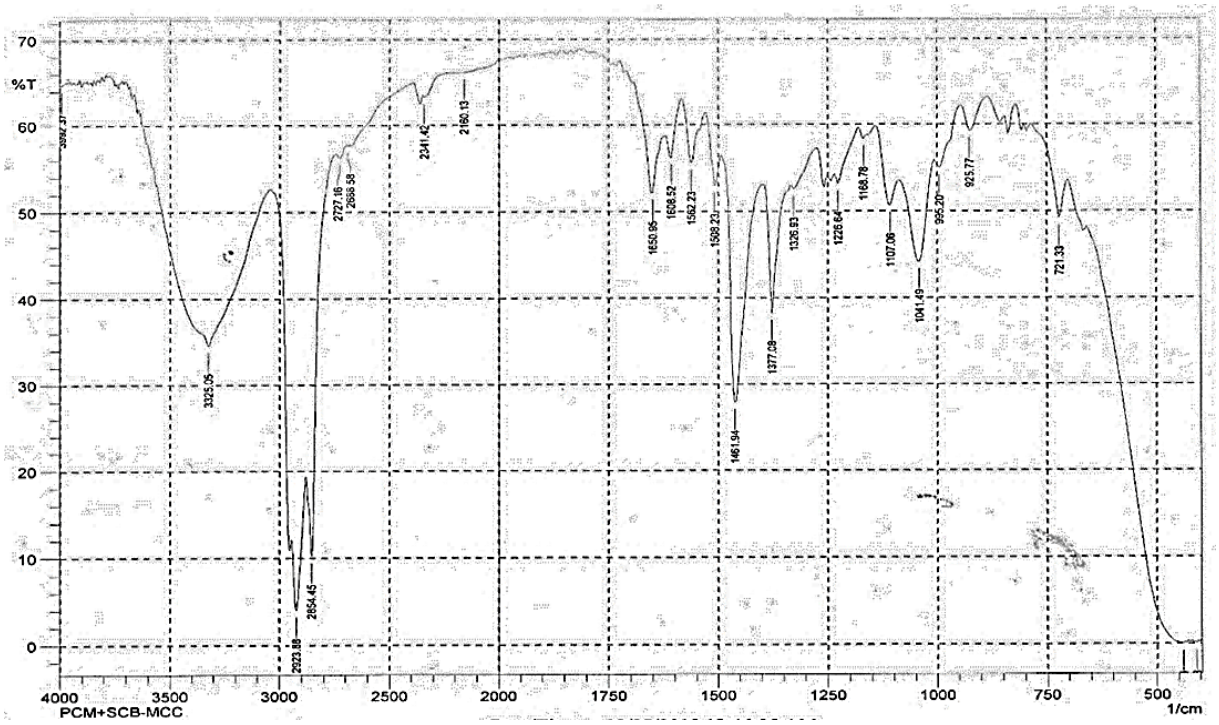

Figure 3-15: FTIR spectrum physical mixture of paracetamol and SCB-MCC.

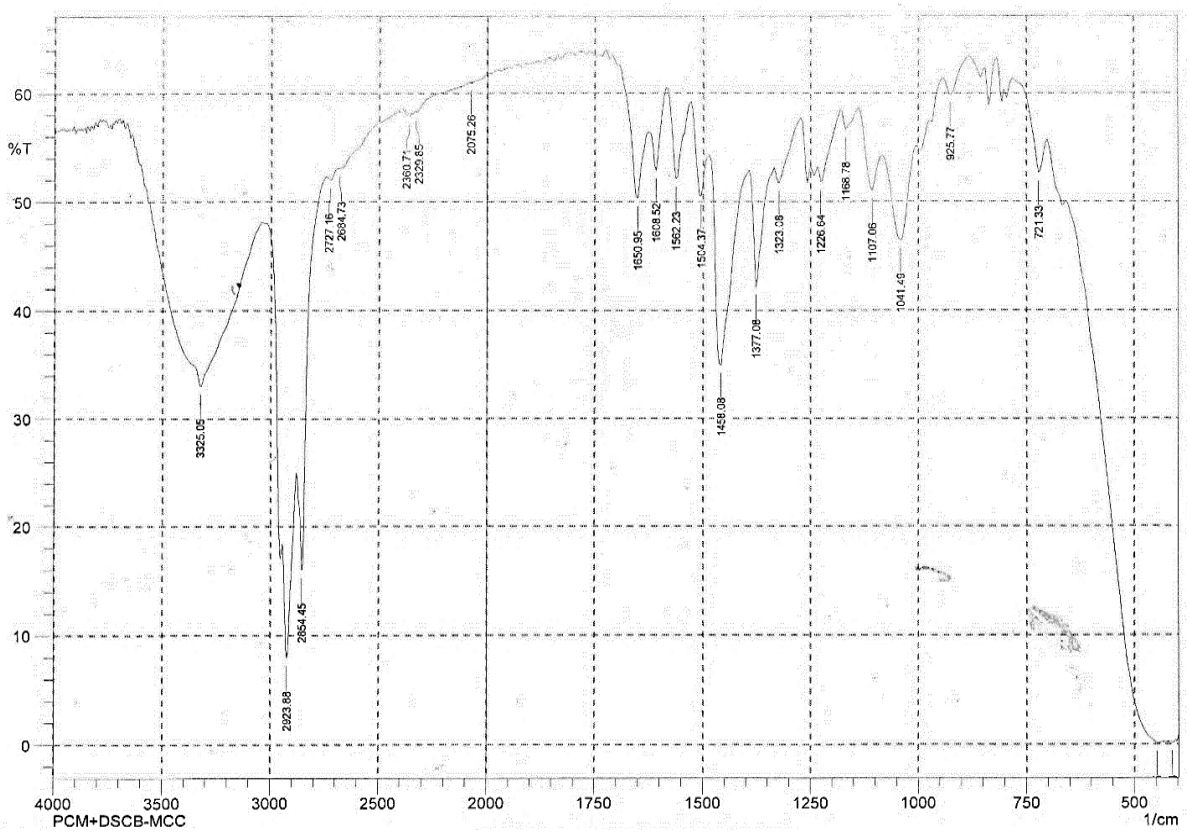

Figure 3-16: FTIR spectrum physical mixture of paracetamol and DSCB-MCC.

An extremely broad band that appeared around 3570-3200 cm^{-1} is attributed to O-H stretching. The peak at 3321 cm^{-1}, at 3325 cm^{-1} in case of mixture of paracetamol with SCB-MCC and DSCB-MCC, originates from N-H stretching (secondary amine has broad band with one sharp spike). The absorption band at 1650 cm^{-1} is associated with C=O stretching. The peaks at 1608, 1562 and 1226 cm^{-1} are attributed to C=C stretching, N-H bending and C−N stretching, respectively. A peak at 810 cm^{-1} is associated with aromatic C-H bending (Silverstein *et al.*, 1962). The peaks observed from FTIR studies suggest that there is no prominent interactions between paracetamol and MCC samples thereby showing compatibility between the samples.

3.8. Dilution Potential

Dilution potential can be defined as the amount of an active ingredient that can be satisfactorily compressed into tablets with a given directly compressible excipient. In general, it can be an indicator of the maximum amount of active pharmaceutical ingredient that can be compressed with the excipient while still obtaining tablets of acceptable quality, i.e., acceptable average

crushing strength (not less than 4 Kg or 40 N), friability (< 1.0%), good disintegration time (< 15 min), and must meet the requirement of Pharmacopeia weight variation limit test (± 5%) (Allen and Ansel, 2013; Bolhuis and de Waard, 2011; De Villiers, 2005). Dilution potential of SCB-MCCOD, SCB-MCCSD, DSCB-MCCOD, DSCB-MCCSD and Avicel PH-101 was evaluated by using paracetamol as a model drug. For the purpose of comparison, all tablets were compressed at a fixed compression force.

3.8.1. Weight variation and thickness

The paracetamol tablets prepared with SCB-MCCOD, SCB-MCCSD, DSCB-MCCOD, DSCB-MCCSD and Avicel PH-101 were examined for their weight and thickness uniformity. The results are summarized in Table 3.9. The tablets were within acceptable range of weight variation (± 5%) as per the British Pharmacopoeia for tablets weighing 250 mg or more (BP, 2009). The slightly lower average weight of the SCB-MCCOD and SCB-MCCSD containing tablets is because of their larger porosity associated with lower bulk density and hence comparable volumes of feed which result in tablets with reduced weights. The mean tablet thickness of all the formulations did not show any significant variations ($P > 0.05$).

Table 3.9: Paracetamol tablet weight and thickness at different paracetamol concentration.

Parameters	Paracetamol Conc. (%)	SCB-MCCOD	SCB-MCCSD	DSCB-MCCOD	DSCB-MCCSD	Avicel PH-101
Weight (mg)	25	386.7 ± 9.09	385.9 ± 5.52	394.1 ± 7.88	393.7 ± 6.41	394.6 ± 8.29
	40	384.2 ± 6.11	382.3 ± 4.09	390.4 ± 5.82	390.2 ± 3.30	389.3 ± 6.89
	55	382.5 ± 5.7	380.5 ± 6.58	384.9 ± 6.08	385.2 ± 4.35	385.7 ± 4.71
Thickness (mm)	25	4.89 ± 0.05	4.86 ± 0.03	4.92 ± 0.04	4.91 ± 0.04	4.87 ± 0.03
	40	4.91 ± 0.04	4.91 ± 0.06	4.94 ± 0.03	4.91 ± 0.05	4.88 ± 0.05
	55	4.93 ± 0.02	4.91 ± 0.03	4.94 ± 0.05	4.92 ± 0.03	4.9 ± 0.04

3.8.2. Crushing strength, tensile strength and friability

The resistance of the tablet to chipping, abrasion or breakage during storage, transportation and handling before usage depends on its hardness. A hardness of 4 to 6 kg (40-60 N) is considered the minimum for a satisfactory tablet (Allen and Ansel, 2013; De Villiers, 2005). The crushing strength of the tablets is plotted as a function of paracetamol concentration (Figure 3-17). When paracetamol concentration increases, the crushing strength of the tablets decreases. This is in agreement with previous work on MCC as diluent by Pesonen and Paronen (1986). Crushing

strengths of tablet preparations containing 25 and 40% paracetamol were above 40 N and could be considered strong enough to withstand rigors of handling and transportation (Nkemakolam and Ifeanyi, 2017). As shown in Figure 3-17, DSCB-MCCSD gave tablets with greater crushing strength than those made with DSCB-MCCOD ($P < 0.05$). Non-dewaxed MCC gave tablets with slightly higher ($P > 0.05$) crushing strength than those made with respective dewaxed MCC. At 70% paracetamol concentration all MCC samples produced soft tablets. Unlike to oven dried MCC, spray dried MCC and Avicel PH-101 tablet preparations containing 55% paracetamol were above minimum acceptable average crushing strength (40 N). The poorer compression properties of the oven dried MCC could be the consequence of wide particle size distribution (as reflected by their higher span value) (Padmadisastra and Gonda, 1989). Invariably, tablet formulations containing paracetamol 25, 40 and 55%, prepared with Avicel PH-101 showed significantly higher crushing strengths than those prepared with SCB-MCCOD, SCB-MCCSD, DSCB-MCCOD and DSCB- MCCSD. This might be due to higher crystallinity of Avicel PH-101 resulting in a stronger packing under the application of compression force.

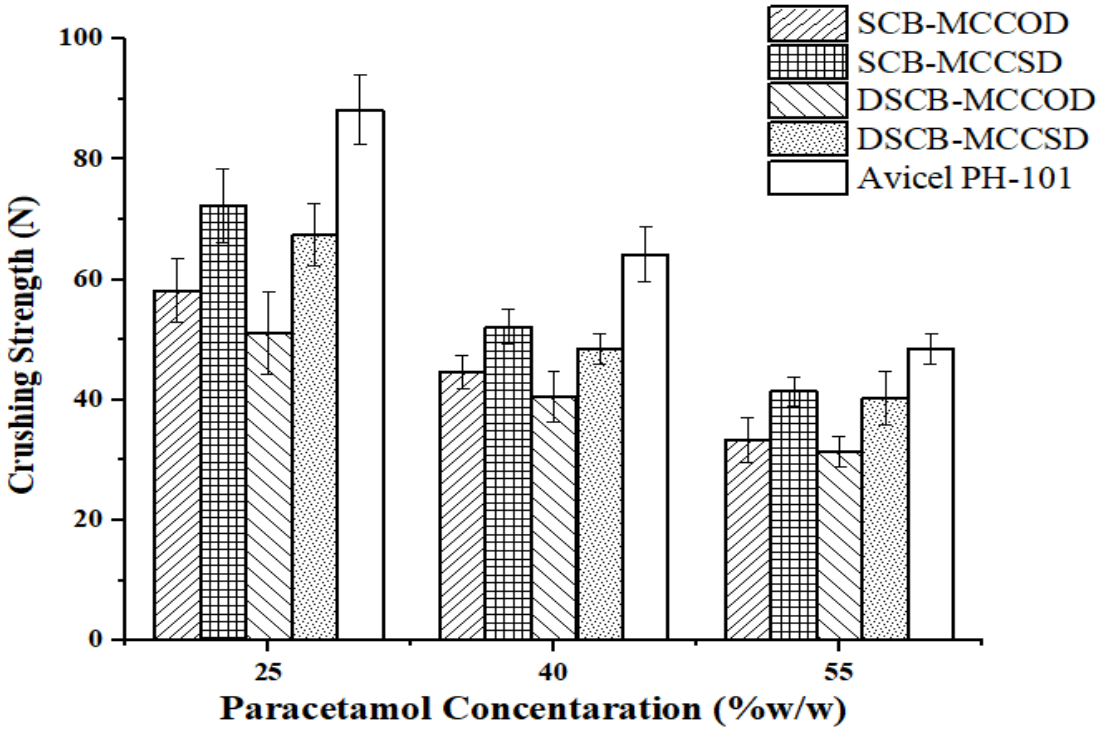

Figure 3-17: Effects of concentration of paracetamol on the hardness of tablets.

Tensile strength, which describes tablet strength, is a critical parameter which maintains consistency of property if the size of the tablet is changed (Jarosz and Parrott, 1981). The tensile

strengths of SCB-MCCOD, SCB-MCCSD, DSCB-MCCOD, DSCB-MCCSD and Avicel PH-101 tablets are depicted in Figure 3-18. Oven dried MCC tablets had lower tensile strength value than spray dried MCC tablets. Avicel PH-101 gave tablets with significantly higher ($P < 0.05$) tensile strength than MCC prepared from SCB at 25, 40 and 55% of paracetamol concentrations. This might have resulted from a high crushing strength of Avicel PH-101 tablets.

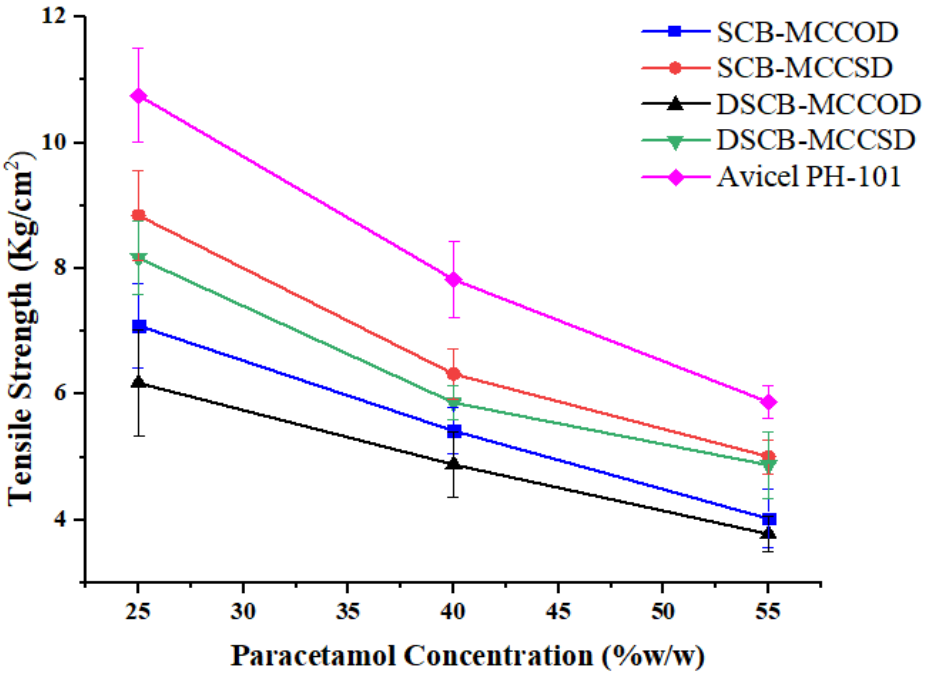

Figure 3-18: Effects of concentration of paracetamol on the tensile strength of tablets.

Friability is a measure of inter-particular cohesiveness in tablets. Conventional tablets that lose less than 1.0% of their weight are generally acceptable (BP, 2009). Friability values of SCB-MCCOD, SCB-MCCSD, DSCB-MCCOD, DSCB-MCCSD and Avicel PH-101 tablets are displayed in Figure 3-19. DSCB-MCCOD tablets had highest friability values at different paracetamol concentrations. The least hardness values of DSCB-MCCOD tablets might contribute to its highest friability. In general, a decrease in tablet hardness causes an increase in friability.

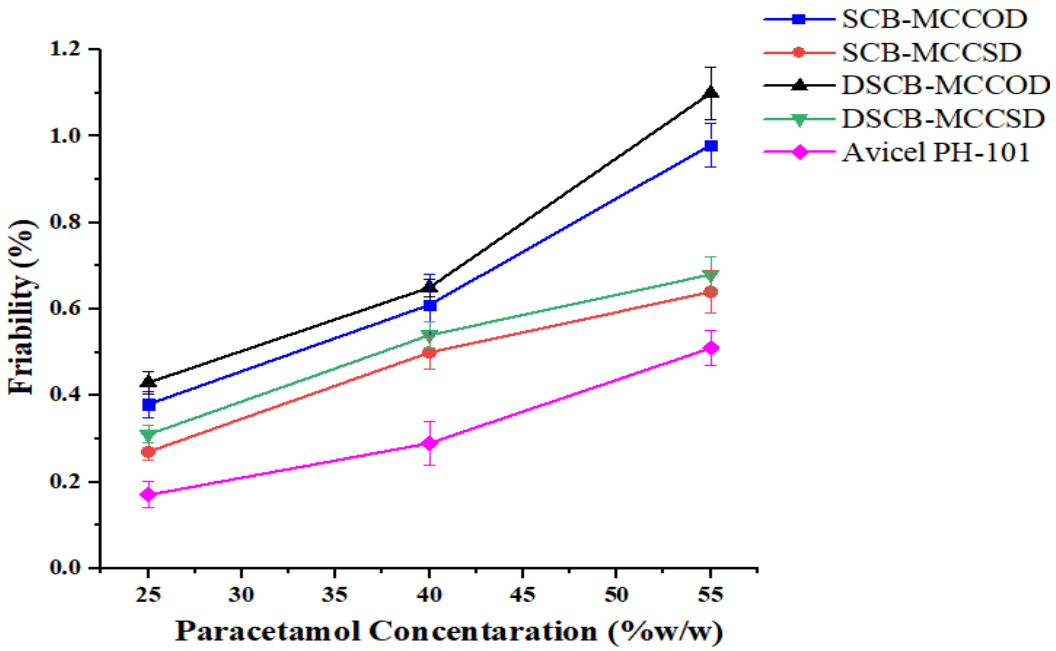

Figure 3-19: Effects of concentration of paracetamol on the friability of tablets.

3.8.3. Disintegration time of directly compressed paracetamol tablets

Disintegration test is performed to ensure that the drug substance is fully available for dissolution and absorption from the gastrointestinal tract. The disintegration test indicates the time required for a tablet to break into many small particles with a much greater total surface than the intact tablet. The disintegration of MCC tablets resulted from the penetration of water into tablet matrix by means of capillary pores and the subsequent breaking of the hydrogen bonding between cellulose microcrystals (Allen and Ansel, 2013; De Villiers, 2005; Lahdenpää *et al.*, 1997; Lowenthal *et al.*, 1972).

Disintegration times of DSCB-MCCOD, DSCB-MCCSD and Avicel PH-101 are shown in Figure 3-20 A. The disintegration times of tablets formulated by DSCB-MCCOD, DSCB-MCCSD and Avicel PH-101 decreased upon increasing of paracetamol concentration. Reduction of disintegration times might be explained on the base of tablet weakness with paracetamol content increment. Generally, the disintegration time is related to hardness. When the hardness increases, the disintegration time increased and the dissolution rate also delayed. In this study, the disintegration times of DSCB-MCCOD, DSCB-MCCSD and Avicel PH-101 paracetamol tablets were less than 15 min as given in the USP/NF specification (USP 30/NF 25, 2007).

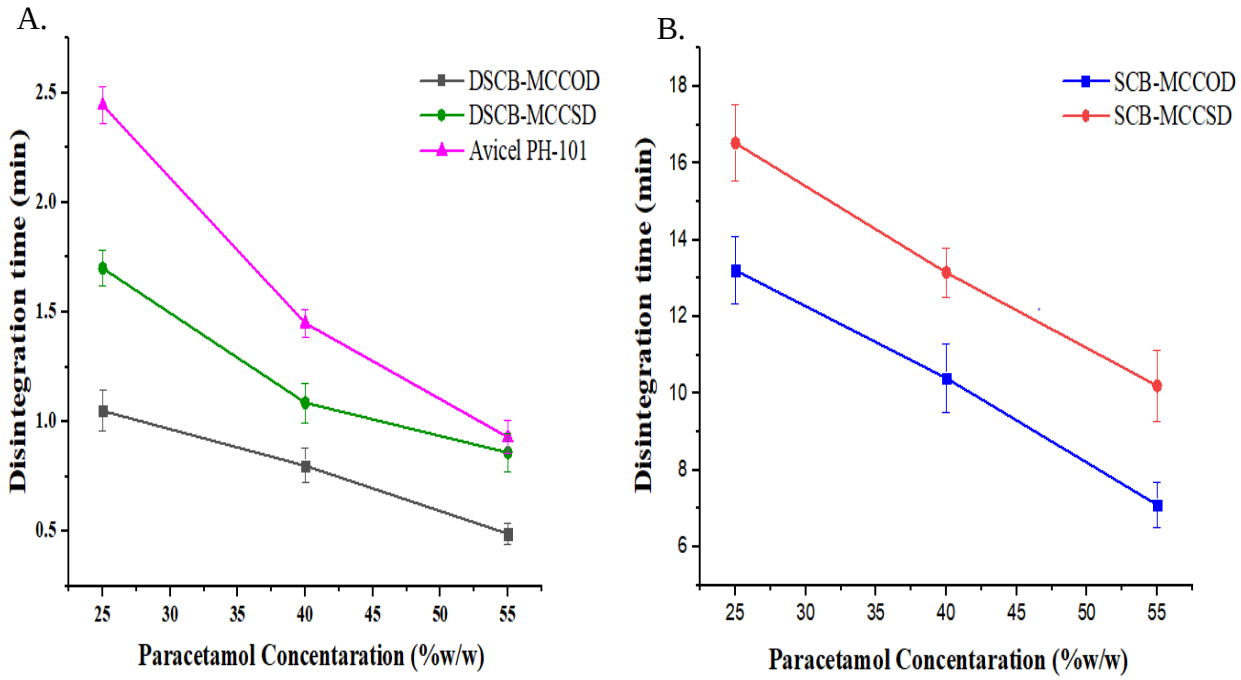

Figure 3-20: Effects of concentration of paracetamol on the disintegration times of tablets containing, DSCB-MCCOD, DSCB-MCCSD and Avicel PH-101 (A) and SCB-MCCOD and SCB-MCCSD (B).

As can be noted from Figure 3-20 B, tablets prepared from SCB-MCCOD and SCB-MCCSD had higher disintegration times, at all paracetamol concentrations, than those prepared from DSCB-MCCOD, DSCB-MCCSD and Avicel PH-101. Thus, the behaviour of the SCB-MCCOD and SCB-MCCSD based tablets was comparatively poor. Satisfactory friability (< 1.0%) corresponding to hardness in excess of 40 N was accompanied by slow disintegration. This might be caused by sufficiently high levels of wax left in MCC prepared from non-dewaxed SCB which would result in poor water uptake properties of this material and therefore long disintegration time. Tablets composed of MCC prepared from dewaxed SCB had excellent disintegration properties because they took up water and swelled up very rapidly (Padmadisastra *et al.*, 1987). Disintegration times of SCB-MCCSD tablets containing 25% paracetamol were above than 15 min and did not fulfill the acceptable quality.

3.8.4. UV calibration curve of paracetamol

From stock solution of 200 µg/ml of paracetamol in phosphate buffer (pH 5.8), standard calibration curve was plotted at nine different concentrations (µg/ml). The absorbance (at 243 nm) versus concentration of the solutions was plotted and a calibration curve with a linear

regression equation of Y = 0.056889X - 0.01167 (where Y is the absorbance and X is the concentration in µg/ml) and a correlation coefficient of 0.9997 was obtained (Figure 3-21).

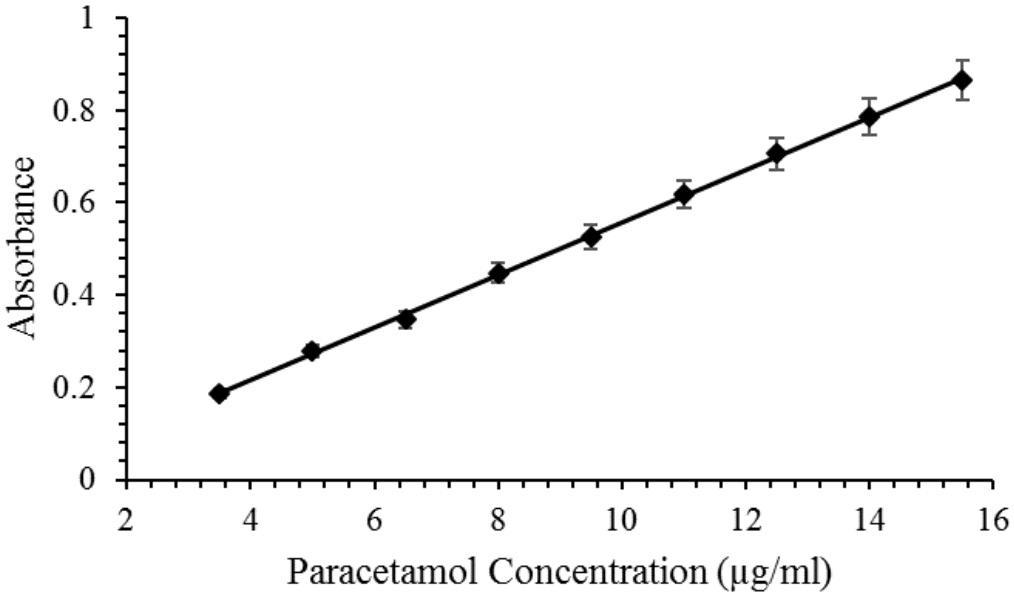

Figure 3-21: Standard calibration curve of paracetamol in phosphate buffer (pH = 5.8) at 243 nm with 95% confidence bands for the mean; (R^2 = 0.9997)

3.8.5. Dissolution of directly compressed paracetamol tablets

The bioavailability of drugs from tablets can be markedly influenced by the rate and efficiency of the initial disintegration and dissolution processes. The goal of *in-vitro* dissolution testing is to provide as far as possible, a reasonable prediction of, or correlation with, the product's *in-vivo* bioavailability (Allen and Ansel, 2013; De Villiers, 2005). The dissolution profiles of the paracetamol tablets (25%, 40% and 55% w/w) produced from different MCC samples are shown in Figure 3-22. All formulations which contain DSCB-MCCOD, DSCB-MCCSD and Avicel PH-101 fulfilled the specification of the USP/NF (USP 30/NF 25, 2007) i.e., > 80% of the tablet content should be released within 30 min, and > 90% of the tablet content should be released within 45 min. Although SCB-MCCOD tablets containing 55% of paracetamol fulfilled both of the specifications, these tablets had crushing strength < 40 N. The poor disintegration and dissolution performances of the SCB-MCCOD and SCB-MCCSD tablets could have resulted from sufficiently high levels of wax. The hydrophobic residue could reduce surface wettability, decreasing dissolution rates and prolonging disintegration times of these product.

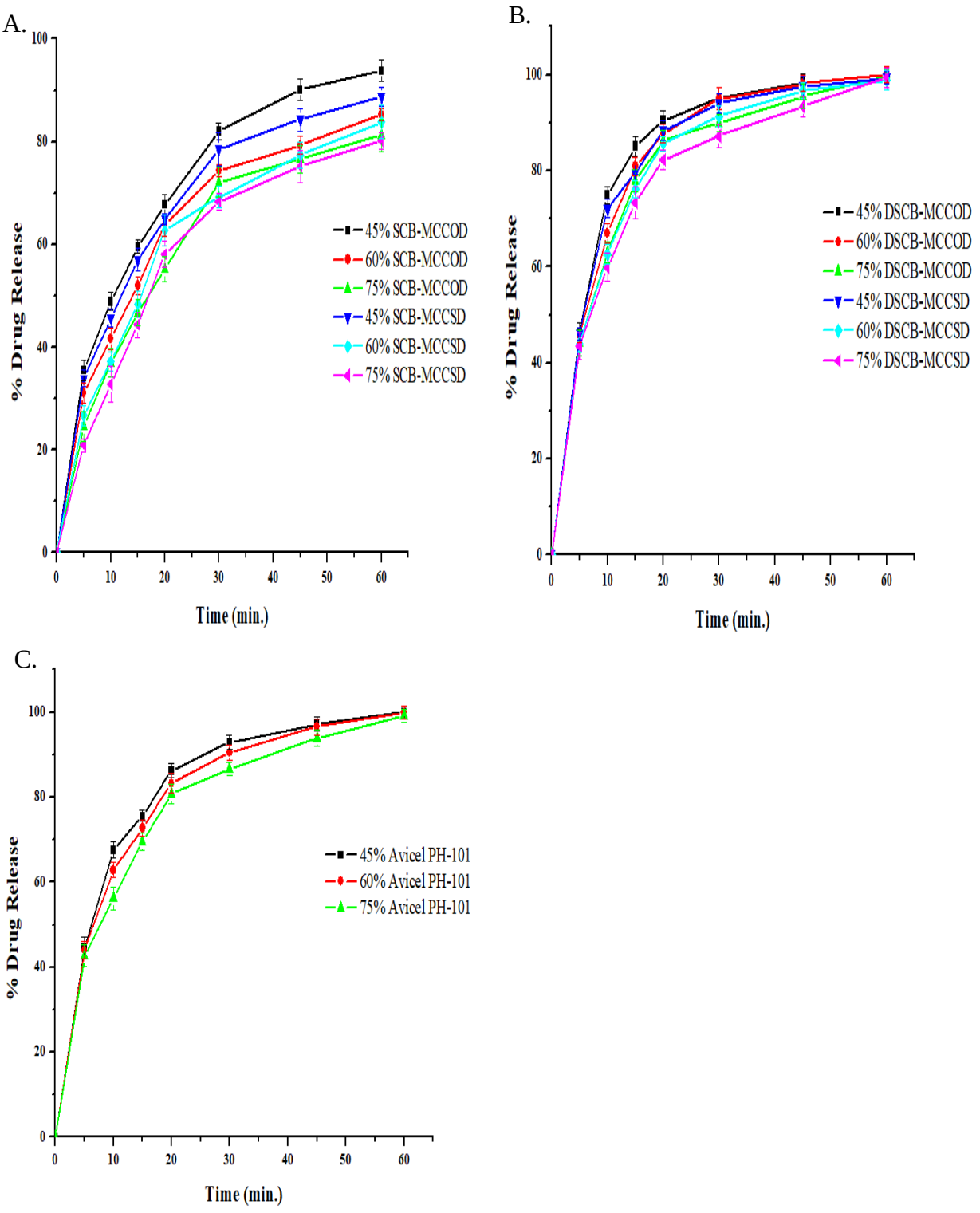

Figure 3-22: Dissolution profiles of non-dewaxed SCB MCC (A), dewaxed SCB MCC (B) and Avicel PH-101 (C) tablets with different concentrations of paracetamol.

4. CONCLUSIONS

Chemical composition and physico-chemical characteristics of cellulose and MCC varied depending on the effectiveness of the extraction method employed. Combining a dewaxing procedure with acid pretreatment provided high-quality cellulose and MCC. Cellulose and MCC yields of dewaxed SCB were comparable with reported values for standard counter-parts. TGA analyses of dewaxed SCB cellulose and MCC confirmed their relative purity. SEM of DSCBC showed characteristic morphology that was fibrous while SEM of DSCB-MCCI revealed it was rod in shape. DP of all MCC preparations was within USP/NF specification. Except SCB-MCCI and DSCB-MCCI, all prepared MCC had monomodal normal particle size distribution. When compared to Avicel PH-101, all MCC samples had lower crushing and tensile strength. Spray dried products had better hardness and tensile strength than their respective oven dried products. Plain tablets of SCB-MCCOD and SCB-MCCSD had longer disintegration times than DSCB-MCCOD, DSCB-MCCSD and Avicel PH-101. DSCB-MCCOD had the highest LSR while other MCC preparations had comparatively low LSR than Avicel PH-101. Spray dried products had better dilution potential than their respective oven dried products. With similar compression force and paracetamol concentration, the MCC preparations had lower tablet quality attributes than Avicel PH-101. However, at a comparable crushing strength, DSCB-MCCOD, DSCB-MCCSD and Avicel PH-101 had comparable friability, disintegration time and dissolution profile. Yet, SCB-MCCOD and SCB-MCCOD had a long disintegration time and retarded *in-vitro* dissolution. Thus, dewaxed SCB could be a promising locally available potential source of cellulose and MCC for pharmaceutical applications.

5. SUGGESTIONS FOR FURTHER WORK

Further work should be undertaken on the following:

- Morphological characterization of SCBC, SCB-MCCI, SCB-MCCOD, SCB-MCCSD, DSCB-MCCOD and DSCB-MCCSD;
- Crystallinity improving techniques for SCB-MCCOD, SCB-MCCSD, DSCB-MCCOD and DSCB-MCCSD;
- Deformation characteristics of SCB-MCCOD, SCB-MCCSD, DSCB-MCCOD and DSCB-MCCSD; and
- Long- and short-term stability studies of tablets produced from SCB-MCCOD, SCB-MCCSD, DSCB-MCCOD and DSCB-MCCSD.

REFERENCES

Adedokun, M., Essien, G., Uwah, T., Umoh, R., Josiah, I. and Jackson, C., 2014. Evaluation of the release properties of microcrystalline cellulose derived from Saccharum officinarum L. in paracetamol tablet formulation. *J Pharm Sci & Res* **6**: 2014, 342-346.

Adel, A.M., El-Wahab, Z.H.A., Ibrahim, A.A. and Al-Shemy, M.T., 2011. Characterization of microcrystalline cellulose prepared from lignocellulosic materials. Part II: Physico-chemical properties. *Carbohydr Polym* **83**: 676-687.

Ahvenainen, P., Kontro, I. and Svedström, K., 2016. Comparison of sample crystallinity determination methods by X-ray diffraction for challenging cellulose I materials. *Cellulose* **23**: 1073-1086.

Akgeyik, E., Kaynak, M.S., Çelebier, M., Altınöz, S. and Şahin, S., 2016. Evaluation of pharmaceutical quality of conventional dosage forms containing paracetamol and caffeine available in the Turkish drug market. *Dissolut Technol* **23**: 36-41.

Alemdar, A. and Sain, M., 2008. Isolation and characterization of nanofibers from agricultural residues–Wheat straw and soy hulls. *Bioresour Technol* **99**: 1664-1671.

Allen, L. and Ansel, H.C., 2013. Solid dosage forms and solid oral modified-release dosage forms. In: Allen, L.V., Popovich, N.G., and Ansel, H.C. eds, *Ansel's Pharmaceutical Dosage Forms and Drug Delivery Systems*, 9^{nth} edn, Lippincott Williams & Wilkins, China, pp 233-235.

Amin, F.R., Khalid, H., Zhang, H., u Rahman, S., Zhang, R., Liu, G. and Chen, C., 2017. Pretreatment methods of lignocellulosic biomass for anaerobic digestion. *AMB Express* **7**:72.

Asl SA, Mousavi M, Labbafi M., 2017. Synthesis and characterization of carboxymethyl cellulose from sugarcane bagasse. *J Food Process Technol* **8**: 687.

ASTM D1348-94., 2003. Standard test methods for moisture in cellulose, ASTM International, West Conshohocken, PA, 2003, www.astm.org

Attard, T.M., McElroy, C.R., Rezende, C.A., Polikarpov, I., Clark, J.H. and Hunt, A.J., 2015. Sugarcane waste as a valuable source of lipophilic molecules. *Ind Crops Prod* **76**: 95-103.

Battista, O.A. and Smith, P.A., 1962. Microcrystalline cellulose. *Ind Eng Chem* **54**: 20-29.

Battista, O.A., 1950. Hydrolysis and crystallization of cellulose. *Ind Eng Chem* **42**: 502-507.

Bezerra, T.L. and Ragauskas, A.J., 2016. A review of sugarcane bagasse for second-generation bioethanol and biopower production. *Biofuels Bioprod Biorefin* **10**: 634-647.

Bhimte, N.A. and Tayade, P.T., 2007. Evaluation of microcrystalline cellulose prepared from sisal fibers as a tablet excipient: A technical note. *Aaps Pharmscitech* **8**: 56-E62.

Bolhuis, G.K. and de Waard, H., 2011. Compaction properties of directly compressible materials. In: Çelik, M. ed, *Pharmaceutical Powder Compaction Technology,* 2nd edn, Informa Healthcare, London, pp 152-217.

Bolhuis, G.K. and Holzer, A.W., 2011. Lubrication issues in direct compaction. In: Çelik, M. ed, *Pharmaceutical Powder Compaction Technology,* 2nd edn, Informa Healthcare, London, pp 218-247.

Bos, C.E., Bolhuis, G.K., Van Doorne, H. and Lerk, C.F., 1987. Native starch in tablet formulations: properties on compaction. *Pharm Weekbl* **9**: 274-282.

British Pharmacopoeia., 2009. British Pharmacopoeia: The Pharmaceutical Press, Her Majesty‟s Stationery Office, London, vol. I−VI.

Brodeur, G., Yau, E., Badal, K., Collier, J., Ramachandran, K.B. and Ramakrishnan, S., 2011. Chemical and physico-chemical pretreatment of lignocellulosic biomass. *Enzyme Res* **2011**: 1-18.

Burgina, E.B., Baltakhinov, V.P., Boldyreva, E.V. and Shakhtschneider, T.P., 2004. IR spectra of paracetamol and phenacetin. 1. Theoretical and experimental studies. *J Struct Chem* **45**: 64-73.

Candido, R.G. and Gonçalves, A.R., 2016. Synthesis of cellulose acetate and carboxymethylcellulose from sugarcane straw. *Carbohydr Polym* **152**: 679-686.

Chen, W., Yu, H., Liu, Y., Chen, P., Zhang, M. and Hai, Y., 2011. Individualization of cellulose nanofibers from wood using high-intensity ultrasonication combined with chemical pretreatments. *Carbohydr Polym* **83**: 1804-1811.

Ciacco, G.T., Ramos, L.A., Frollini, E. And Ass, B.A., 2008. Sisal, sugarcane bagasse and microcrystalline celluloses: influence of the composition of the solvent system N, Ndimethylacetamide/lithium chloride on the solubility and acetylation of these polysaccharides. *e-Polym* **8**: 226-236.

Coates, J., 2000. Interpretation of infrared spectra, a practical approach. In: *Encyclopedia of Analytical Chemistry: Applications, Theory and Instrumentation*, John Wiley & Sons, USA, pp 1-23.

Coffey, D.G., Bell, D.A. and Henderson, A., 2006. Cellulose and cellulose derivatives. In: Stephen, A.M., Phillips, G.O., and Williams, P.A. eds, *Food Polysaccharides and Their Applications*, 2nd edn, Taylor & Francis, New York, pp 147-180.

Cybulska, J., Szymańska-Chargot, M., Zdunek, A., Psonka-Antonczyk, K.M. and Stokke, B.T., 2011. Crystallinity and nanostructure of cellulose from different sources. *ICEF* **11**: 1-4.

De Villiers, M.M., 2004. Oral conventional solid dosage forms: Powders and granules, tablets, lozenges, and capsules. In: Ghosh, T.K., and Jasti, B.R. eds, *Theory and Practice of Contemporary Pharmaceutics*, 1st edn, CRC press, USA, pp 307-310.

Deepa, B., Abraham, E., Koshy, R.R., Pothan, L.A. and Thomas, S., 2015. Extraction and characterization of cellulose nanofibers from banana plant. In: Pandey, J.K., Takagi, H., Nakagaito, A.N., and Kim, H.J. eds. *Handbook of Polymer Nanocomposites. Processing, Performance and Application,* Volume C, Springer, Berlin, pp 65-80.

Doelker, E., 1993. Comparative compaction properties of various microcrystalline cellulose types and generic products. *Drug Dev Ind Pharm* **19**: 2399-2471.

Doelker, E., Massuelle, D., Veuillez, F. and Humbert-Droz, P., 1995. Morphological, packing, flow and tableting properties of new Avicel types. *Drug Dev Ind Pharm* **21**: 643-661.

Doelker, E., Mordier, D., Iten, H. and Humbert-Droz, P., 1987. Comparative tableting properties of sixteen microcrystalline celluloses. *Drug Dev Ind Pharm* **13**: 1847-1875.

Draman, S.F.S., Daik, R. and Mohd, N., 2016. Eco-Friendly Extraction and Characterization of Cellulose from Lignocellulosoic Fiber. *ARPN J Eng Appl Sci* **11**: 9591-9595.

Edge, S., Steele, D.F., Chen, A., Tobyn, M.J. and Staniforth, J.N., 2000. The mechanical properties of compacts of microcrystalline cellulose and silicified microcrystalline cellulose. *Int J Pharm* **200**: 67-72.

El-Sakhawy, M. and Hassan, M.L., 2007. Physical and mechanical properties of microcrystalline cellulose prepared from agricultural residues. *Carbohydr Polym* **67**: 1-10.

Ethiopian Sugar Corporation Omo-Kuraz Sugar Factory III to be inaugurated on Sunday(https://semonegna.com/omo-kuraz-sugar-factory-iii-inaugurated/v).

Fahma, F., Iwamoto, S., Hori, N., Iwata, T. and Takemura, A., 2010. Isolation, preparation, and characterization of nanofibers from oil palm empty-fruit-bunch (OPEFB). *Cellulose* **17**: 977-985.

Fan, L.S., Zhu, C., 1998. Size and properties of particles. In: *Principles of Gas-Solid Flow*, Cambridge University Press, Cambridge, pp 3-24.

Fenta, D.T., 2010. The economic significance of using bagasse as a source of raw material for pulp manufacturing: a case of Ethiopia (Doctoral dissertation, University of South Africa, South Africa).

Figueiredo, J.A., Ismael, M.I., Anjo, C.M.S. and Duarte, A.P., 2010. Cellulose and derivatives from wood and fibers as renewable sources of raw-materials. In: Rauter, A.P., Vogel, P., and Queneau, Y. eds, *Carbohydrates in Sustainable Development I*, Volume 294, Springer, Berlin, pp 117-128.

FMC (2003). Avicel® PH-101microcrystalline cellulose NF, Ph. Eur., JP., FMC Corporation, Philadelphia.

Gbenga, B.L. and Fatimah, O.F., 2014. Investigation of α-cellulose content of sugarcane scrappings and bagasse as tablet disintegrant. *J Basic Appl Sci* **10**: 142-148.

Gohel, M.C. and Jogani, P.D., 2005. A review of co-processed directly compressible excipients. *J Pharm Pharm Sci* **8**: 76-93.

Granström, M., 2009. Cellulose derivatives: synthesis, properties and applications (Academic dissertation, University of Helsinki, Helsinki).

Gurgel, L.V.A., Marabezi, K., Ramos, L.A. and da Silva Curvelo, A.A., 2012. Characterization of depolymerized residues from extremely low acid hydrolysis (ELA) of sugarcane bagasse cellulose: Effects of degree of polymerization, crystallinity and crystallite size on thermal decomposition. *Ind Crops Prod* **36**: 560-571.

Habib, Y., Augsburger, L., Reier, G., Wheatley, T. and Shangraw, R., 1996. Dilution potential: a new perspective. *Pharm Dev Technol* **1**: 205-212.

Hassan, M.L., 2015. Bagasse and rice straw nanocellulosic materials and their applications. In: Pandey J.K., Takagi H., Nakagaito A.N., and Kim H.J. eds. *Handbook of Polymer Nanocomposites. Processing, Performance and Application,* Volume C, Springer, Berlin, pp 47-64.

Hidayati, S., Zuidar, A.S. and Satyajaya, W., 2017. Effect of acetic acid: Formic acid ratio on characteristics of pulp from oil palm empty fruit bunches (OPEFB). *ARPN J Eng Appl Sci* **12**: 3802-3807.

Ho, T.T.T., Zimmermann, T., Hauert, R. and Caseri, W., 2011. Preparation and characterization of cationic nanofibrillated cellulose from etherification and high-shear disintegration processes. *Cellulose* **18**: 391-1406.

Huang, K.L., Wang, B., Peng, X.Y., Wang, Z.F., Li, K.X., Wu, R. and Wang, J.S., 2012. The preparation of sugarcane bagasse microcrystaline cellulose in Subcritical Water/CO2. *Adv Mater Res* **396**:1769-1772.

Ibrahim, M.M., El-Zawawy, W.K., Jüttke, Y., Koschella, A. and Heinze, T., 2013. Cellulose and microcrystalline cellulose from rice straw and banana plant waste: preparation and characterization. *Cellulose* **20**: 2403-2416.

Jahan, M.S., Rumee, J.N., Rahman, M.M. and Quaiyyum, A., 2014. Formic acid/acetic acid/water pulping of agricultural wastes. *Cellul Chem Technol* **48**:111-118

Jahan, M.S., Saeed, A., He, Z. and Ni, Y., 2011. Jute as raw material for the preparation of microcrystalline cellulose. *Cellulose* **18**: 451-459.

Jarosz, P.J. and Parrott, E.L., 1982. Tensile strengths and hardness of tablets. *J Pharm Sci* **71**: 705-707.

Kachrimanis, K., Noisternig, M.F., Griesser, U.J. and Malamataris, S., 2006. Dynamic moisture sorption and desorption of standard and silicified microcrystalline cellulose. *Eur J Pharm Biopharm* **64**: 307-315.

Karande, V.S., Bharimalla, A.K., Hadge, G.B., Mhaske, S.T. and Vigneshwaran, N., 2011. Nanofibrillation of cotton fibers by disc refiner and its characterization. *Fibers Polym* **12**: 399.

Karim, M., Chowdhury, Z., Hamid, S. and Ali, M., 2014. Statistical optimization for acid hydrolysis of microcrystalline cellulose and its physiochemical characterization by using metal ion catalyst. *Materials **7***: 6982-6999.

Kim, S.H., Lee, C.M. and Kafle, K., 2013. Characterization of crystalline cellulose in biomass: basic principles, applications, and limitations of XRD, NMR, IR, Raman, and SFG. *Korean J Chem Eng* **30**: 2127-2141.

Klemm, D., Philpp, B., Heinze, T., Heinze, U. and Wagenknecht, W., 1998. Experimental protocols for the analysis of cellulose. In: Klemm, D., Philpp, B., Heinze, T., Heinze, U. and Wagenknecht, W. *Comprehensive Cellulose Chemistry. Volume 1: Fundamentals and Analytical Methods*, Volume 1, Wiley-VCH Verlag Weinheim, Germany, pp 234-235.

Kothari, S.H., Kumar, V. and Banker, G.S., 2002. Comparative evaluations of powder and mechanical properties of low crystallinity celluloses, microcrystalline celluloses, and powdered celluloses. *Int J Pharm* **232**: 69-80.

Kuentz, M. and Leuenberger, H., 2000. A new theoretical approach to tablet strength of a binary mixture consisting of a well and a poorly compactable substance. *Eur J Pharm Biopharm* **49**: 151-159.

Kumar, C.G., Kumar, M.P., Gupta, S., Sunder, M.S., Rao, K.V.M., Jagadeesh, B., Swapna, V. and Kamal, A., 2015. Isolation and characterization of cellulose from sweet sorghum Bagasse. *Sugar Tech* **17**: 395-403.

Kumar, V. and Kothari, S.H., 1999. Effect of compressional force on the crystallinity of directly compressible cellulose excipients. *Int J Pharm* **177**: 173-182.

Kusumattaqiin, F. and Chonkaew, W., 2015. Preparation and characterization of microcrystalline cellulose (MCC) by acid hydrolysis using microwave assisted method from cotton wool. *Macromol Symp* **354**: 35-41.

Lahdenpää, E., Niskanen, M. and Yliruusi, J., 1997. Crushing strength, disintegration time and weight variation of tablets compressed from three Avicel® PH grades and their mixtures. *Eur J Pharm Biopharm* **43**: 315-322.

Lam, N.T., Chollakup, R., Smitthipong, W., Nimchua, T. and Sukyai, P., 2017. Characterization of cellulose nanocrystals extracted from sugarcane bagasse for potential biomedical materials. *Sugar Tech* **19**: 539-552.

Laopaiboon, P., Thani, A., Leelavatcharamas, V. and Laopaiboon, L., 2010. Acid hydrolysis of sugarcane bagasse for lactic acid production. *Bioresour Technol* **101**: 1036-1043.

Leão, R.M., Miléo, P.C., Maia, J.M. and Luz, S.M., 2017. Environmental and technical feasibility of cellulose nanocrystal manufacturing from sugarcane bagasse. *Carbohydr Polym* **175**: 518-529.

Liao, Z., Zhang, N., Zhao, G., Zhang, J., Liang, X., Zhong, S., Wang, G. and Chen, X., 2012. Multivariate analysis approach for correlations between material properties and tablet tensile strength of microcrystalline cellulose. *Die Pharmazie- Int J Pharm Sci* **67**: 774-780.

Liu, C.F., Ren, J.L., Xu, F., Liu, J.J., Sun, J.X. and Sun, R.C., 2006. Isolation and characterization of cellulose obtained from ultrasonic irradiated sugarcane bagasse. *J Agric Food Chem* **54**: 5742-5748.

Lowenthal, W., 1972. Disintegration of tablets. *J Pharm Sci* **61**: 695-1711.

Lu, P. and Hsieh, Y.L., 2012. Preparation and characterization of cellulose nanocrystals from rice straw. *Carbohydr Polym* **87**: 564-573.

Mallah, M.A., Sherazi, S.T.H., Bhanger, M.I., Mahesar, S.A. and Bajeer, M.A., 2015. A rapid Fourier-transform infrared (FTIR) spectroscopic method for direct quantification of paracetamol content in solid pharmaceutical formulations. *Spectrochim Acta Part A* **141**: 64-70.

Mandal, A. and Chakrabarty, D., 2011. Isolation of nanocellulose from waste sugarcane bagasse (SCB) and its characterization. *Carbohydr Polym* **86**: 1291-1299.

Marques-Marinho, F.D. and Vianna-Soares, C.D., 2013. Cellulose and its derivatives use in the pharmaceutical compounding practice. In: Ven, T. ed, *Cellulose-Medical, Pharmaceutical and Electronic Applications*, InTech, Canada, pp 141-162.

Mashego, D.V., 2016. Preparation, isolation and characterization of nanocellulose from sugarcane bagasse (Doctoral dissertation, Durban University of Technology, South Africa).

McMillan, J.D., 1994. Pretreatment of lignocellulosic biomass. *ACS symposium series* **566**: 292-321.

Michel, D., Bachelier, B., Drean, J.Y. and Harzallah, O., 2013. Preparation of cellulosic fibers from sugarcane for textile use. *Conf Pap Sci* **2013**: 1-6.

Mihranyan, A., Llagostera, A.P., Karmhag, R., Strømme, M. and Ek, R., 2004. Moisture sorption by cellulose powders of varying crystallinity. *Int J Pharm* **269**: 433-442.

Moon, R.J., Martini, A., Nairn, J., Simonsen, J. and Youngblood, J., 2011. Cellulose nanomaterials review: structure, properties and nanocomposites. *Chem Soc Rev* **40**: 3941-3994.

Morán, J.I., Alvarez, V.A., Cyras, V.P. and Vázquez, A., 2008. Extraction of cellulose and preparation of nanocellulose from sisal fibers. *Cellulose* **15**: 149-159.

Mothé, C.G. and de Miranda, I.C., 2009. Characterization of sugarcane and coconut fibers by thermal analysis and FTIR. *J Therm Anal Calorim* **97**: 661.

Mužíková, J. and Nováková, P., 2007. A study of the properties of compacts from silicified microcrystalline celluloses. *Drug Dev Ind Pharm* **33**: 775-781.

Nakai, Y., Fukuoka, E., Nakajima, S. and Hasegawa, J., 1977. Crystallinity and physical characteristics of microcrystalline cellulose. *Chem Pharm Bull* **25**: 96-101.

Nazir, M.S., Wahjoedi, B.A., Yussof, A.W. and Abdullah, M.A., 2013. Eco-friendly extraction and characterization of cellulose from oil palm empty fruit bunches. *BioResources* **8**: 2161-2172.

Nkemakolam, N. and Ifeanyi, O.S., 2017. Effect of drying methods on the powder and compaction properties of microcrystalline cellulose derived from Cocos nucifera. *Br J Pharm Res* **20**.

Nogami, H., Nagai, T., Fukuoka, E. and Sonobe, T., 1969. Disintegration of the aspirin tablets containing potato starch and microcrystalline cellulose in various concentrations. *Chem Pharm Bull* **17**: 1450-1455.

Nokhodchi, A., 2005. Effect of moisture on compaction and compression. *Pharm Tech* **6**: 46-66.

Obae, K., Iijima, H. and Imada, K., 1999. Morphological effect of microcrystalline cellulose particles on tablet tensile strength. *Int J Pharm* **182**: 155-164.

Ohwoavworhua, F.O. and Adelakun, T.A., 2010. Non-wood fibre production of microcrystalline cellulose from Sorghum caudatum: Characterisation and tableting properties. *Indian J Pharm Sci* **72**: 295.

Padmadisastra, Y. and Gonda, I., 1989. Preliminary studies of the development of a direct compression cellulose excipient from bagasse. *J Pharm Sci* **78**: 508-514.

Padmadisastra, Y., Sawayanagi, Y., Nagai, T. and Gonda, I., 1987. Development of a tablet excipient from bagasse. *Chem Pharm Bull* **35**: 289-293.

Patel, S., Kaushal, A.M. and Bansal, A.K., 2006. Compression physics in the formulation development of tablets. *Crit Rev Ther Drug Carrier Syst **23***.

Peng, Y., Han, Y. and Gardner, D.J., 2012. Spray-drying cellulose nanofibrils: effect of drying process parameters on particle morphology and size distribution. *Wood Fiber Sci* **44**: 448-461.

Pesonen, T. and Paronen, P., 1986. Evaluation of a new cellulose material as binding agent for direct compression of tablets. *Drug Dev Ind Pharm* **12**: 2091-2111.

Pesonen, T., Paronen, P. and Puurunen, T., 1989. Evaluation of a novel cellulose powder as a filler-binder for direct compression of tablets. *Pharm Weekbl* **11**: 13-19.

Podczeck, F. and Révész, P., 1993. Evaluation of the properties of microcrystalline and microfine cellulose powders. *Int J Pharm* **91**: 183-193.

Poletto, M., Ornaghi, H.L. and Zattera, A.J., 2014. Native cellulose: structure, characterization and thermal properties. *Materials* **7**: 6105-6119.

Poopak, S. and Reza, A.R., 2012. Environmental benefit of using bagasse in paper production. A case study of LCA in Iran. In: Singh, B.R. ed, *Global Warming-Impacts and Future Perspective*, InTech, England, pp 205-225.

Popescu, M.C., Popescu, C.M., Lisa, G. and Sakata, Y., 2011. Evaluation of morphological and chemical aspects of different wood species by spectroscopy and thermal methods. *J Mol Struct* **988**: 65-72.

Princi, E., Vicini, S., Pedemonte, E., Mulas, A., Franceschi, E., Luciano, G. and Trefiletti, V., 2005. Thermal analysis and characterisation of cellulose grafted with acrylic monomers. *Thermochim Acta* **425**: 173-179.

Qi, G., Peng, F., Xiong, L., Lin, X., Huang, C., Li, H., Chen, X. and Chen, X., 2017. Extraction and characterization of wax from sugarcane bagasse and the enzymatic hydrolysis of dewaxed sugarcane bagasse. *Prep Biochem Biotechnol* **47**: 276-281.

Radotić, K. and Mićić, M., 2016. Methods for extraction and purification of lignin and cellulose from plant tissues. In: Mićić, M. ed, *Sample Preparation Techniques for Soil, Plant, and Animal Samples*, Springer Protocols Handbooks, Humana Press, New York, pp 365-376.

Ramos, L.P., 2003. The chemistry involved in the steam treatment of lignocellulosic materials. *Quim. Nova* **26**: 863-871.

Rípoli, T.C.C., Molina Jr, W.F. and Rípoli, M.L.C., 2000. Energy potential of sugar cane biomass in Brazil. *Sci Agric* **57**: 677-681.

Rohan, 2015. Cellulose fiber market: Available at: (http://www.marketsandmarkets.com/PressReleases/cellulose-fiber.asp). Accessed on 19/10/2017.

Rojas, J.J., Aristizabal, J. and Henao, M., 2013. Screening of several excipients for direct compression of tablets: A new perspective based on functional properties. *Rev Cienc Farm Basica Apl* **34**: 17-23.

Rosli, N.A., Ahmad, I. and Abdullah, I., 2013. Isolation and characterization of cellulose nanocrystals from Agave angustifolia fibre. *BioResources* **8**: 1893-1908.

Rowe, R.C., Sheskey, P.J., and Quinn, M.E. eds, 2009. Microcrystalline cellulose. In: *Handbook of Pharmaceutical Excipients*, 6th edn, Pharmaceutical press, USA, pp 129-131.

Roy, D., Semsarilar, M., Guthrie, J.T. and Perrier, S., 2009. Cellulose modification by polymer grafting: a review. *Chem Soc Rev* **38**: 2046-2064.

Rumman, M., 2009. Understanding the functionality of MCC rapid as an excipient for DC-moving towards QbD (Doctoral dissertation, University of Basel, Basel).

Segal, L.G.J.M.A., Creely, J.J., Martin Jr, A.E. and Conrad, C.M., 1959. An empirical method for estimating the degree of crystallinity of native cellulose using the X-ray diffractometer. *Text Res J* **29**: 786–794.

Shanmugam, N., Nagarkar, R.D. and Kurhade, M., 2015. Microcrystalline cellulose powder from banana pseudostem fibres using bio-chemical route. *Indian J Nat Prod Resour* **6**: 42-50.

Shokri, J. and Adibkia, K., 2013. Application of cellulose and cellulose derivatives in pharmaceutical industries, In: Ven, T. and Godbout, L., *Cellulose-Medical, Pharmaceutical and Electronic Applications*, InTech, Canada, pp 47-66.

Silverstein, R.M., Webster F.X. and Kiemle D.J. (eds), 2005. Spectrometric Identification of Organic Compounds, 7th edn, John Wiley and Sons, USA, pp 99-103.

Sin, E.H., 2012. The extraction and fractionation of waxes from biomass (Doctoral dissertation, University of York, UK).

Singh, Y. (ed), 2006. Martin's Physical Pharmacy and Pharmaceutical Sciences, 6th edn, Wolters Kluwer/ Lippincott Williams & Wilkins, London, pp 442-443.

Sun, C.C., 2008. Mechanism of moisture induced variations in true density and compaction properties of microcrystalline cellulose. *Int J Pharm* **346**: 93–101.

Sun, J.X., Sun, X.F., Zhao, H. and Sun, R.C., 2004. Isolation and characterization of cellulose from sugarcane bagasse. *Polym Degrad Stab* **84**: 331-339.

Sun, R.C. and Tompkinson, J., 2003. Comparative study of organic solvent and water-soluble lipophilic extractives from wheat straw I: yield and chemical composition. *J Wood Sci* **49**: 0047-0052.

Sun, X.F., Xu, F., Sun, R.C., Fowler, P. and Baird, M.S., 2005. Characteristics of degraded cellulose obtained from steam-exploded wheat straw. *Carbohydr Res* **340**: 97-106.

Suvachitanont, S. and Ratanapan, P., 2011. Evaluation of microcrystalline cellulose from corn cob for development to the pharmaceutical industry. *TIChE Int Conf* ms012:1-5.

Suzuki, T. and Nakagami, H., 1999. Effect of crystallinity of microcrystalline cellulose on the compactability and dissolution of tablets. *Eur J Pharm Biopharm* **47**: 225-230.

Terinte, N., Ibbett, R. and Schuster, K.C., 2011. Overview on native cellulose and microcrystalline cellulose I structure studied by X-ray diffraction (WAXD): Comparison between measurement techniques. *Lenzinger Ber* **89**: 118-131.

Thoorens, G., Krier, F., Leclercq, B., Carlin, B. and Evrard, B., 2014. Microcrystalline cellulose, a direct compression binder in a quality by design environment–A review. *Int J Pharm* **473**: 64–72.

Trache, D., Hussin, M.H., Chuin, C.T.H., Sabar, S., Fazita, M.N., Taiwo, O.F., Hassan, T.M. and Haafiz, M.M., 2016. Microcrystalline cellulose: Isolation, characterization and bio-composites application—A review. *Int J Biol Macromol* **93**: 789-804.

Umeh, O.N.C., Nworah, A.C. and Ofoefule, S.I., 2014. Physico-chemical properties of microcrystalline cellulose derived from Indian bamboo (Bambusa vulgaris). *Int J Pharm Sci Rev Res* **29**: 5-9.

United States Pharmacopoeia 30th ed. National Formulary 25 ed. (USP 30/NF 25) (2007). The United states Pharmacopeial Convention, Inc., Rockville, Maryland.

United States Pharmacopoeia, Stage 6 Harmonization (USP <616>, 2015). The United States Pharmacopeial Convention.

United States Pharmacopoeia. 30(6) Harmonization: <1174> POWDER FLOW (USP <1174>, 2016).

Westermarck, S., Juppo, A.M., Kervinen, L. and Yliruusi, J., 1999. Microcrystalline cellulose and its microstructure in pharmaceutical processing. *Eur J Pharm Biopharm* **48**: 199-206.

Williams, R.O., Sriwongjanya, M. and Barron, M.K., 1997. Compaction properties of microcrystalline cellulose using tableting indices. *Drug Dev Ind Pharm* **23**: 695-704.

Yang, H., Yan, R., Chen, H., Lee, D.H. and Zheng, C., 2007. Characteristics of hemicellulose, cellulose and lignin pyrolysis. *Fuel* **86**: 1781-1788.

Yiannoulakis, H., 2015. Pulp and Paper Application of MgO. Research and Development Center Technical Note/Version 2/02.03.13

Yu, H., Liu, R., Shen, D., Jiang, Y. and Huang, Y., 2005. Study on morphology and orientation of cellulose in the vascular bundle of wheat straw. *Polymer* **46**: 5689-5694.

Yuliasmi, S. and Husnita, A., 2017, March. Characterization of microcrystalline from pineapple leaf (Ananas comosus L. Merr). IOP Conference Series. *Mater Sci Eng* **180**: 012267.

Zhong, C., Wang, C., Huang, F., Jia, H. and Wei, P., 2013. Wheat straw cellulose dissolution and isolation by tetra-n-butylammonium hydroxide. *Carbohydr Polym* **94**: 38-45.

Zugenmaier, P., 2008. Cellulose. In: Timell, T.E. and Wimmer, R. eds, *Crystalline Cellulose and Derivatives,* Springer, Berlin, pp 101-174.